Dean Vidakovic, BSc

# Synthesis and Characterization of silylated heavier Group 14 anions

**MASTER'S THESIS**

to achieve the university degree of

Master of Science

Master's degree programme:

Chemie

submitted to

**Graz University of Technology**

**Supervisor**

Assoc.Prof. Dipl.-Ing. Dr.techn. Roland Fischer

Institute of Inorganic Chemistry

Graz, June 2022

## AFFIDAVIT

I declare that I have authored this thesis independently, that I have not used other than the declared sources/resources, and that I have explicitly indicated all material which has been quoted either literally or by content from the sources used. The text document uploaded to TUGRAZonline is identical to the present master's thesis.

Date, Signature

# Danksagung

An dieser Stelle möchte ich mich bei all denjenigen bedanken, ohne die diese Masterarbeit nicht möglich gewesen wäre.

Mein größter Dank geht in erster Linie an Roland Fischer, der mir die Möglichkeit gab, mich mit einem interessanten und spannenden Thema auseinanderzusetzen. Vielen Dank für die zahlreichen motivierenden und fachlichen Gespräche, die dazu beigetragen haben, mich stets weiterzuentwickeln und weitergreifende Zusammenhänge zu erkennen (oder auch zu verstehen). Aber vor Allem möchte ich mich für die Unterstützung während meines verletzungsbedingten Ausfalles bedanken. Vielen Dank auch für die NMR-Messungen und die Kristallstrukturanalysen.

Bedanken möchte ich mich auch bei den ganzen Mitgliedern des Instituts für Anorganische Chemie, insbesondere bei denen der Arbeitsgruppe Flock/Uhlig/Fischer. Ja, wir im 5.Stock sind schon etwas Besonderes. Namentlich möchte ich mich hierbei bei meinen SchreibraumkollegInnen Clara, Meli und Flo für das gute Arbeitsklima und die Späße zwischendurch bedanken. Weiters zu nennen wären Doris, Freskida, Gernot, Schmidi, 2* Phillip und Christoph, die mir bei Fragen stets geholfen haben, aber auch abseits des Laboralltages für lustige Stunden sorgten.

Natürlich möchte ich mich auch bei all meinen Freunden bedanken. Besonders hervorheben möchte ich hier Cher, Dominik, Hannes, Maxi, und Stefan, die mich immer unterstützt oder auch gestützt haben.

Meiner Freundin Magdalena gilt ein besonderer Dank. Du bist immer für mich da und hast stets ein offenes Ohr, wenn es gebraucht wird. Deine ruhige und humorvolle Art trägt dazu bei, dass ich mich jeden Tag aufs Neue auf unseren gemeinsamen Feierabend freue.

Zu guter Letzt möchte ich mich bei meinen Eltern, Mila und Boško, bedanken, ohne deren finanzieller Unterstützung dies alles nicht möglich gewesen wäre. Die Tatsache, dass ihr euch teilweise mehr über bestandene Prüfungen gefreut habt als ich selbst, aber auch Verständnis dafür hattet, wenn etwas nicht auf Anhieb klappte, hat mich enorm bekräftigt und mir auch eine wohltuende Sicherheit gegeben – ***Hvala vam od srca***.

# Abstract

In this work, various silylated organocompounds of the heavier group 14 elements (i.e. silicon, germanium and tin) and their anionic forms are studied. For this purpose, some methods known in the literature such as the Wurtz-type coupling or metalation with potassium *tert*-butoxide are used to prepare these compounds. However, there is little data in the literature on the structure or isolation of chiral anions in this class of compounds. Here we show, starting from tetrakis(trimethylsilyl) group 14 compounds, the introduction of the *tert*-butyldimethylsilyl group followed by selective methylation and the preparation of new tris(trimethylsilyl) organotin compounds. With this, we were able to isolate and characterize these novel compounds in terms of multinuclear NMR spectroscopy ($^{1}$H, $^{13}$C, $^{29}$Si and $^{119}$Sn). In addition, the 18-crown-6 * potassium anions of the *tert*-butyldimethylsilyl compounds and, in the next step, methylated compounds of the heavier analogs of group 14 were determined by multinuclear NMR spectroscopy and X-Ray crystallography. It is shown how the substitution pattern affects the structure and that the degree of pyramidalization increases from silicon to germanium to tin within the same compound class.

# Kurzfassung

In dieser Arbeit werden verschiedene silylierte Organoverbindungen der schwereren Elemente der Gruppe 14 (d.h. Silizium, Germanium und Zinn) und ihre anionischen Formen untersucht. Zu diesem Zweck werden einige in der Literatur bekannte Methoden, wie die Wurtz-Kupplung oder die Metallierung mit Kalium-*tert*.-butanolat, zur Herstellung dieser Verbindungen verwendet. Allerdings gibt es in der Literatur nur wenige Daten über die Struktur oder die Isolierung der chiralen Anionen in dieser Verbindungsklasse. Hier zeigen wir, ausgehend von Tetrakis(trimethylsilyl)-verbindungen der Gruppe 14, die Einführung der *tert*-Butyldimethylsilylgruppe mit anschließender selektiver Methylierung und die Herstellung neuer Tris(trimethylsilyl)organozinnverbindungen. Auf diese Weise konnten wir diese neuen Verbindungen isolieren und mit Hilfe von multinuklearer NMR-Spektroskopie ($^{1}$H, $^{13}$C, $^{29}$Si und $^{119}$Sn) charakterisieren. Darüber hinaus wurden die 18-Kronen-6*-Kaliumanionen der *tert*-Butyldimethylsilylverbindungen und, in einem nächsten Schritt, die methylierten Verbindungen der schwereren Analoga der Gruppe 14 durch multinukleare NMR Spektroskopie und Röntgenkristallographie bestimmt. Es wird gezeigt, wie sich das Substitutionsmuster auf die Struktur auswirkt und, dass der Grad der Pyramidalisierung innerhalb der gleichen Verbindungsklasse von Silizium über Germanium zu Zinn zunimmt.

**Contents**

# 1 Introduction

## 1.1 $R_3Si$-E Compounds in Group 14 (E = C, Si, Ge, Sn, Pb)

Triorganosilyl substituted group 14 compounds are of high interest, as the silyl group is cleaved off rather easily to generate reactive intermediates or to stabilize those. Their anionic moieties play an important role in the organometallic synthesis (E= Si [1,2], Ge [3], Sn [4]).

The first tetrakis(trialkysilyl) compound was synthesized by Gilman and Smith in 1964, which was the tetrakis(trimethylsilyl)silane.[5] Therefore, lithium wires were added to an excess of chlorotrimethylsilane in THF, followed by slow addition of $SiCl_4$. This proved to be a promising reaction route for further tetrakis(trialkylsilyl) substituted group 14 analogues (Scheme 1-1 (I)). In 1965 Merker and Scott prepared the tetrakis(trimethylsilyl)methane derivate using different polyhalides $CBr_nCl_{4-n}$ (n=0-4).[6] Bürger and Goetze used $GeCl_4$ and $SnCl_4$ to obtain tetrakis(tristrimethylsilyl)germane and -stannane back in 1968 by a similar method.[7] The analogous plumbane was prepared some years later by a slightly different method using $PbCl_2$ and $Mg(SiMe_3)_2$ (Scheme 1-1 (II)).[8] Following this procedure elemental lead is produced as a side product. The synthesis of the tetrakis(trimethylsilyl) substituted compounds was the starting point of further organosilyl group 14 compounds of the type $R_{4-n}E(SiMe_3)_n$.

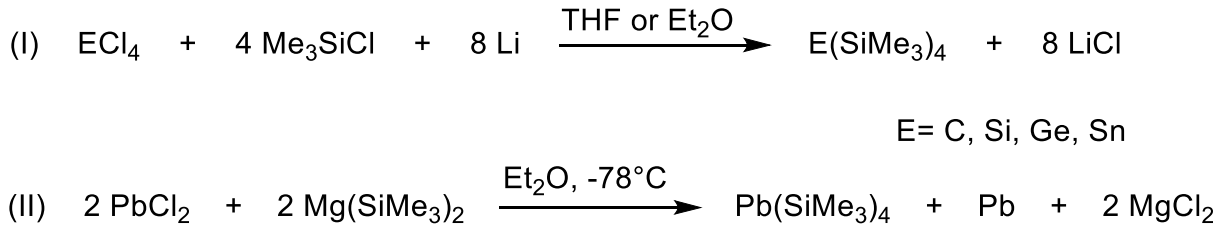


**Scheme 1-1.** Reaction schemes for the preparation of $(Me_3Si)_4E$ (E= C, Si, Ge, Sn) (I) and $Pb(SiMe_3)_4$ (II)

The Wurtz reaction and salt elimination reaction for synthesizing group 14 triorganosilyl derivatives are shown in Scheme 1-2. This is a promising route for the synthesis of this type of compounds since the stoichiometry is easily controlled. However, the purification of byproducts from the Wurtz-type coupling remains a major challenge.

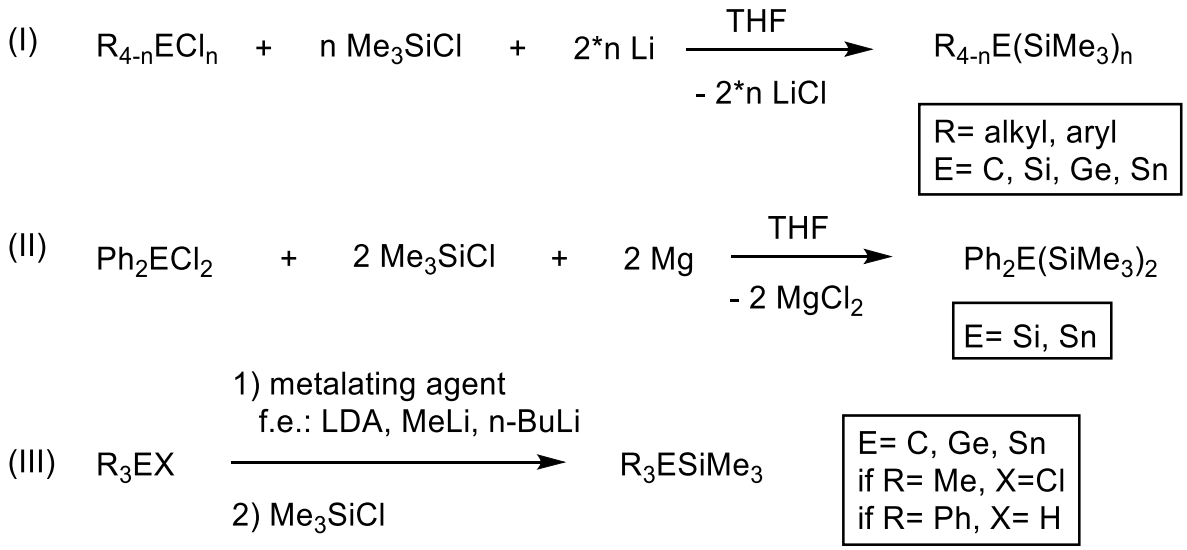


**Scheme 1-2.** Overall reaction scheme of the Wurtz-type coupling with lithium (I) or magnesium (II) and salt elimination reactions with metalating agents (III)

For review, the syntheses for the compounds $R_nE(SiMe_3)_3$ (E = C, Si, Ge, Sn; R= 1-3) are summarized in Table 1.1. Most compounds are prepared by the proven Wurtz-type coupling with lithium metal. Nevertheless, for the synthesis of the $Ph_2E(SiMe_3)_2$ (E =-Si, Sn) compounds Mg was the metal of choice.[9,10] In contrast to the silicon analogous, the outcome of preparing the tin compound changed with the reaction time.[10] Initially, the formation of dodecaphenylcyclohexastannane after 30 min was reported. Subsequently, within 90 minutes, the bis(trimethylsilyl)tetraphenyldistannane was formed, and after 24 h of reaction time, the bis(trimethylsilyl)diphenylstannane was afforded. Hence, the last step, which is metalating the central E-E bond of $(R_3Si)_nR_{n-1}E\text{-}ER_{n-1}(SiR_3)_n$ followed by silylation is also used for the preparation of $Me_2Si(SiMe_3)_2$[11] and $Me_3Sn(SiMe_3)$[12]. However, in the preparation of the $R_3ESiMe_3$ compounds (E = C, Ge, Sn), metalation of the starting material with a reactive group (X = H, Cl) and subsequent quenching with the chlorosilane resulted in the desired product. Hence, the formation of $(SiMe_3)_3GePh$ was obtained by Brook et al. in 1986, by initial formation of the $(SiMe_3)_3GeLi$ anion, which was then reacted with PhBr.[13] Further, the group of Mochida synthesized the $(SiMe_3)_3GeMe$ compound. [14] Therefore, they allowed the intermediate $(Me_3Si)_3GeZnGe(SiMe_3)_3$ to react with MeI for two days. Thus, the $(Me_3Si)_3ER$ compounds are only known for E= carbon, silicon, and germanium.

**Table 1-1.** Review for the synthesis of $R_{4-n}E(SiMe_3)_n$ (E= C, Si, Ge, Sn; R= Me, Ph); if not stated otherwise, in all reactions the quenching reagent was trimethylchlorosilane

| $R_{4-n}E(SiMe_3)_n$ | Starting material | Metalating agent | ref. |
|---|---|---|---|
| **E = C, R = Me, Ph** | | | |
| $RE(SiMe_3)_3$ | $RCX_3$ (X= Cl ,F), R = Me, Ph | Li, cat. DTBB | (15) |
| $R_2E(SiMe_3)_2$ | $R_2CCl_2$ , R = Me, Ph | Li | (16) |
| $R_3E(SiMe_3)_3$ | t-$BuMe_2SiCl$ | MeLi | (17) |
| | $Ph_3CH$ | n-BuLi | (18) |
| **E = Si, R = Me, Ph** | | | |
| $RE(SiMe_3)_3$ | $RSiCl_3$ | Li | (19) |
| $R_2E(SiMe_3)_2$ | $Ph_2SiCl_2$ | Mg | (9) |
| | $Me_3SiSiMe_2Cl$ | Li | (11) |
| $R_3E(SiMe_3)$ | $Ph_3SiCl$ | Li | (11) |
| | $Me_3SiCl$ | Li | (20) |
| **E = Ge, R = Me, Ph** | | | |
| $RE(SiMe_3)_3$ | $(SiMe_3)_4Ge$, then PhBr | MeLi | (13) |
| | $(Me_3Si)_3GeZnGe(SiMe_3)_3$, MeI | | (14) |
| $R_2E(SiMe_3)_2$ | $Cl_2GeR_2$ | Li | (21) |
| $R_3E(SiMe_3)$ | $Me_3GeCl$ | MeLi | (22) |
| | $Ph_3GeH$ | n-BuLi | (23) |
| **E = Sn, R = Me, Ph** | | | |
| $R_2E(SiMe_3)_2$ | $Me_2SnCl_2$ | Li | (10) |
| | $Ph_2SnCl_2$ | Mg | (10) |
| $R_3E(SiMe_3)$ | $Me_3SnSnMe_3$ | n-BuLi | (12) |
| | $Ph_3SnH$ | LDA | (24) |

## 1.2 E-SiMe$_3$ Bond (E = C, Si, Ge, Sn, Pb)

To understand the bonding properties of the E-SiR$_3$ moiety, one must first look at the atomic properties within group 14. These are summarized in Table 1-2. Going from the 1$^{st}$ to the 2$^{nd}$ row within group 14 implies a drastic change in the atomic radii of almost a double, i.e. from 0.77 Å for carbon → 1.17 Å for silicon.[25] The reason for this is that the core of the 2$^{nd}$ row nuclei within group 14 contains s- and p- atomic orbitals, while the core of the 1$^{st}$ row nuclei only contain s- atomic orbitals and upon desceding the group, the energy difference between ns- and np- orbitals increases.[26] However, the increase of the atomic radii is not as drastic as we move from silicon downwards the group 14. This is due to the d and f orbitals, in which the ns- and np- valence electrons are ineffectively shielded. Hence, the additional f-orbitals in Pb ineffectively shield the nucleus from the valence electrons and therefore the ionization potential increases compared to Sn. However, Allred and Rochow stated that the order of decreasing electronegativity within group 14 is C > Pb > Ge > Sn > Si.[27] Therefore, the tendency to hypervalency increases down the group 14, compared to carbon compounds. Several examples are reported in the literature.[28,29] This is essentially a consequence of larger radii and the more electropositive atoms.

**Table 1-2.** Comparison of the atomic properties in group 14, adapted from ref.[30]

| | C | Si | Ge | Sn | Pb | Ref |
|---|---|---|---|---|---|---|
| **Atomic number** | 6 | 15 | 32 | 50 | 82 | |
| **Atomic weight** | 12.011 | 28.0855 | 72.59 | 118.69 | 207.2 | (31) |
| **Covalent radius (Å)** | 0.77 | 1.17 | 1.22 | 1.42 | 1.48 | (31) |
| **Van der Waals radius (Å)** | 1.70 | 2.10 | 2.15 | 2.17 | 2.02 | (32) |
| **Ionization Potential (eV)** | 11.26 | 8.15 | 7.88 | 7.34 | 7.42 | (31) |
| **Electronegativity** | 2.60 | 1.90 | 2.00 | 1.93 | 2.45 | (27) |

The data from Table 1-3 are reflected for the tetrakis(trimethylsilyl) compounds of group 14. Here, the carbon and silicon congeners can be stored under ambient conditions for months, whereas the oxophilicity drastically increases from germanium to lead. Therefore, they need to be stored under inert conditions. The E-$SiR_3$ bond is attacked under basic conditions and by alcohols. All of them show high solubility in etheral solvents and hydrocarbons.[33]

The bond dissociation energies (BDE) for the diatomic molecule of Si-E (E = C, Si, Ge, Sn) are shown in Table 1-3. The atomic properties are reflected here, as the BDE decreases from C-Si to Pb-Si.

**Table 1-3.** Bond dissociation energies (BDE) for the diatomic molecules Si-E

| | **BDE [kJ/mol]** | **Ref.** |
|---|---|---|
| **C-Si** | 447 | (34) |
| **Si-Si** | 310 | (34) |
| **Ge-Si** | 297 | (34) |
| **Sn-Si** | 233 ± 7.8 | (35) |
| **Pb-Si** | 169 ± 7 | (36) |

## 1.3 Formation of $(R_3Si)_nE$-Anions (E= C, Si, Ge, Sn, Pb)

Trivalent group 14 compounds with a lone pair at the central atom bearing a negative charge are useful synthons in synthetic chemistry. The first synthesized and investigated group 14 centered anion, the carbanion, is already known for decades. Indeed, in the early 1900s Grignard reagents[37] and organolithium[38] were the first studied anions and are therefore the most powerful alkylating agents used nowadays. The carbanion is electron rich, and hence can act as both, a strong Lewis base and a strong nucleophile. The preparation of these carbanions is usually carried out using strong bases for the deprotonation of hydrocarbons. If the compound is not sufficiently acidic for direct deprotonation, transmetalation of alkyl halides with alkyl lithiums or Grignard reagents can be used instead.

In general, using the same synthetic methods for the generation of higher anionic homologues of group 14 does not work. This has two reasons[39]:

- Due to electronegativity differences, the E-H (E = Si, Ge, Sn) bond is polarized towards H, therefore the H atom is more hydridic. On the contrary, C-H bond is negatively polarized towards C, therefore the H atom is acidic, and deprotonation is more readily possible. Nevertheless, deprotonation of f.e. silyl hydrides is known for cases where the anion is stabilized by a silyl or phenyl group.
- The use of silyl, germyl or stannyl halides with metals like Mg rather leads to Wurtz type coupling, as the halides are excellent electrophiles and are immediately attacked by nucleophiles. Hence, substitution via salt elimination is favoured over transmetalation reactions.

From the 1950s the investigation of the heavy group 14 element centered silylated anions started with the study of oligosilyl anions. At this time, Gilman et al.[40] described the first synthesis of $(SiMe_3)_3SiLi$, which was further improved by Brook and coworkers[41] in the beginning of the 1980s. They used the readily available $Si(SiMe_3)_4$, where the Si-Si bond was cleaved by MeLi in THF. It was in 1986 when again Brook et al. prepared the tris(trimethylsilyl)germyllithium[13] and in 1992 the tris(trimethylsilyl)stannyllithium was synthesized by Preuss and coworkers via a similar route as used for the silicon analogue (see Scheme 1-3).[42] Recrystallization in THF resulted in the isolation and structural characterization of $(Me_3Si)_3ELi$ *3 THF.

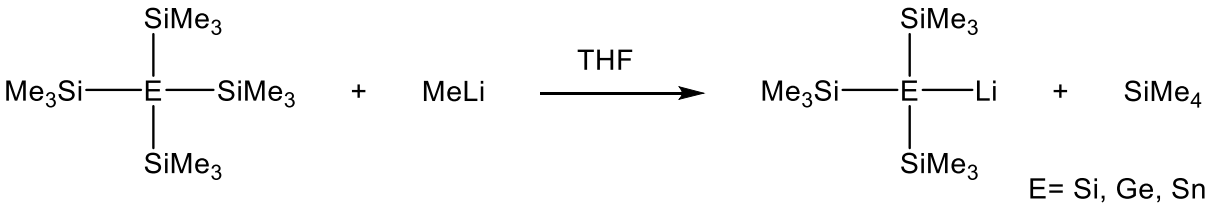


**Scheme 1-3.** Route of preparation for the first tris(trimethylsilyl) group 14 anions

Since then, the $(Me_3Si)_3SiLi$ moiety has been the most widely studied compound in terms of structure and application to synthesis. The tris(trimethylsilyl)silyl moiety is widely used as a substituent in main group and transition metal chemistry because of its steric and electronic properties to stabilize anionic or radical compounds.[43]

Marschner et al. reported the first synthesis of the $(Me_3Si)_3SiK$ by using $KO^tBu$ in etheral solvents like THF or DME (see Scheme 1-4).[44] In contrast to the method employed by Gilman with MeLi, the stoichiometry can be controlled rather easily as $KO^tBu$ is a solid and the reaction is almost quantitative. Also the potassium compounds show increased reactivity and solubility in nonpolar solvents compared to the lithium compound. In this case, the silyl ether $^tBuOSiMe_3$ is formed as a cleavage product in contrast to tetramethylsilane when MeLi is employed.

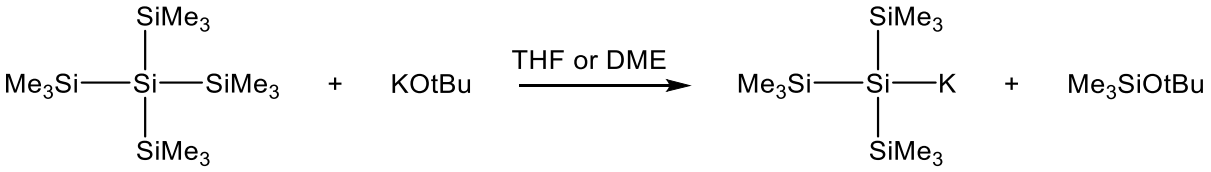


**Scheme 1-4.** Generation of the hypersilylanion following Marschner's route

However, the electronic and steric stabilizing effect of the $(Me_3Si)_3Si$-moiety sometimes do not meet the requirement for synthesizing labile compounds. An example of this is the synthesis of the extremely sensitive tetrasilatetrahedrane. For this, Wiberg used the even more stabilizing supersilyl group $Si^tBu_3$ as in $Si(Si^tBu_3)$ (see Figure 1.1).[45]

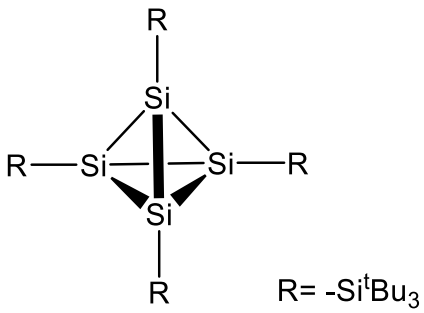


**Figure 1-1.** Wiberg's tetrasilatetrahedrane

The route followed by Marschner resulted in new ways for introducing even bulkier silyl groups to the silanide (see Scheme 1-5). Sterically more shielding silyl groups like $^{t}BuMe_2Si$ (TBDMS), $^{i}Pr_3Si$ (TIPS) or 2,3-dimethyl-2-butyldimethylsilyl (ThexylMe$_2$Si) are by far less accessible to cleavage by potassium tert-butoxide. Further treatment of these compounds with KO$^{t}$Bu reacted with selective removal of the SiMe$_3$ group, but only if no phenyl groups were present.[46]

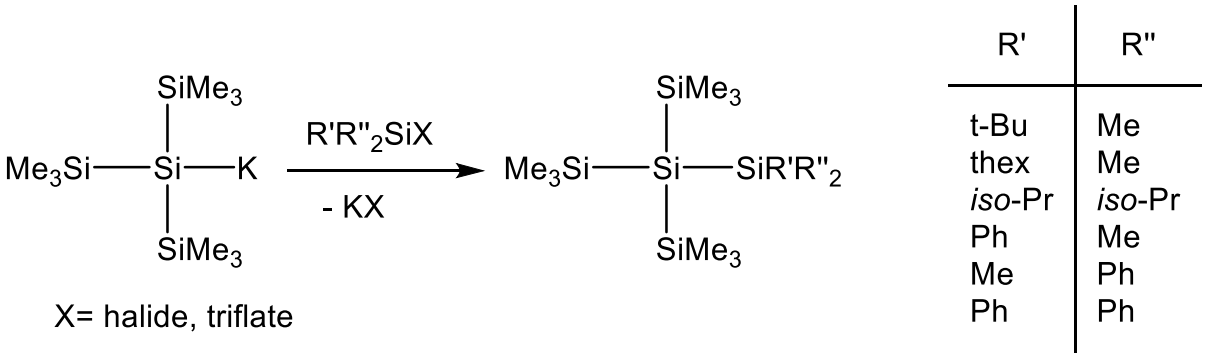


**Scheme 1-5.** Generation of bulkier silyls, adapted from ref.[2]

Prior to the method introduced by Marschner, Klinkhammer et al. prepared the unsolvated and base free hypersilyl anion by transmetalation of [Si(SiMe$_3$)$_3$]$_2$M (M= Zn, Cd, Hg) with an alkali metal (M'= K, Rb, Cs) (see Scheme 1-6).[47,48] The reaction rates increased by employing both, the heavier homologues of alkali metals and the zinc group. Therefore this route is rather disadvantageous as toxic Hg(II) is used in order to reach high conversion rates. As the group 10 derivatives of (Me$_3$Si)$_3$Si-M-Si(SiMe$_3$)$_3$ can be obtained from (Me$_3$Si)$_3$SiH and R$_2$M (M=Zn, Cd, Hg) in alkanes, and further derivatization is also possible in hydrocarbon solvents, this method allows the preparation of oxygen-donor free silylanions.

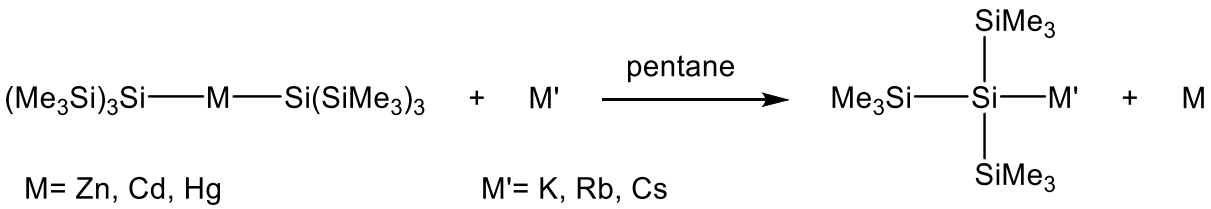


**Scheme 1-6.** Hypersilylanion preparation by the method of Klinkhammer

The route employed by Marschner provides convenient and widely variable access to novel oligosilanylanions, as shown in the case for $Si_2(SiMe_3)_6$ (see Scheme 1-7) .[44] $KO^tBu$, in contrast to the use of MeLi, specifically cleaves the terminal Si-$SiMe_3$ bond and not the internal Si-Si bond.[49,50]

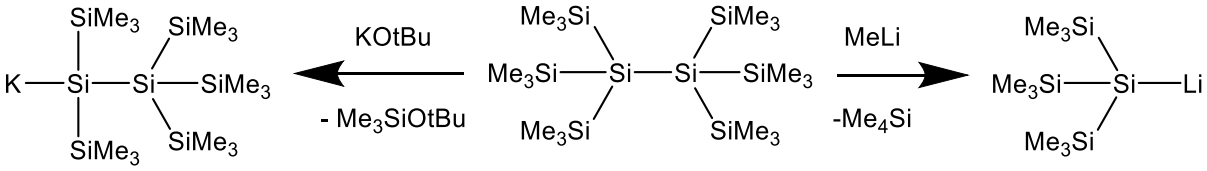


**Scheme 1-7.** Oligosilyl anion preparation by using MeLi or KOtBu

In comparison to silyl centered anions, the chemistry of alkali silylgermanides was limited to the lithium hypersilylgermanide, following the procedure developed by Brook in the mid-80s, as mentioned above. It was in 2004, when Teng and Ruhlandt-Senge prepared the $KGe(SiMe_3)_3$ analogous to the preparation of the potassium silanide as mentioned above.[51] They used the intermediate for preparation and characterization of the heavy alkaline earth germanides $M(THF)_n(Ge(SiMe_3)_3)_2$ (M= Ca, Sr, n= 3; M= Ba, n= 4) by reacting it with the corresponding alkaline earth metal iodides in THF. Like the observations for the potassium silanide [52], the corresponding germanide also showed redox chemistry, by $SiMe_3$ group migration, if kept for too long in THF. The byproducts are $Ge(SiMe_3)_4$ and elemental germanium. Therefore, reaction times should be kept as short as possible to avoid such side reactions. Consequently, the working group of Marschner in 2005 investigated the follow up reactions of the silylgermylpotassium compounds following the same way as for the hypersilylpotassium.[3] The reaction was performed in either THF or in aromatic solvent with the aid of a sequestering polyether, e.g. a crown ether like 18cr6. Though, the latter required the use of crown ether.

As with the hypersilylsilanide congener, the hypersilylgermanide shows similar reactivities towards different electrophiles (as shown in Scheme 1-8). It was also shown that in a $(Me_3Si)_3Ge\text{-}E(SiMe_3)_3$ (E= Si, Ge) moiety only the terminal Ge-$SiMe_3$ bond is cleaved, if employing 1 eq of $KO^tBu$. Hence, the use of 2 eq of KOtBu resulted in the formation of a dianion, where additionally the E-$SiMe_3$ bond was cleaved to yield 1,2-dianionis $K(Me_3Si)_2SiE(SiMe_3)_2K$.

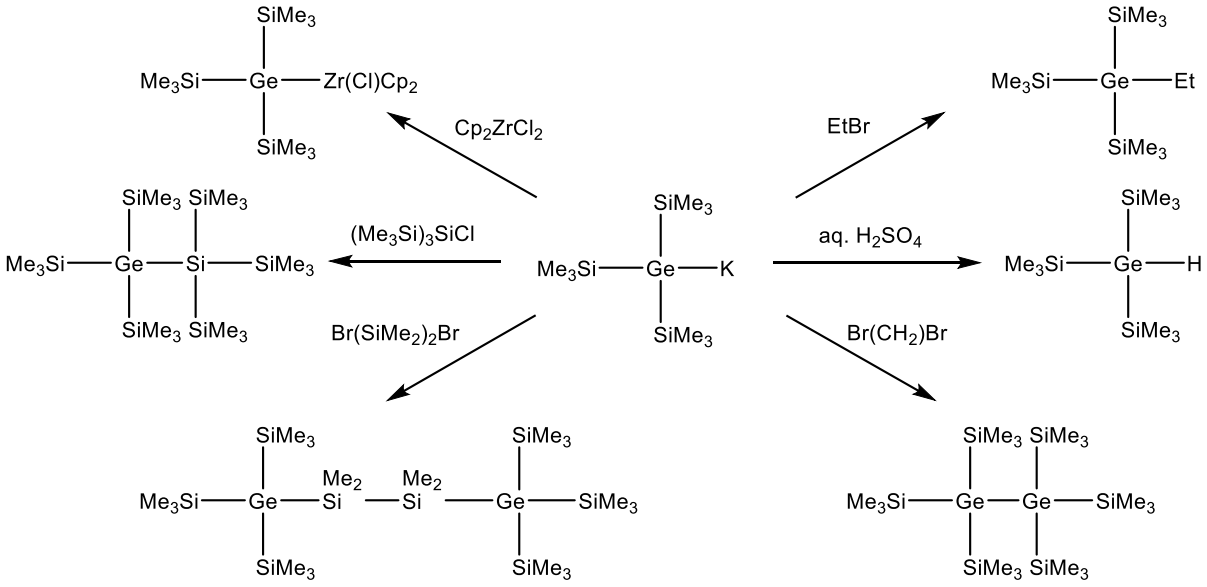


**Scheme 1-8.** Reactions of the $(Me_3Si)_3GeK$ with electrophiles, adapted from ref.[3]

Like the tris(trimethylsilyl)germanide alkali compound, the tris(trimethylsilyl)stannyl alkali derivative was limited to lithium as the counterion. In 2005 Fischer showed that the reaction with MeLi also works in benzene.[53] Moreover, they investigated the anion preparation starting from tetrakis(trimethylsilyl) stannane using alkali tert-butoxides $^tBuOM$ (M= Na, K, Rb, Cs) (see Scheme 1-9). As for the silicon and germanium congener the reactions were performed in polar etheral solvents, like THF or DME, or aromatic solvents. Hence, again the later required at least one equivalent of crown ether. It was shown that the tin derivative is easier to metalate than the silicon derivative. Therefore, the metalation of $E(SiMe_3)_4$ (E= Si, Sn) with NaOtBu in THF was compared. While the silicon moiety takes up to 24 h at temperatures around 50 °C, the metalation of the tin analogous is completed within 10 minutes at room temperature. Moreover, the rubidium derivative showed the highest reactivity among the alkali metal tert-butanolates. Therefore, stochiometric amounts and removal of $Me_3SiO^tBu$ *in vacuo* are necessary to avoid side reactions like reduction to elemental tin and decomposition under silyl group migration under partial regeneration of the starting material or

dimerization. To this end, they synthesized $(Me_3Si)_3Sn$-Cs*18cr6 via fluoride mediated cleavage of the Sn-Si bond using CsF to form the anion and trimethylfluorosilane via the energetically highly favored Si-F bond.

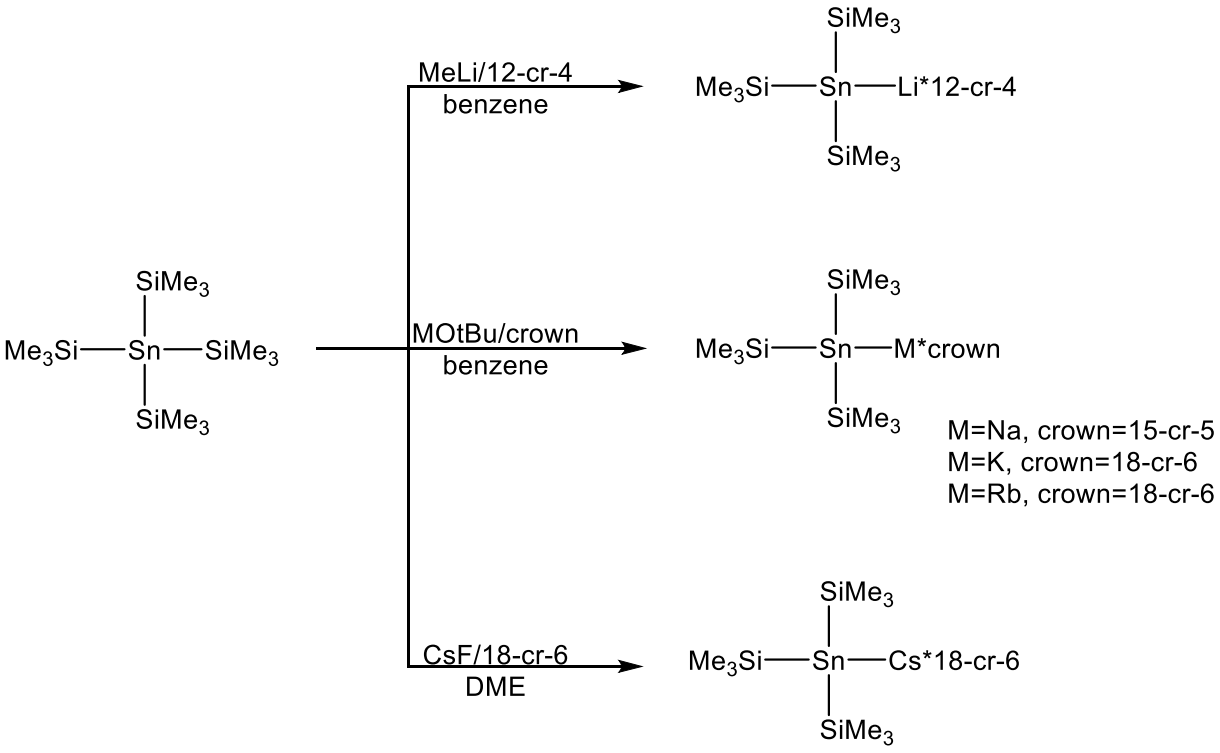


**Scheme 1-9.** Anion preparation starting from $Sn(SiMe_3)_4$, adapted from ref.[53]

## 1.4 Structure of $R_3Si$-E Anions

X-Ray and NMR studies of group 14 anions remain highly interesting, as they give insights into the structure (planar vs. pyramidal), aggregation with donor solvents, inversion barrier and the type of bonding interaction between the metal and the anionic center (i.e. covalent vs. ionic).

In general, the pyramidal inversion is the result of $sp^3$-hybridization, where the lone pair has more s-character than in a planar configuration (only p-hybridized) and therefore gains additional stability. The influence on s-orbital contribution is also reflected by the drastic increase of the electron binding energy with increasing s-character, when going from $H_3C\text{-}CH_2^-$ ($sp^3$) to $H_2C{=}CH^-$ ($sp^2$) to $HCC^-$ (sp).[54] Therefore, if the energy gaps between s- and p- orbitals become larger upon descending a group, the bond to other elements gain higher p-character. Indeed, the inversion barrier increases going downwards inside a group. This holds also true for the isoelectronic ammonia and phosphine molecules. The inversion barrier of the two molecules is for $NH_3$ = 25 kJ $mol^{-1}$ and for $PH_3$ = 140 kJ $mol^{-1}$.[55] Hence, ammonia or the resulting amines typically show racemization at room temperature, whereby the phosphine derivatives give an optical pure isomer as the racemization rate is slow. Effectively, the inversion barrier can be seen as the activation energy needed to go through a planar transition state to the other enantiomeric form (see Figure 1-2).

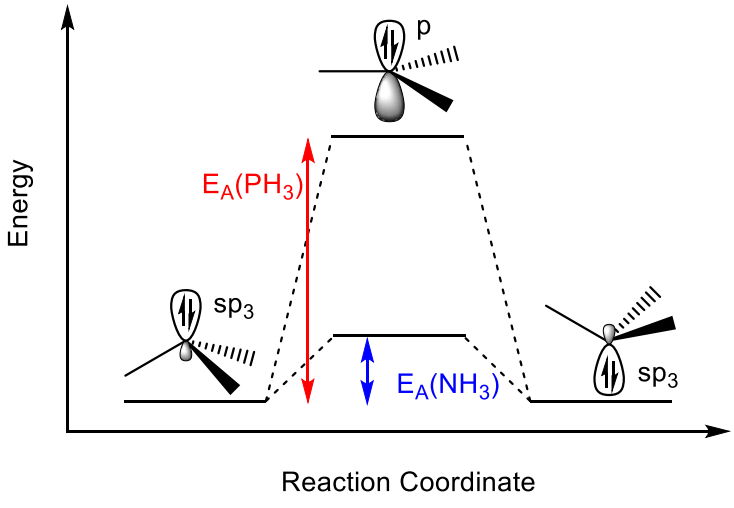


**Figure 1-2.** Qualitative representation of the pyramidal inversion and the inversion barrier (i.e. $E_A$) differences between $NH_3$ and $PH_3$, adapted from ref.[56]

This degree of pyramidalization is also depicted in the bond angles of those two molecules. In $NH_3$ the H-N-H angle is 107.3°, which is slightly less than for a

tetrahedron (109.5°). Instead, in the $PH_3$ molecule the average H-P-H angle is 93.5° and therefore more pyramidal. An important characteristic in this context is the sum of angles around the central atom, which is 360° for a planar structure and smaller the more pyramidalized the structure is.

Especially for the silylated group 14 anions experimental studies about the inversion barriers are rare. In 2003 Fischer et al. conducted an experimental investigation on the inversion barrier of the chiral oligosilyl moiety shown in Scheme 1-10.[57] To synthesize the desired oligosilylanion, the authors took advantage of the selective cleavage of the -$SiMe_3$ group upon introduction of a more bulky silyl group. (i.e. -$SiMe_2{}^tBu$).This was demonstrated by Kayser et al. in 2002, where the selective cleavage of alkyl substituted silyl groups in the neopentasilanes studied was determined by their steric bulk.[58] This means that the less bulky silyl group (f.e. -$SiMe_3$) is cleaved off before the more bulky one (f.e. -$SiMe_2{}^tBu$). The final chiral silyl anion in Scheme 1-10. was obtained by transmetallation of the silyl potassium with lithium chloride.

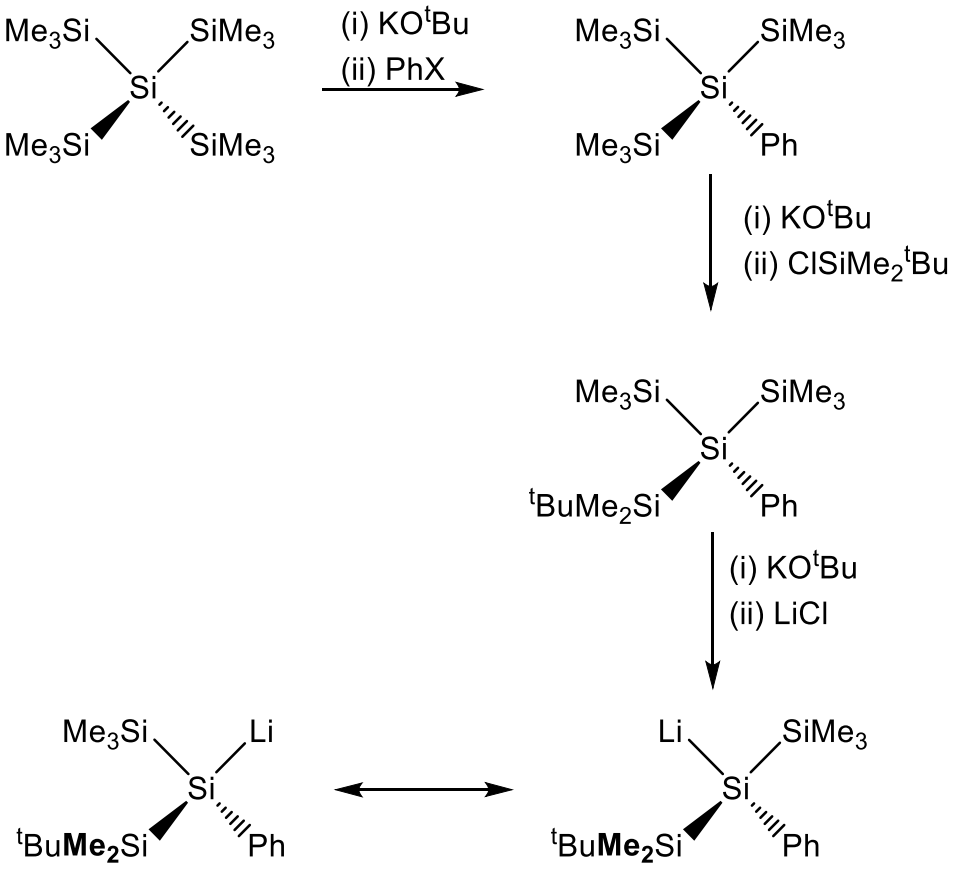


**Scheme 1-10.** Route of preparation for the oligosilylanion from ref.[57]

They used the data derived from temperature dependent $^{1}H$ NMR (shown in Figure 1-3.) of the highlighted methyl groups in Scheme 1-10. Here, the diastereotropic methyl groups give two distinctly separate signals at -40°C, while they exhibit coalescence and finally merge into one signal as the temperature is increased. Hence, the -$SiMe_3$ group stays unaffected. Moreover, they were able to show that the barrier increases if a less electropositive cation, i.e. lithium or magnesium, is used instead of sodium or potassium. In addition, it was shown that the inversion barrier also depends on the Si-cation bond type and the planarity of the anion. Therefore, the inversion barrier of the investigated oligosilyl anion decreases in the following order: benzene as solvent > etheral solvents > crown ether.

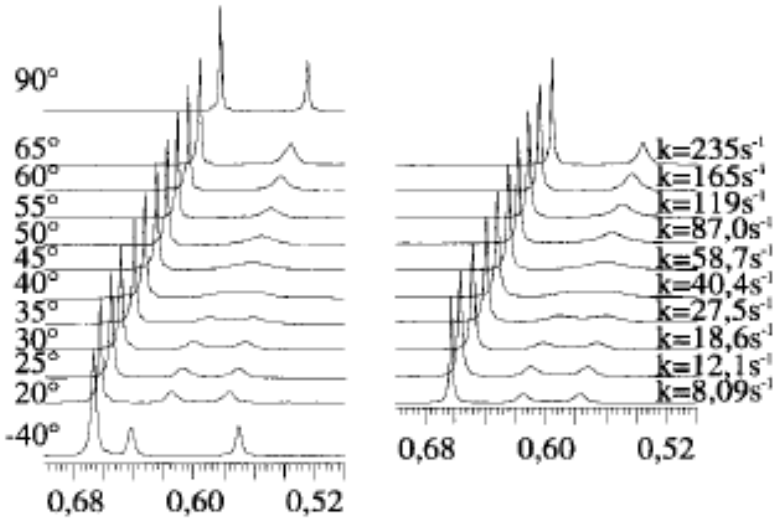


**Figure 1-3.** Temperature dependent $^{1}H$ NMR with rate constants, reprinted form ref.[57]

X-Ray crystallography is a comprehensive tool for studying the pyramidalization, the bonding type between anion-cation and the aggregation state with donor solvents. Therefore, the available X-Ray data for the $E(SiMe_3)$ E = Si, Ge, Sn family and their anionic form are compared concerning cone angles and E-M bond distances as shown in Figure 1-4.

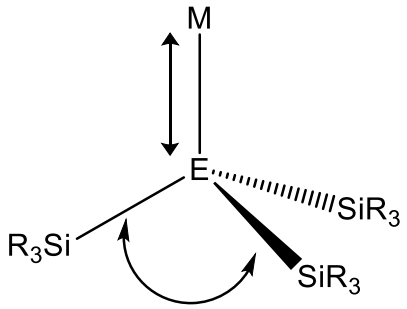


**Figure 1-4.** Compared cone angles between Si-E-Si and bond distances of the E-M bond

In general, the bond distances between the E-Si do not change significantly if the corresponding anion is formed. Moreover, a drastic change is observed in the bond angle spanned by the silyl groups and the central group 14 atom. This means going from an ideal tetrahedral bond angle of 109.5° to 102.4°,100.9° and 98.8°, as this is the case for the trisolvated THF $LiE(SiMe_3)_3$ anion where E = Si, Ge, Sn. Hence, the pyramidalization for the anion type of $LiE(SiMe_3)_3$ increases if going from Si over Ge to Sn. This implies sufficiently more p-character bonding, as the s-electrons are more stabilized and less available for bonding. Therefore, the degree of pyramidalization increases. By using other counterions, i.e. potassium or sodium, the degree of pyramidalization does not change drastically. The structural data from different anions are compared in Table 1-4. The alkali metal group 14 distance drastically varies in the solid state structures as a consequence of the solvation of the cation. This trend, however, is not reflected in NMR data on inversion barriers, as crown ether adducts usually show direct E-M contact in the solid state, but dissociate in solution and show lower inversion barriers.

**Table 1-4.** Comparison of structural data for $E(SiMe_3)_4$ and $(Me_3Si)_3EM$ for E= Si,Ge,Sn

| | mean E-Si [Å] | E-M [Å] | mean ∢ Si-E-Si [°] | Ref. |
|---|---|---|---|---|
| **E = Si** | | | | |
| $E(SiMe_3)_4$ | 2.346(1) | | 109.5(1) | (59) |
| $(Me_3Si)_3ELi * 3THF$ | 2.330(2) | 2.644(12) | 102.4(1) | (59) |
| $(Me_3Si)_3EK * 3C_6H_6$ | 2.336 | 3.33 | 101.5 | (48) |
| **E = Ge** | | | | |
| $E(SiMe_3)_4$ | 2.374(1) | | 109.46(7) | (60) |
| $(Me_3Si)_3ELi * 3THF$ | 2.374(1) | 2.666(6) | 100.89(4) | (60) |
| $(Me_3Si)_3EK * 18cr6$ | 2.383 | 3.399(8) | 100.9 | (61) |
| **E = Sn** | | | | |
| $(Me_3Si)_3ELi * 3THF$ | 2.5718(8) | 2.865(5) | 98.75(3) | (62) |
| $(Me_3Si)_3ENa * 15cr5$ | 2.593(5) | 3.0775(18) | 99.13 | (53) |

Yet, the structures of group 14 anions with sterically demanding silyl substituents strongly differs from the tris(trimethylsilyl) substituted anions. This was shown by the working group of Sekiguchi, where they investigated the anions of the form $(t\text{-}Bu_2MeSi)_3EM$ for E = Si, Ge, Sn.[63] The anions were prepared by one electron reduction of the corresponding radical using either hexane or THF as solvent (see Scheme 1-11). The crystallographic data for the monomeric, unsolvated anions showed for both a nearly planar structure, i.e. an average bond angel for Si-Si-Si = 119.7° and for Si-Ge-Si = 117.5 ° respectively. The reasons for the high degree of planarity were described as following:

- hyperconjugation between anionic center and σ*-orbital of Si-C bonds
- Li--CH agostic interactions
- shorter E-Li bonds compared to pyramidal structures

Therefore, the introduction of sterically demanding electropositive silyl substituents also favors to planarity. This is accompanied by the decrease of the inversion barriers, as shown in our group by computational methods.[64] Thus, similar observations were found for the isoelectronic compound $(^{i}Pr_3Si)_3P$.[65] Additionally, Sekiguchi and coworkers isolated the solvent separated ion pairs (SSIP) by performing the reaction in THF (see Scheme 1-11). Herein, the pyramidalization increases, as an average bond angle for Si-Si-Si = 116.7° and for Si-Ge-Si = 114.5° is found. Hence, this is attributed to the absence of agostic interactions between Li--CH.

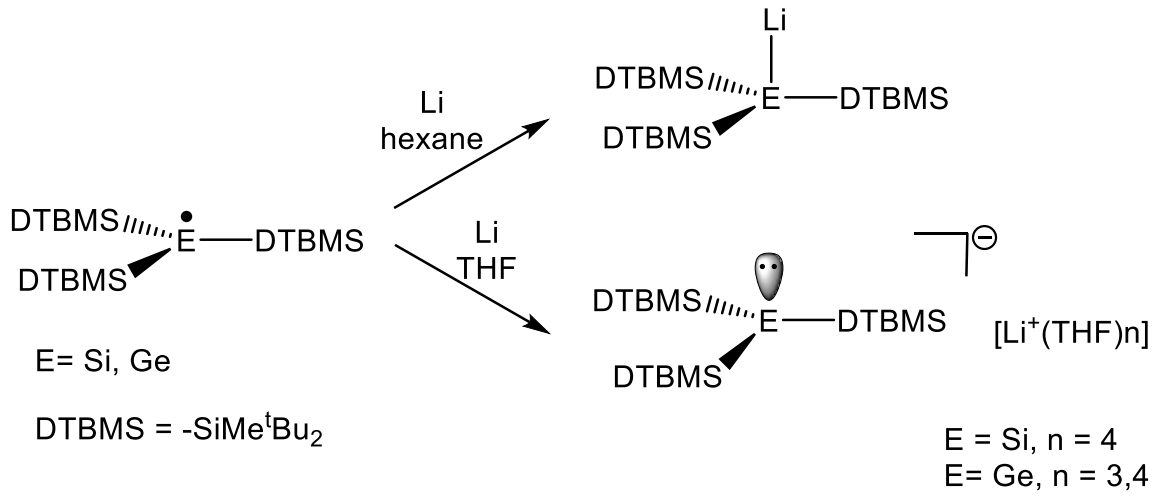


**Scheme 1-11.** Investigated $(DTBMS)_3ELi$ (E= Si, Ge) anions by Sekiguchi et al.[63]

Moreover, Sekiguchi and coworkers studied the anion formation of the analogous tin radical $[(^{t}Bu_2MeSi)_3Sn]^{\cdot}$.[66] In contrast to the silicon and germanium congener, the tin radical species showed different behavior in the anion formation (see Scheme 1-12). Hence, if the one electron reduction is performed in THF with lithium the tin species resulted in the formation of a THF coordinated stannyllithium. In contrast, the silyl and germyl analogous resulted in the formation of SSIP. This is explained by the fact that tin has a larger atomic radius than silicon or germanium and therefore the bonds to the substituents are significantly longer, as crystallographic data imply. Furthermore, this leaves enough space for the lithium cation to come close to the tin anion. Indeed, if the anion formation is performed with potassium and [2.2.2]cryptand in THF, the free anion is observed. Comparing the average cone angles between the free anions of the silyl, germyl, and stannyl analogs (Si = 116.7°; Ge = 114.5°; Sn = 111.6°), reveals the trend of increasing pyramidalization if descending the group. Reduction of the tin radical in a nonpolar solvent, i.e. heptane, resulted in the formation of a dimeric species rather than the monomeric anion, as in the case of silyl and germyl.

Additionally, a solvated anion with $\eta^6$ coordinated lithium to the aromatic solvent is observed when benzene is used as solvent.

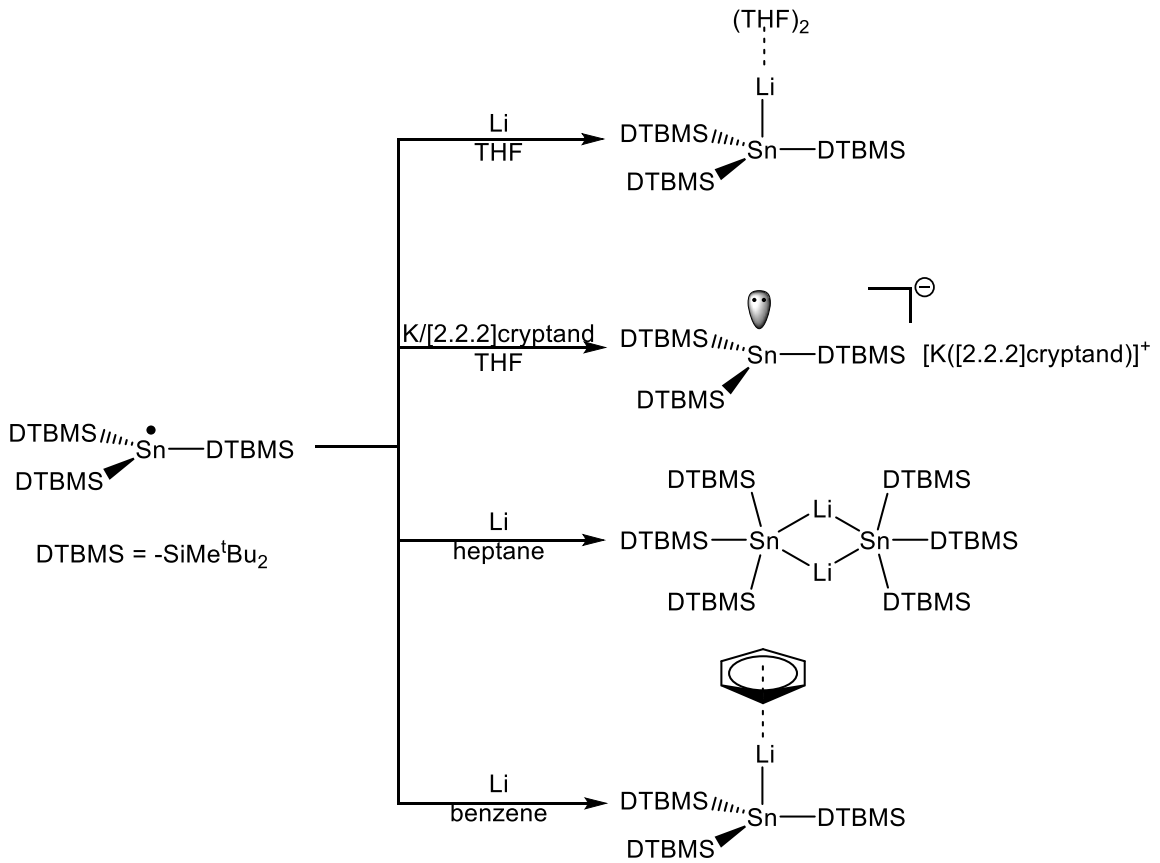


**Scheme 1-12.** Reduction of $[(^tBu_2MeSi)_3Sn]^\cdot$ radical, studied by Sekiguchi et al.[66]

However, the X-ray structures of the stannyl anions in Scheme 1-12 do not show a high degree of pyramidalization with average Si-Sn-Si bond angles ranging from 111.6° to 114.1°. This is attributed to the large steric demand of the used silyl group. Similar planarization was found with the sterically high demanding “supersilyl” ligand in $[(Me_3Si)_3Si]_3SnNa\text{-}(C_7H_8)$, with an average bond angle of 109.9°.[48]

In general, the following aspects are responsible for the degree of pyramidalization of a group 14 substituted silyl anion, that is:

- steric influence of the silyl group, as seen above for $(Me_3Si)_3SnLi$ * 3 THF (av. cone angle = 98.8°) vs. $(t\text{-}Bu_2MeSi)_3SnLi$ * 2THF (av. cone angle = 112.6°)
- nature of the cation and type of cation-anion interaction, i.e. contact ion pair (CIP) or solvent separated ion pair (SSIP)
- type of central atom, as pyramidalization increases within a group.

# 2 Aim of the Project

The aim of the master's thesis was the synthesis of novel organo silane, germane and tin compounds from which chiral anions should be studied in solution (NMR) and by X-Ray structure analysis. The target was the investigation of the inversion barriers and the degree of pyramidalization, which should increase from silicon towards tin. The target racemic mixture is shown in Scheme 2-1.

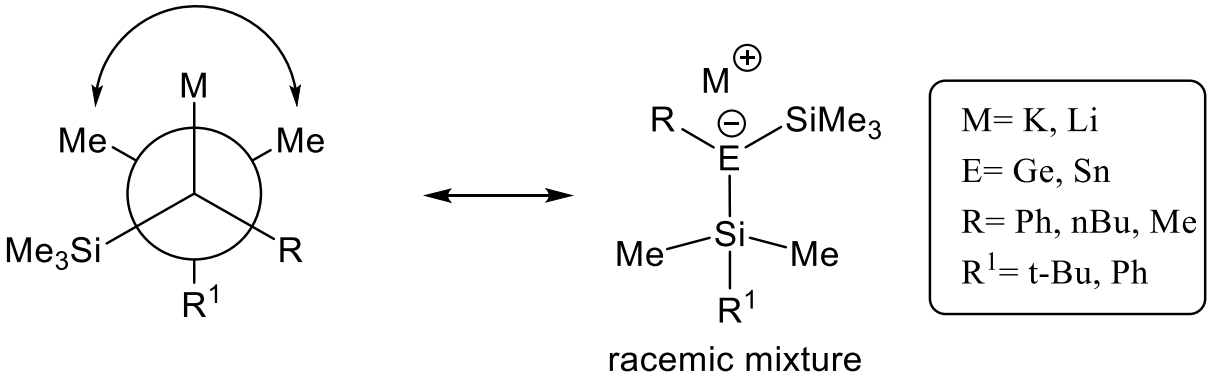


**Scheme 2-1.** Target molecule with diastereotopic methyl groups of the TBDMS group

As a starting material for the preparation of chiral group 14 anions, compounds of general formula $^{t}BuMe_2Si(Me_3Si)_2RE$ were chosen, as the methyl groups of the $^{t}BuMe_2Si$ substituents are diasterotopic and hence anisochronous in NMR spectra after cleavage of one of the trimethylsilyl groups.

The synthetic route followed is shown in Scheme 2-2. Following route (I), we tried to synthesize the tris(trimethylsilyl)organostannane by Wurtz type coupling. The next step is the introduction of a sterically more demanding silyl group, i.e. $-SiMe_2{}^{t}Bu$. This is done by initial anion formation with $KO^{t}Bu$ and subsequent reaction with the silyl halide. The sterically demanding silyl group is needed for the selective cleavage of the $-SiMe_3$, as described above, to obtain a chiral silyl, germyl or stannyl anion.

In route (II) we wanted to start with the readily available tetrakis(trimethylsilyl)silane, -germane or- stannane. Again, a sterically more demanding silyl group (i.e. $-SiMe_2{}^{t}Bu$) is introduced with the already known procedure. Subsequent anion formation and alkylation with an alkylating agent leads to the desired precursor for the chiral silyl, germyl or stannyl anion.

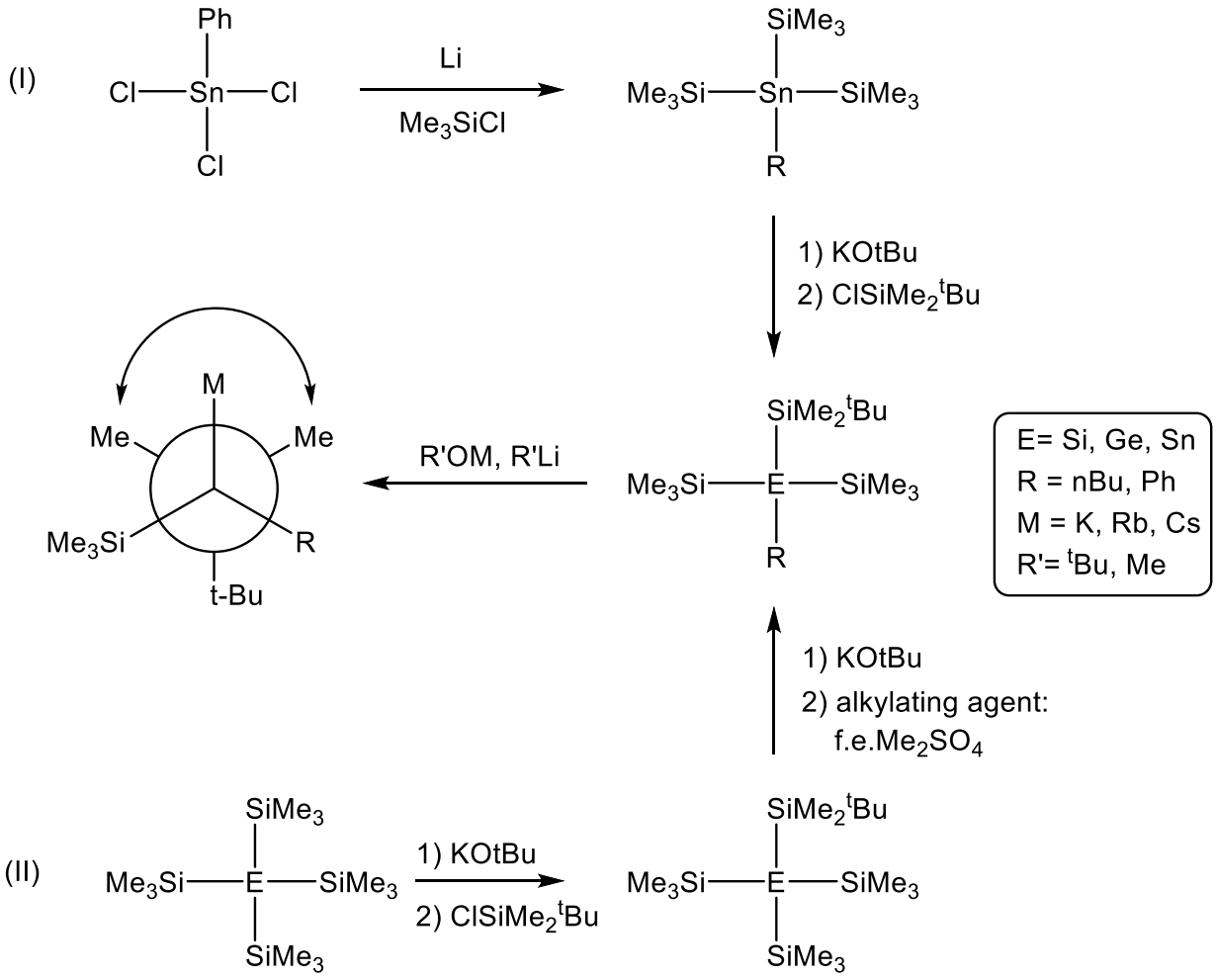


**Scheme 2-2.** Synthetic route followed to a chiral anion

# 3 Results and Discussion

## 3.1 Kocheshkov redistribution reaction of $SnCl_4$ and $Ph_3SnCl$

To synthesize dichlorodiphenylstannane (**1**) and chlorotriphenylstannane (**2**), the pioneering Kocheshkov reaction is the way of choice.[67,68] By controlling the stoichiometry of $SnCl_4$ and $Ph_3SnCl$ the outcome of the redistribution reaction at elevated temperatures can be controlled smoothly (see Scheme 3-1). The reaction control was monitored via $Sn^{119}$ NMR. To facilitate the control of stoichiometry, (**1**) was recrystallized in n-hexane. Recrystallization of (**2**) in dry THF leaded to an off-white shiny solid. The complex formation of (**2**)*THF was confirmed via $^1H$ NMR. However, the complex showed decomposition after approximately two weeks. This was confirmed by $^{119}Sn$ NMR and the waxy aggregation formed. Therefore, the dark brown liquid was used without further workup for the consecutive reactions.

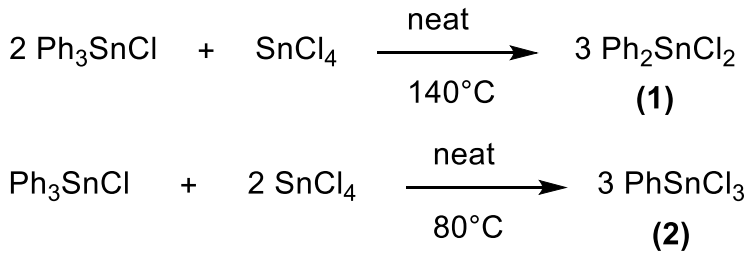


**Scheme 3-1.** Kocheshkov redistribution reaction

## 3.2 Synthesis of $Ph_2Sn(SiMe_3)_2$ (3)

The starting material bis(trimethylsilyl)diphenylstannane (**3**) was synthesized according to the published procedure via Wurtz type coupling.[10] As discussed in the introduction chapter this reaction shows strong time dependence and therefore a prolonged reaction time is needed. However, the reaction progress is monitored by $^{119}Sn$ NMR and compared to the published data.[10]

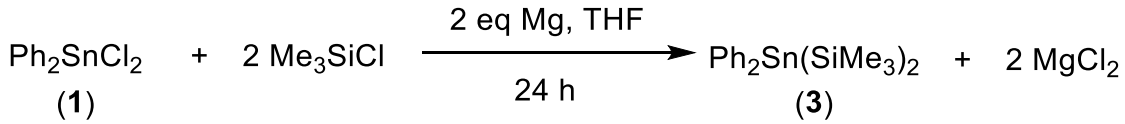


**Scheme 3-2.** Synthesis of (**3**) according to the published procedure

### 3.2.1 Halogenation attempts of $Ph_2Sn(SiMe_3)_2$

The intention was to synthesize the halogenated reactive intermediate $PhXSn(SiMe_3)_2$ by splitting off the phenyl group from $Ph_2Sn(SiMe_3)_2$ and replacing it by a halogen (X=Cl or Br). This was attempted with various methods already known in the literature, wherein different organotin or -silicon compounds were used (see Scheme 3-3).

The first method tested was the use of excess etheral hydrochloric acid described by the work of Jukschat et.al., wherein an organotin dimer connected through a carbon spacer was used.[69–71] The advantage of this method is the selective removal of the phenyl group at the central tin atom and the easy workup of the byproduct, as the resulting benzene can be removed rather easily *in vacuo*. However, in our case mainly the starting material remained and a not assignable peak at – 547 ppm was observed in the $^{119}Sn$ spectrum.

The second method tested was the halogenation with bromine.[72] Here, the reaction was performed in the dark to avoid byproducts from the radical reactions, as bromine is light sensitive. Nevertheless, the $^{119}Sn$ spectrum showed formation of unclassifiable byproducts, whereby the starting material was consumed entirely.

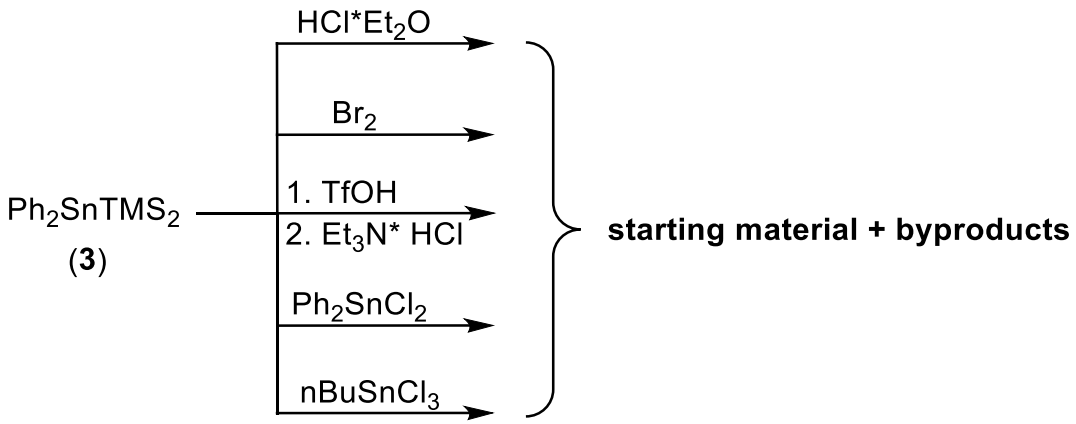


**Scheme 3-3.** Chlorination attempts of $Ph_2Sn(SiMe_3)_2$ (**3**)

Furthermore, the chlorination was tried with TfOH (Tf= $CF_3SO_3$) and $Et_3N$*HCl. In the literature this was shown with various organosilicon and -tin compounds, which are connected through a carbon spacer (e.g. $(CH_2)_n$) between the two silicon or tin centers.[73,74] Here, the triflate group replaces the phenyl group and, upon addition of $Et_3N$*HCl, the acid group is cleaved off again to form the desired chlorosilane or -stannane. Furthermore, it was reported that exact stoichiometry, performing the reactions at low temperatures and the choice of solvents is essential. Even small deviations lead to product mixtures that are hardly separable. However, in our case the reaction outcome was mainly the starting material with some byproducts.

The last method of choice was the Kocheshkov redistribution with $Ph_2SnCl_2$ or $^nBuSnCl_3$. Nevertheless, elevated temperatures and prolonged reaction times did not improve the reaction outcome as the starting materials remained in the end.

As a result, the halogenation attempts on $Ph_2Sn(SiMe_3)_2$ was unsuccessful with various methods known to the literature. Therefore, the investigation of those was not studied further.

## 3.3 Silylation reactions of $RSnCl_3$ with Mg or Li (R= Ph, nBu)

### 3.3.1 Synthesis of $PhSn(SiMe_3)_3$ (4)

In attempts to synthesize the $PhSn(SiMe_3)_3$ (**4**) via Wurtz-type coupling the reaction temperature, solvent mixtures and the type of alkali/earth alkali metal have a big impact to the outcome of the reaction. Therefore, different conditions were tested to establish the best reaction outcome.

The initial reaction was performed with Mg in THF at 0°C, analogously to the procedure for the synthesis of $Ph_2Sn(SiMe_3)_2$, but with adjusted stoichiometry. However, it was found that this type of reaction leads to the formation of $SnCl_2$ and the Grignard reagent PhMgCl (see Scheme 3-4). The formation of $SnCl_2$ was confirmed by X-Ray analysis. The initial formation of the Grignard reagent explains the obtained product mixtures, which are $Ph_2Sn(SiMe_3)_2$, $Ph_3SnSiMe_3$ and $Ph_4Sn$.

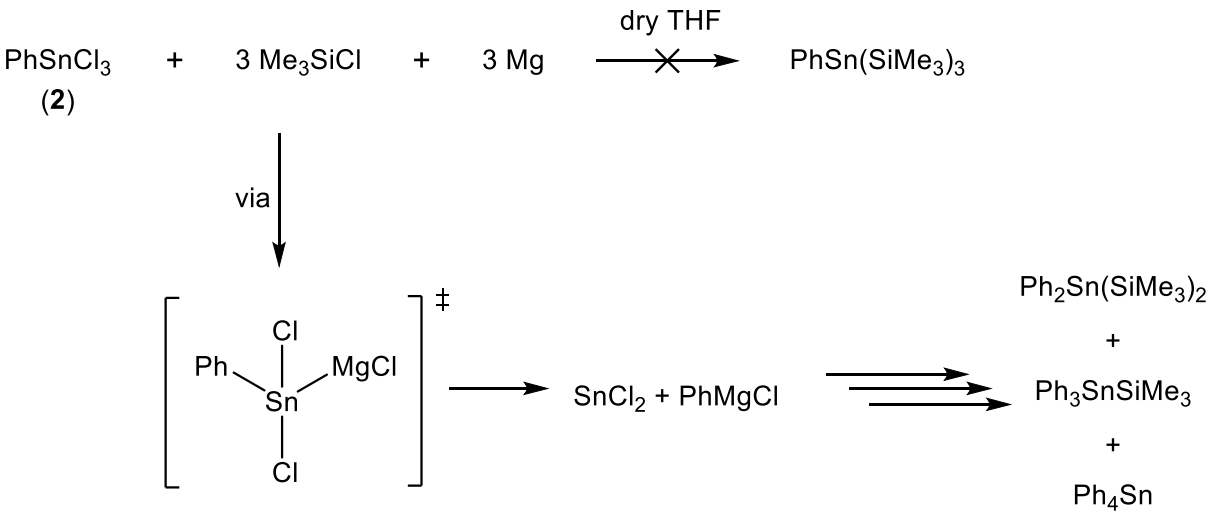


**Scheme 3-4.** Reaction pathway when Mg is used for the synthesis of (**4**)

Consequently, Li was chosen for further reactions (see Scheme 3-5). The reactions with the Li-granulate did not consume all the staring material and the products formed, monitored via $^{119}Sn$ NMR, were mainly $Sn(SiMe_3)_4$ and $Ph_2Sn(SiMe_3)_3$, when performed in THF at -30°C. However, when the same reaction was carried out in $Et_2O$, the conditions proved to be too harsh and numerous by-products were formed in addition to $Sn(SiMe_3)_4$. Thus a solvent mixture of $Et_2O$/THF (7:2) was used and the $^{119}Sn$ NMR showed the formation of $Ph_2Sn(SiMe_3)_2$, $PhSn(SiMe_3)_2$ and $Sn(SiMe_3)_4$ in an approximated ratio of 1:2.6:1.3. These ratios are derived from the relative intensities of the $^{119}Sn$ NMR spectrum.

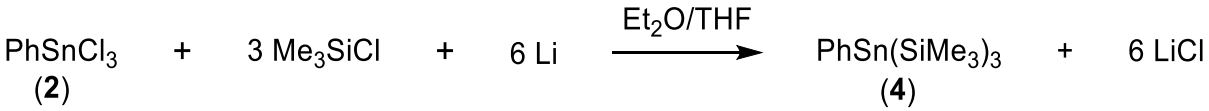


**Scheme 3-5.** Wurtz coupling to synthesize (**4**)

However, switching to the more reactive Li-band, lower temperatures (- 50°C), and maintaining the solvent mixture $Et_2O$/THF in the ratio of 7:2 improved the composition of the products as the peak for $PhSn(SiMe_3)_3$ (- 409 ppm) became more intense. In Figure 3-1 a representative $^{119}Sn$ NMR is shown for the composition of the products. Here the approximated ratio of $Ph_2Sn(SiMe_3)_2$, $PhSn(SiMe_3)_3$ and $Sn(SiMe_3)_4$ is 4.1:7.5:1. This relative ratio is derived from the intensities in the $^{119}Sn$ NMR spectrum. The peaks at – 253 ppm and – 664 ppm are accounted to the literature known compounds $Ph_2Sn(SiMe_3)_2$ and $Sn(SiMe_3)_4$, respectively.[10,53]

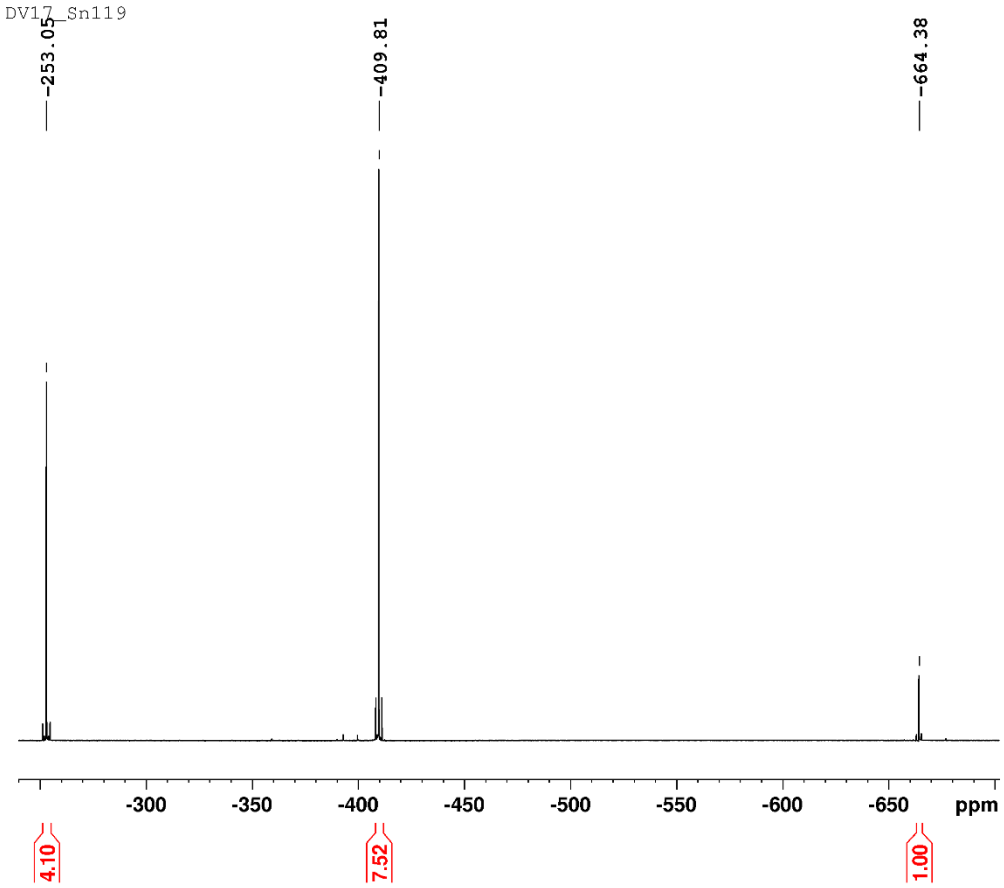


**Figure 3-1.** $^{119}Sn$ NMR of the product mixture

In addition, long reaction times of about 48 hours at room temperature are required till all starting material is consumed. Performing the reaction longer than 48 h did not improve the reaction outcome. As a result, Table 3-1 gives an overview of the conditions under which the Wurtz coupling yields the best product composition so far.

**Table 3-1.** Wurtz coupling conditions for the synthesis of (**4**)

| | |
|---|---|
| **Earth alkali metal** | Li-band |
| **Solvent mixture** | $Et_2O$/THF (7:2) |
| **Reagent addition temperature** | -50°C |
| **Reaction time at room temperature** | 48 h |

Regarding this, the product isolation was performed by inert flash chromatography in dry heptane. This gives well separated spots for the different silylated organotin compounds $Ph_nSn(SiMe_3)_{4-n}$ on the TLC (Thin Layer Chromatography) as shown in Figure 3-2. The spots are detected under UV-light at 350 nm. Thus, the spot with an Rf value of 0.62 is accounted to the $PhSn(SiMe_3)_3$. This is consistent with the Rf value reported for $PhSi(SiMe_3)_3$ in n-hexane, which is 0.74.[75] The higher Rf value for $PhSi(SiMe_3)_3$ can therefore be attributed to the electronegativity difference between silicon and tin and the slightly more polar solvent used (n-hexane more polar than n-heptane).

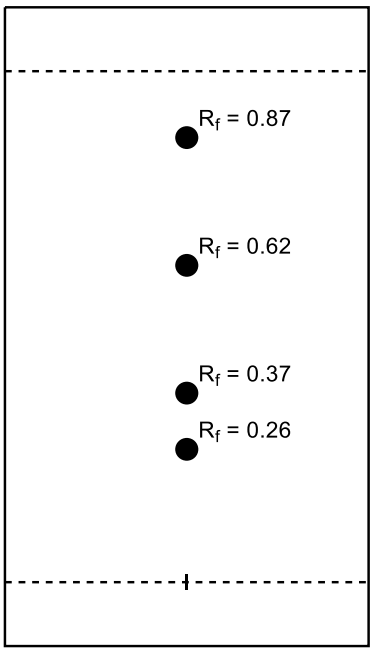


| $R_f$ | Compound |
|---|---|
| 0.87 | $Sn(SiMe_3)_4$ |
| 0.62 | $PhSn(SiMe_3)_3$ |
| *0.37* | $Ph_2Sn(SiMe_3)_2$ |
| 0.26 | $Ph_3SnSiMe_3$ |

**Figure 3-2.** TLC of the product mixture run in heptane

Moreover, we were able to isolate crystals of $Ph_3SnSiMe_3$ suitable for X-Ray analysis. The crystal structure of the colorless shiny plates is shown in Figure 3-3. The Isolation was done by fractionated crystallization in pentane from the reaction mixture.

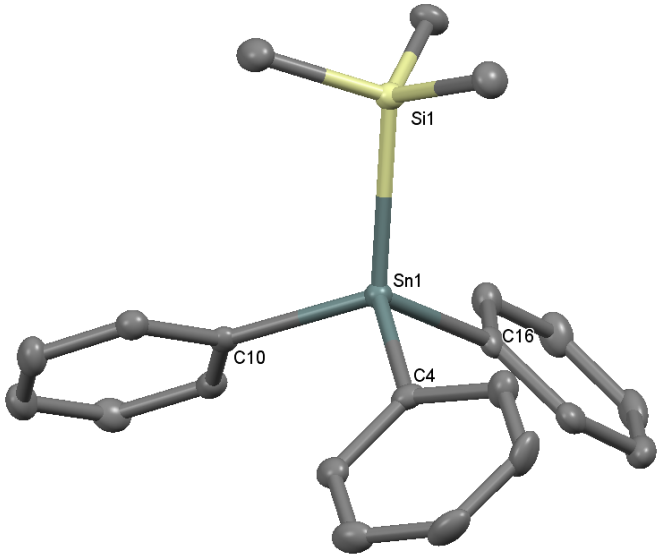


**Figure 3-3.** Crystal structure of $Ph_3SnSiMe_3$ (**5**). H-atoms are omitted for clarity. Selected bond lengths [Å] and angles [°]: Sn1-Si1 2.572(1), Sn1-C4 2.147(4), Sn1-C10 2.155(4), Sn1-C16 2.150(4); Si1-Sn1-C4 11.8(1), Si1-Sn1-C10 112.8(1), Si1-Sn1-C 16.113.5(1), C4-Sn1-C10 106.4(1), C4-Sn1-C16 105.8(1), C10-Sn1-C16 105.9(1).

In Table 3-2 the bond angles of ∢ C-E-C are compared between E = C, Si, Ge and Sn. Here, the trend towards a higher degree of pyramidalization can be observed when descending group 14 within the same product class. This is shown by the decrease of the bond angles when going from E= C (∢ = 331.2°) to E= Sn (∢ = 318.0°).

**Table 3-2.** Comparison of bond angles for $Ph_3ESiMe_3$, E= C, Si, Ge, Sn

| **$Ph_3ESiMe_3$** | **Sum of ∢ C-E-C [°]** | **Reference** |
|---|---|---|
| E = C | 331.2 | (76) |
| E = Si | 326.1 | (77) |
| E = Ge | 323.7 | (78) |
| E = Sn | 318.0 | this work |

Isolation with flash column chromatography run in heptane yielded $PhSn(SiMe_3)_3$ (**4**) as a colorless oil. The characterization was done with TLC in heptane, $^{1}H$, $^{13}C$, $^{29}Si$ and $^{119}Sn$ NMR spectroscopy. Figure 3-4 shows clean product formation in the $^{119}Sn$ NMR and well assignable couplings. The absolute values for the couplings derived from the $^{119}Sn$ spectrum are given in Table 3-3.

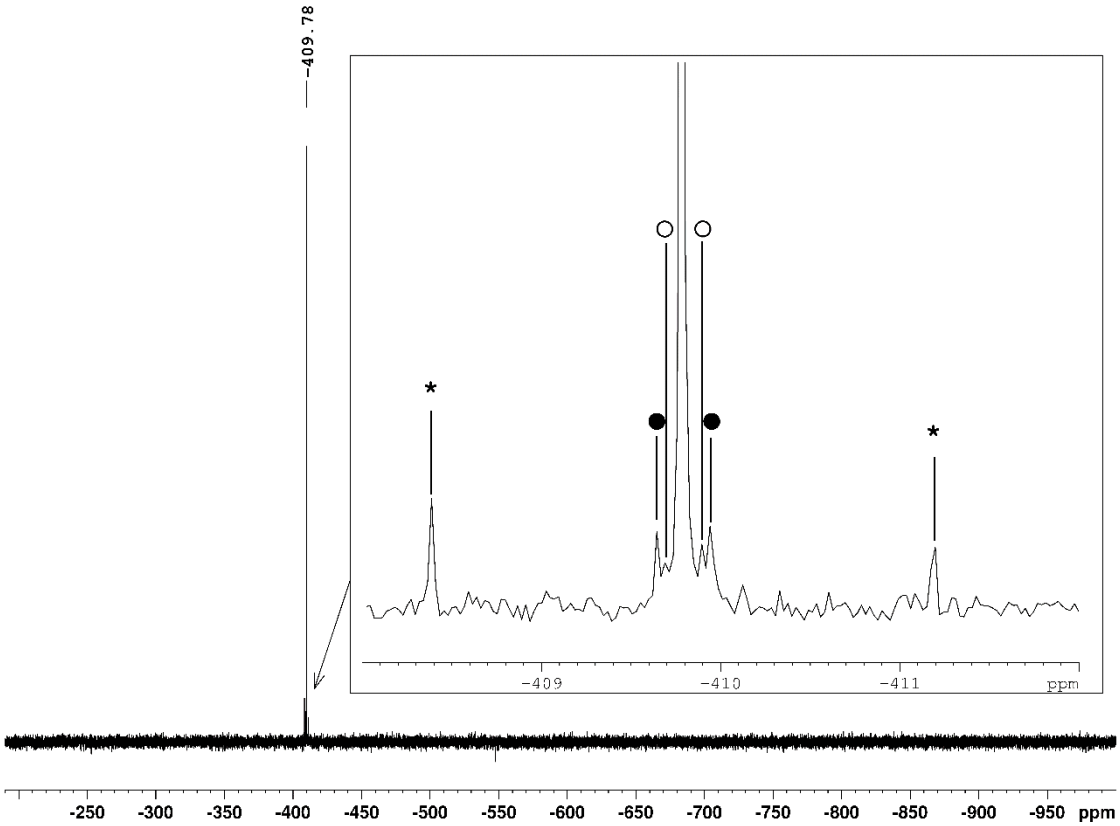


**Figure 3-4.** $^{119}Sn$ NMR of $PhSn(SiMe_3)_3$ (**4**) in $C_6D_6$; marked couplings are assigned in Table 3-3

**Table 3-3.** Assigned couplings from Figure 3-3.

| Label | Coupling constant J [Hz] | Assignment |
|---|---|---|
| ○ | 30.1 | $^{2}J(^{119}Sn\text{-}^{1}H)$ |
| ● | 44.44 | $^{1}J(^{119}Sn\text{-}^{13}C)$ |
| ★ | 418.64 | $^{1}J(^{119}Sn\text{-}^{29}Si)$ |

### 3.3.2 Synthesis of $nBuSn(SiMe_3)_3$ (6)

The preparation of $nBuSn(SiMe_3)_3$ (**6**) was performed in a similar manner to the previously discussed synthesis of $PhSn(SiMe_3)_3$ (see Scheme 3-6). In this case, using a solvent mixture as in (**4**) did not improve the reaction result and, so dry THF was the solvent of choice. In addition, cooling to more than -50°C is not possible as the $^{n}BuSnCl_3$ starts to precipitate. Therefore, the reaction could not be performed at lower temperatures. The reaction time required was similar to that for the phenyl congener, which was about 48 h. After a simple workup, which included washing with pentane and filtration through canula, a black oil was obtained. This was purified by filtration through celite and sublimation to give a colorless oil.

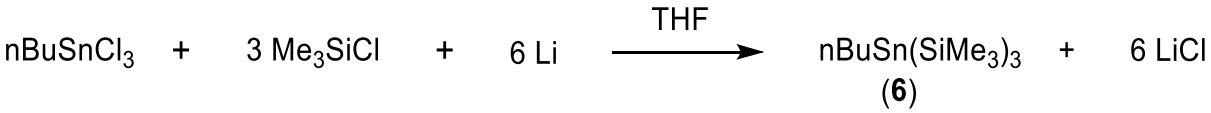


**Scheme 3-6.** Wurtz coupling to synthesize (**6**)

However, here $SnCl_2$ formation is even more dominant than in the case of $PhSnCl_3$, as shown by the fast crystallization of $SnCl_2$ in the NMR samples and X-Ray analysis of the crystals. Also, separate formation of $Sn(SiMe_3)_4$ was observed during the Wurtz-type coupling. Moreover, it turned out that column chromatography was also not suitable for the purification, because $Sn(SiMe_3)_4$ and $nBuSn(SiMe_3)_3$ are inseparable based on TLC experiments. This is even the case if the TCL is run in the nonpolar n-heptane. Therefore, traces of $Sn(SiMe_3)_4$ are still present in the final product mixture, as shown in Figure 3-5. The approximate ratio of $nBuSn(SiMe_3)_3$ : $Sn(SiMe_3)_4$ (18.8 : 1) is derived from the $^{119}Sn$ spectrum. Also, the absolute values for the couplings derived from the $^{119}Sn$ spectrum are given in Table 3-4.

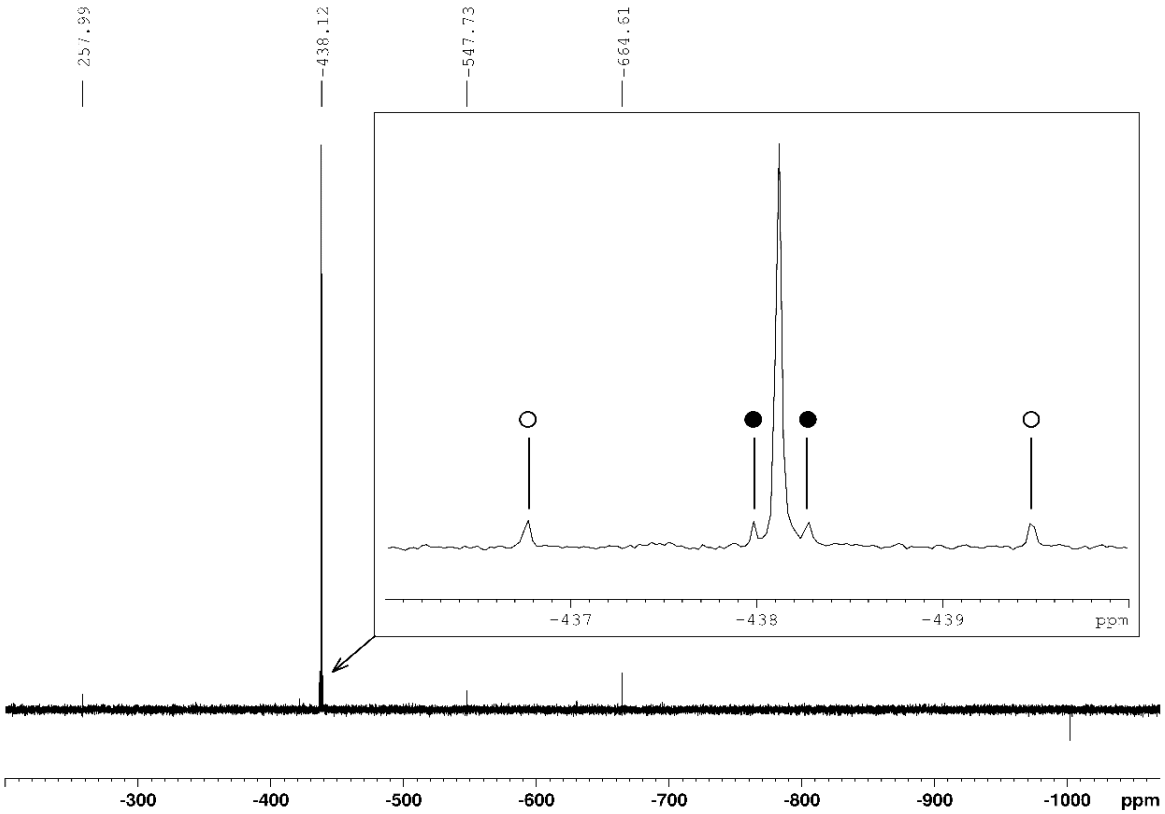


**Figure 3-5.** $^{119}$Sn NMR of nBuSn(SiMe$_3$)$_3$ (**6**) ; couplings are assigned in Table 3-4

**Table 3-4.** Assigned couplings from Figure 3-4.

| Label | Coupling constant J [Hz] | Assignment |
|---|---|---|
| ○ | 405.38 | $^{1}$J($^{119}$Sn-$^{29}$Si) |
| ● | 43.48 | $^{1}$J($^{119}$Sn-$^{13}$C) |

## 3.4 Derivatization of $E(SiMe_3)_4$, E = Si, Ge, Sn

### 3.4.1 Synthesis of $E(SiMe_3)_4$, E = Ge, Sn

Tetrakis(trimethylsilyl)germane and -stannane were synthesized in a fairly similar manner according to literature procedures.[7] The Wurtz coupling (see Scheme 3-8) must be carried out at low temperatures and slow addition of $ECl_4$ (E = Ge, Sn). It was found that the yield of the tin congener was more sensitive to higher temperatures (i.e. -30 °C) and the addition time of $ECl_4$ (E = Ge, Sn). The reason for this is that side reactions preferentially occur at higher temperatures. The product is isolated by sublimation to give a colorless solid in both cases.

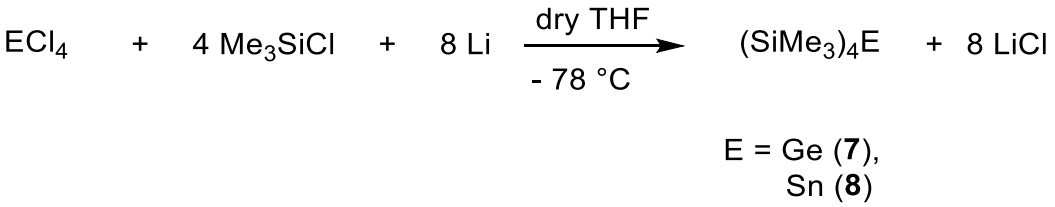


**Scheme 3-7.** Synthesis of $E(SiMe_3)_4$ according to literature[7], E= Ge, Sn

### 3.4.2 Chlorination attempt of $Ge(SiMe_3)_4$ (7)

The first method examined for the preparation of the $(Me_3Si)_3GeCl$ was adapted from the work of Brook et al. in 1986.[13] It is untill now the only published procedure for the synthesis of $(Me_3Si)_3GeCl$.

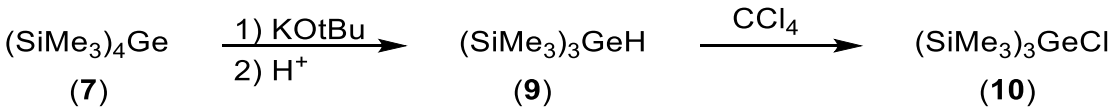


**Scheme 3-8.** Synthetic route for the preparation of $(Me_3Si)_3GeCl$, adapted from ref.[13]

In this work, the initial anion formation was done with KOtBu in DME instead of the originally published procedure using MeLi to generate the anion. The anion was transferred directly into a degassed 5% $H_2SO_4$ solution to form the germanium hydride species. After separation of the layers, the ether phase was dried *in vacuo* to give a colorless oil. Characterization was performed by $^1H$ benchtop NMR.

The tris(trimethylsilyl)germane was then dissolved in $CCl_4$ and allowed to react for 24 h at room temperature. After workup, the yellowish oily residue was characterized by $^1H$ NMR, which also showed the formation of side products. Nevertheless, we were able to isolate crystals, formed when $CCl_4$ was removed *in vacuo* (see Figure 3-6).

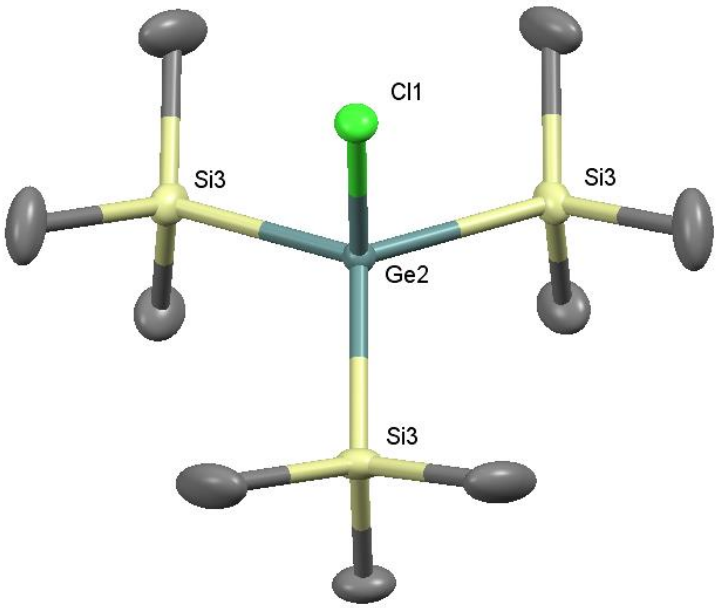


**Figure 3-6.** Crystal structure of $(SiMe_3)_3GeCl$ (**9**). H-atoms are omitted for clarity. Selected bond lengths [Å] and angles [°]: Cl1-Ge2 2.2480(4), Si3-Ge2 2.3855(5); Cl1-Ge2 103.58(2), Si3-Ge2-Si3 114.66(2).

When comparing the structural data of the chlorogermane with the structurally related chlorosilane, an increase in the bond angles (∢ Si-E-Si) from the silane (∑∢ = 339.3°)[79] to the germane (∑∢ = 344.0°) is observed. Here, the bond angles increase from the silane to the germane unit. This can be explained by the slightly larger covalent radius of germanium compared to silicon.

### 3.4.3 Phenylation attempts of $Ge(SiMe_3)_4$ (7)

Here the goal was to synthesize the $PhGe(SiMe_3)_3$ moiety. Starting from the readily available tetrakis(trimethylsilyl)germane, different routes were tested as shown in Scheme 3-9.

In route (I), the anion formed in situ is reacted with 2-bromotoluene in DME. $Fe(acac)_3$ is used to catalyze the cross-coupling. However, in our case, no clear evidence for the formation was found in the $^{29}Si$ spectrum, besides the formation of several unidentified by-products.

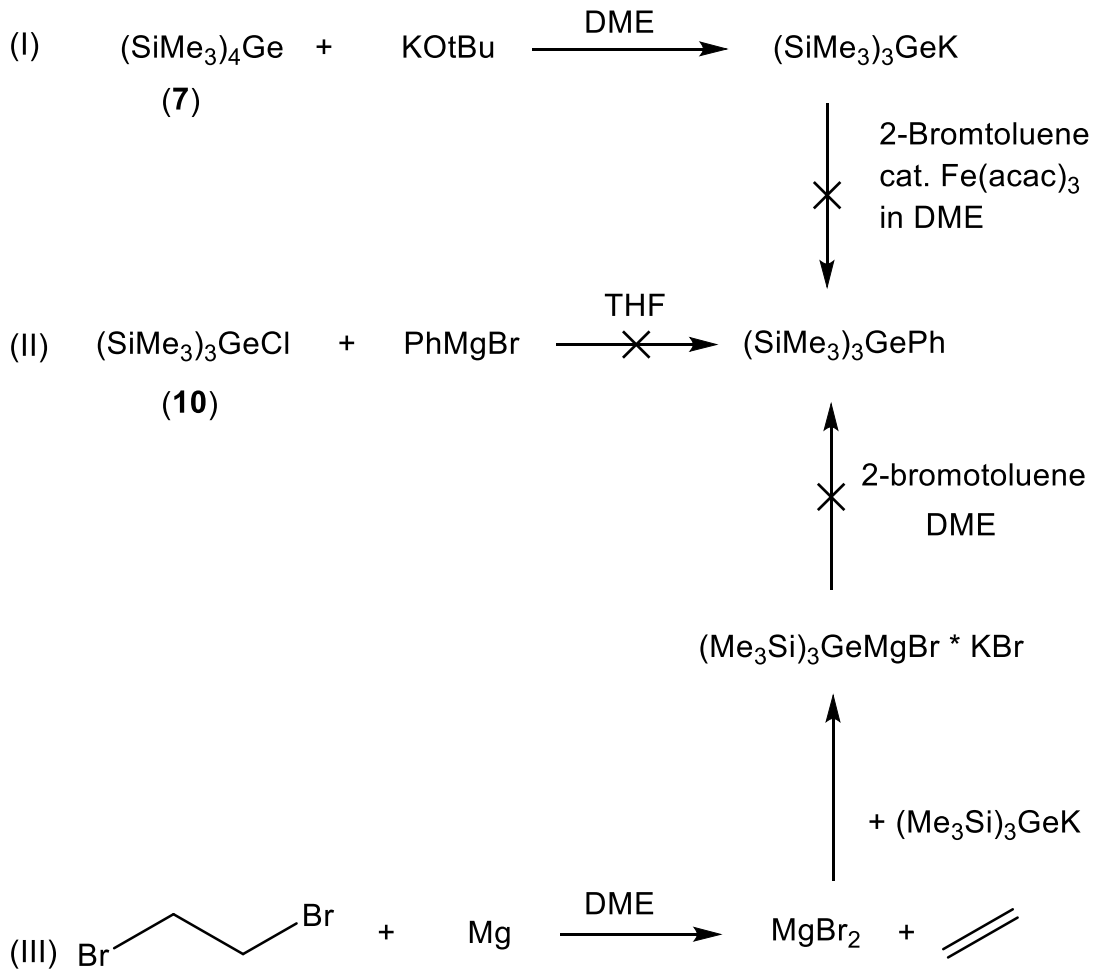


**Scheme 3-9.** Phenylation attempts of $Ge(SiMe)_4$

By path (II) the tris(trimethylsilyl)chlorogermane is reacted with the Grignard reagent PhMgBr formed in situ. The chlorogermane was added slowly at room temperature and no heat evolution was observed. Therefore, the reaction mixture was heated under reflux. However, after workup, the brown residue was characterized via $^{1}H$ NMR and $^{29}Si$ NMR. In the $^{29}Si$ spectrum the major peak is at – 7.09 ppm and a minor one at - 5.8 ppm, which could not be identified.

The last pathway tested, pathway (III), was taken from the literature, where a $Ph_3GeCl$ was quantitatively reacted via Grignard formation with an electrophile E-X (E= alkyl, arly).[80] However, the authors reported that by initial $MgBr_2$ formation and subsequent reaction with the germanium monoanion, the Grignard reagent $R_3GeMgBr$ is formed. Here, it is also accounted that the $MgBr_2$ precipitates immediately when the temperature is lower than 55°C and cannot be redissolved again. Letting the Grignard react with electrophiles leads to the desired organogermane. Nevertheless, in our case, the anion formation was carried out with $KO^tBu$ as the metalating agent and subsequent reaction with 2-bromotoluene led to the formation of by-products. The removal of these by-products was not successful.

Hence, no suitable method for phenylation of $Ge(SiMe_3)_4$ was found within the tested reaction conditions and the idea of phenylation was therefore not pursued longer.

### 3.4.4 Silylation of $E(SiMe_3)_4$ with $(Me_3C)Me_2SiCl$ (E = Si, Ge, Sn)

To provide a larger stabilizing group for subsequent anion formation and to provide the diastereotopic methyl groups in the chiral anion, the *tert*-butyldimethylsilyl group is introduced. Thus, this is done according to the published procedures for the synthesis of the silicon congener.[50,58] Thereby, initial anion formation with $KO^tBu$ is followed by silylation with the silyl chloride. The solvent of choice is toluene, and the reaction is carried out at 0°C. After aqueous work up, a colorless wax was obtained for all three compounds. The product yield is identical, ranging from 79% to 86%. Product characterization was accomplished via $^1H$, $^{13}C$, $^{29}Si$ and $^{119}Sn$ NMR.

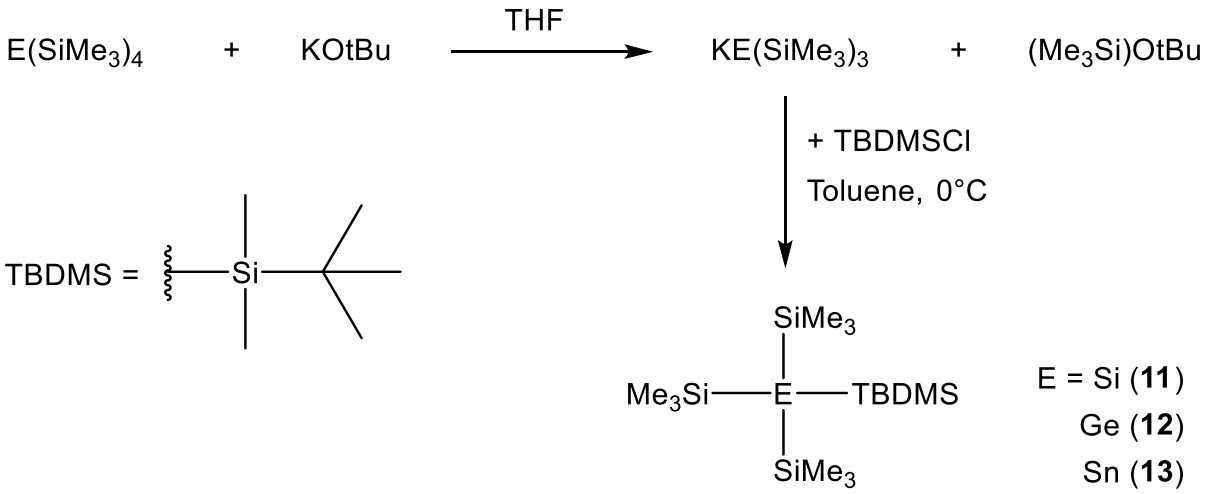


**Scheme 3-10.** Synthesis of $(TBDMS)E(SiMe_3)_3$, E= Si, Ge, Sn

The data for $^{13}C$, $^{29}Si$ and $^{119}Sn$ NMR are summarized in Table 3-5. The coupling constants $^1J(^{13}C\text{-}^{29}Si)$ and $^1J(^{29}Si\text{-}^{13}C)$ for the $-SiMe_3$ groups are all in the expected range of approximately 41-45 Hz.

**Table 3-5.** $^{13}C$, $^{29}Si$ and $^{119}Sn$ NMR data of compounds (**11**), (**12**) and (**13**)

| **$^{13}C$ NMR** | | | | |
|---|---|---|---|---|
| | -Si**Me$_2$**$^t$Bu | -Si-**Me$_3$** | -Si-Me$_2$(**C**Me$_3$)] | -Si-Me$_2$(C**Me$_3$**)] |
| **Compound** | **δ [ppm]** | **δ [ppm]** ***$^1J(^{13}C$-$^{29}Si)$ [Hz]*** | **δ [ppm]** | **δ [ppm]** |
| (**11**)[a] | - 0.95 | 3.45 *44.14* | 18.78 | 28.25 |
| (**12**)[a] | - 0.39 | 3.96 *44.64* | 18.66 | 28.12 |
| (**13**)[b] | -1.55 | 2.58[b] *41.26* | 16.70 | 25.86 |

| **$^{29}Si$ NMR** | | | |
|---|---|---|---|
| | -**Si**-Me$_3$ | -**Si**Me$_2$$^t$Bu | Si-**Si**-Si |
| **Compound** | **δ [ppm]** ***$^1J(^{29}Si$-$^{13}C)$ [Hz]*** | **δ [ppm]** | **δ [ppm]** |
| (**11**)[a] | - 9.71 *44.39* | 4.71 | -138.68 |
| (**12**)[a] | - 5.21 *44.22* | 10.07 | |
| (**13**)[b] | - 10.51[c] *42.84* | 10.35 | |

| **$^{119}Sn$ NMR** | | |
|---|---|---|
| **Compound** | **δ [ppm]**, | **$^1J(^{119}Sn$-$^{13}C)$ [Hz]** |
| (**13**)[b] | - 672.8[d] | 38.88 |

[a] in $CDCl_3$; [b] in $C_6D_6$; [c] Coupling constant: $^1J(^{29}Si$-$^{117/119}Sn)$ = 323.70/338.62 Hz; [d] Coupling constant: $^1J(^{119}Sn$-$^{29}Si)$ = 340.46 Hz.

### 3.4.5 Methylation of $[(Me_3C)Me_2Si]E(SiMe_3)_3$ with $Me_2SO_4$ (E = Si, Ge, Sn)

The next step was the alkylation of (**11**), (**12**) and (**13**) with the strong alkylating agent dimethyl sulfate. This reaction needs to be done with care as $Me_2SO_4$ alkylates the DNA. However, the introduction of the methyl group is essential for the subsequent study of the chiral anions. The procedure for the methylation of the silicon (**11**), germanium (**12**) and the tin compound (**13**) is carried out in a similar manner. Therefore, the anion formation is followed by the reaction with $Me_2SO_4$ in toluene at - 78°C. Slow addition of the anion at cold temperatures is important to avoid heat generation and side reactions. After simple workup the products were isolated all as a colorless waxy solid. Notably, aqueous workup of the tin compound (**16**) also did not lead to decomposition. Product characterization was carried out with $^{1}H$, $^{13}C$, $^{29}Si$ and $^{199}Sn$ NMR spectroscopy.

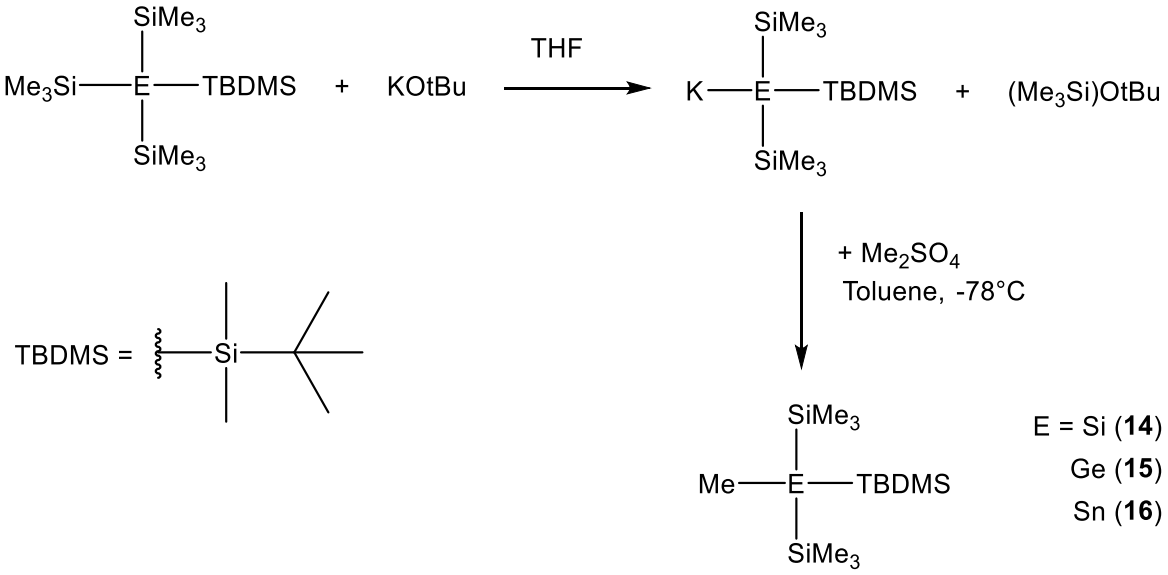


**Scheme 3-11.** Synthesis of $(TBDMS)(Me)E(SiMe_3)_2$ (E= Si, Ge, Sn)

However, distinguishing between the methylated and non-methylated compounds with $^{1}H$ NMR is difficult because the peak for the introduced methyl group overlaps with the peak for the $-SiMe_3$ group. Therefore, $^{13}C$ NMR is the most powerful tool for characterization, since the methyl peak $E-SiMe_3$ for all methylated compounds appears in the high field of the $^{13}C$-NMR at around -12 ppm (E = Si, Ge) and - 23.70 ppm (E = Sn). Moreover, the Si-**Si**-Si in (**14**) is shifted to lower field compared to the nonmethylated species (**11**) in the $^{29}Si$ NMR. The same is true for (**16**), where the $^{119}Sn$ peak is also shifted downfield compared to (**13**). The data for $^{13}C$, $^{29}Si$ and $^{119}Sn$ NMR are summarized in Table 3-6.

**Table 3-6.** $^{13}C$, $^{29}Si$ and $^{119}Sn$ NMR data of compounds (**14**), (**15**) and (**16**)

| **$^{13}C$ NMR** | | | | | |
|---|---|---|---|---|---|
| | -Si**Me$_2$**$^t$Bu | -Si-**Me$_3$** | -(**C**Me$_3$)] | -(C**Me$_3$**)] | -E-**Me** |
| **Compound** | **δ [ppm]** | **δ [ppm]** <br> ***$^1J(^{13}C$-$^{29}Si)$ [Hz]*** | **δ [ppm]** | **δ [ppm]** | **δ [ppm]** |
| (**14**)[a] | - 3.34 | 0.76 <br> *44.50* | 18.51 | 27.83 | -11.52 |
| (**15**)[a] | - 2.76 | 1.37 <br> *44.64* | 18.56 | 27.65 | -12.10 |
| (**16**)[b] | -3.32 | 0.72[b] <br> *43.49* | 16.72 | 25.73 | -23.70 |

| **$^{29}Si$ NMR** | | | |
|---|---|---|---|
| | -**Si**-Me$_3$ | -**Si**Me$_2$$^t$Bu | Si-**Si**-Si |
| **Compound** | **δ [ppm]** <br> ***$^1J(^{29}Si$-$^{13}C)$ [Hz]*** | **δ [ppm]** | **δ [ppm]** |
| (**14**)[a] | - 12.13 | 0.68 | - 89.20 |
| (**15**)[a] | - 5.22 <br> *44.82* | 10.07 | |
| (**16**)[b] | - 10.43[c] <br> *43.60* | 8.15 | |

| **$^{119}Sn$ NMR** | | |
|---|---|---|
| **Compound** | **δ [ppm]** | **$^1J(^{119}Sn$-$^{13}C)$ [Hz]** |
| (**16**)[b] | - 463.3 | 45.6 |

[a] in $CDCl_3$; [b] in $C_6D_6$; [c] Coupling constant: $^1J(^{29}Si$-$^{117/119}Sn)$ = 396.3/415.3 Hz;

[d] Coupling constant: $^1J(^{119}Sn$-$^{29}Si)$ = 414.8 Hz.

## 3.5 Anion formation

### 3.5.1 Formation of $(SiMe_2{}^tBu)(SiMe_3)_2EK$ * 18cr6 (E = Si, Ge, Sn)

The anions of (**11**), (**12**) and (**13**) were prepared identical to the procedures already described for $(Me_3Si)_3SnM$ anions.[53] The anion is prepared with KOtBu as metalating agent and 18cr6 as a host agent for the potassium cation.[81] Crystallization of the anions was achieved from diethyl ether as solvent. From the initial reaction mixtures, the solvent was evaporated until incipient crystallization at room temperature, followed by storage at -35°C to complete the crystallization. Product characterization was carried out via $^1H$, $^{13}C$, and $^{29}Si$ NMR spectroscopy. The stannide was additionally characterized with $^{119}Sn$ NMR. Also, crystals for all three compounds were found suitable for X-Ray analysis.

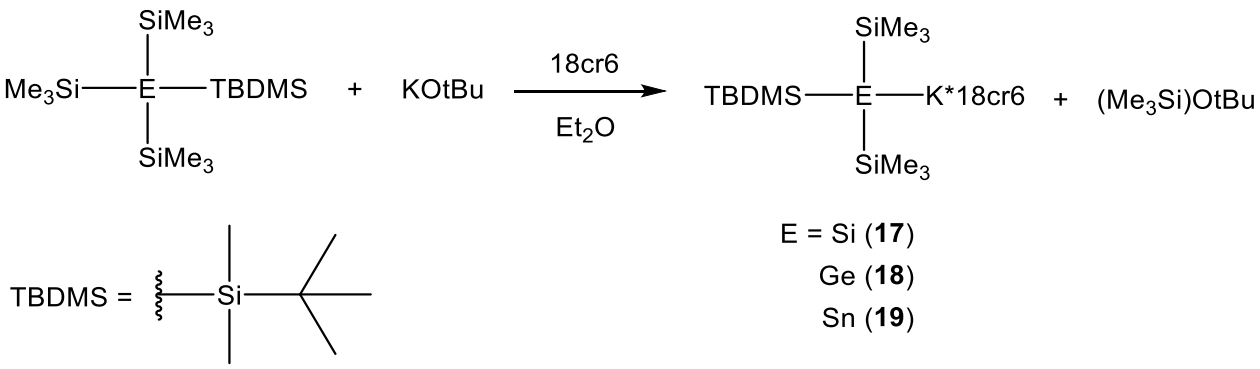


**Scheme 3-12.** Route of preparation for anions (**17**), (**18**) and (**19**)

In Table 3-7. the data for $^{13}C$, $^{29}Si$ and $^{119}Sn$ NMR are summarized. When comparing the starting materials (**11-13**) with their analogous anionic compounds (**17-19**), the E-$(SiMe_3)_3$ shift in $^1H$ and $^{13}C$ NMR is generally observed at a lower field. In the case of E = silicon and germanium, the $^{29}Si$ shift for $(SiMe_3)_3$ in (**17,18**) is observed at a higher field compared to the starting material (**11**, **12**). This is also the true for the Si-Si-Si shift of the central atom in (**17**), where the shift is found at -197.28 ppm compared to (**11**) (-138.68 ppm). This is due to the negative charge at the central atom, which is why a higher shielding is observed. In contrast, the anionic tin compound (**19**) is shifted to the higher field in the $^{29}Si$ for $(SiMe_3)_3$ compared to (**13**). However, the $^{119}Sn$ shift for (**19**) is observed at high field at -904.4 ppm compared to -672.8 ppm for (**13**).

**Table 3-7.** $^{13}C$, $^{29}Si$ and $^{119}Sn$ NMR data of compounds (**17**), (**18**) and (**19**)

| **$^{13}C$ NMR** | | | | |
|---|---|---|---|---|
| | -Si**Me$_2$**$^t$Bu | -Si-**Me$_3$** | -(**C**Me$_3$)] | -(C**Me$_3$**)] |
| **Compound** | **δ [ppm]** | **δ [ppm]** | **δ [ppm]** | **δ [ppm]** |
| (**17**)[a] | 2.63 | 8.36 | 19.28 | 29.44 |
| (**18**)[a] | 3.05 | 8.63 | 19.35 | 29.39 |
| (**19**)[a] | 3.61 | 8.88 | 18.84 | 29.23 |

| **$^{29}Si$ NMR** | | | |
|---|---|---|---|
| | -**Si**-Me$_3$ | -**Si**Me$_2$$^t$Bu | Si-**Si**-Si |
| **Compound** | **δ [ppm]** | **δ [ppm]** | **δ [ppm]** |
| (**17**)[a] | - 4.54 | 10.07 | - 197.28 |
| (**18**)[a] | - 3.72 | 12.01 | |
| (**19**)[a] | - 13.44 | 7.28 | |

| **$^{119}Sn$ NMR** | |
|---|---|
| **Compound** | **δ [ppm]** |
| (**19**)[a] | - 904.4 |

[a] in $C_6D_6$.

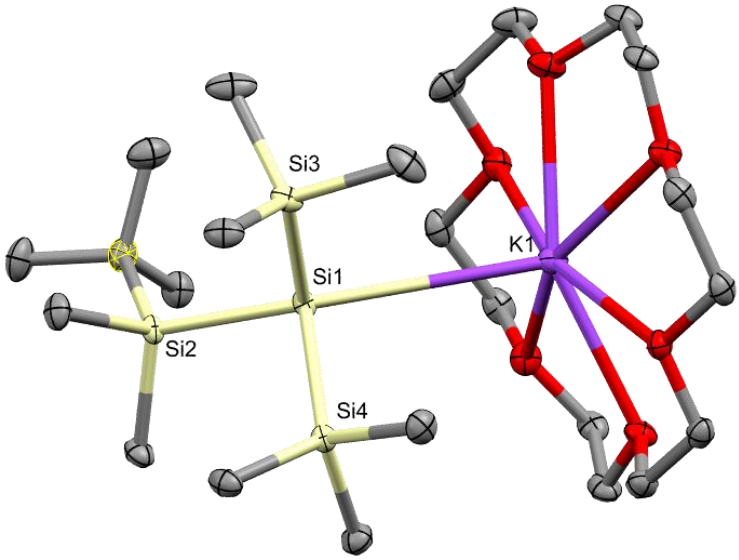


**Figure 3-7.** Crystal structure of (**17**). H-atoms are omitted for clarity. Selected bond lengths [Å] and angles [°]: Si1-K1 3.7031(7), Si1-Si2 2.3504(7), Si1-Si3 2.3434(7), Si1-Si4 2.3423(6); Si2-Si1-Si4 98.47(2), Si2-Si1-Si3 103.87(2), Si4-Si1-Si3 98.56(2).

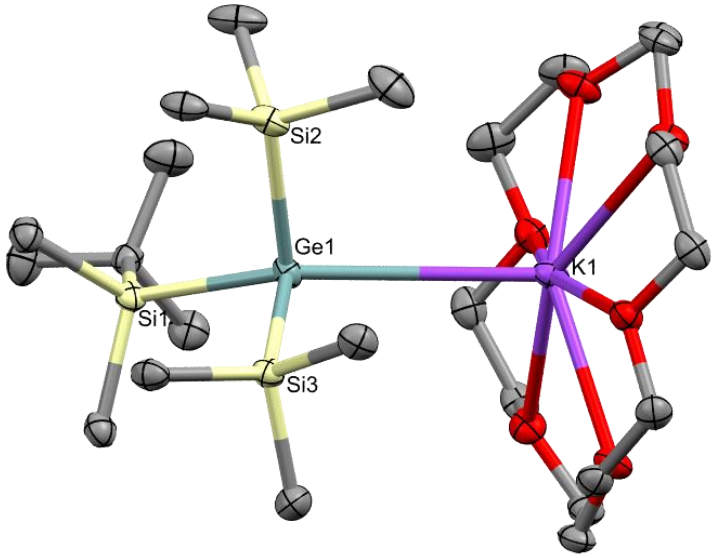


**Figure 3-8.** Crystal structure of (**18**). H-atoms are omitted for clarity. Selected bond lengths [Å] and angles [°]: Ge1-K1 3.6674(8), Ge1-Si1 2.3944(8), Ge1-Si2 2.3956(9), Ge1-Si3 2.3884(9); Si1-Ge1-Si2 96.81(2), Si1-Ge1-Si3 96.76(2), Si2-Ge1-Si3 97.54(3).

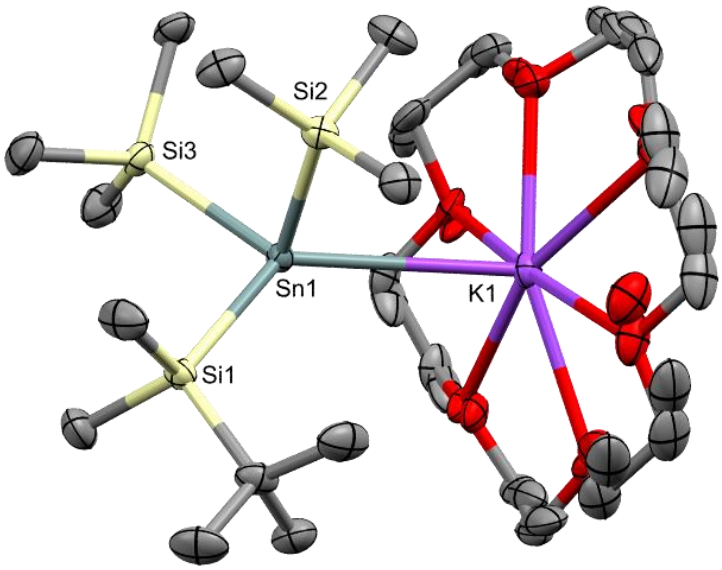


**Figure 3-9.** Crystal structure of (**19**). H-atoms are omitted for clarity. Selected bond lengths [Å] and angles [°]: Sn1-K1 3.7084(7), Sn1-Si1 2.6007(7), Sn1-Si2 2.5992(7), Sn1-Si3 2.6102(8); Si1-Sn1-Si2 98.11(2), Si1-Sn1-Si3 98.02(2) Si3-Sn1-Si2 94.05(2).

The structure of the compounds (**17**)-(**19**) were studied with X-Ray diffractometry. They all crystallize in the monoclinic space group P2(1). The bond distances between E-K are somewhat around 3.70 Å. The E-Si distances increase slightly when going from the silicon to the tin compound. Nevertheless, all structures show a pronounced pyramidalization (∑ of ∢ Si-E-Si < 301°), since the Si-E-Si angles are much smaller than it would be the case for an ideal tetrahedron (∑ of ∢ Si-E-Si = 328.5°). The trend that the pyramidalization within the same compound class increases, while going down within group 14, also continues

In Table 3-8 the crystal structures of the studied anions and similar anions known in the literature are compared. In all cases, the counterion is potassium, coordinated to a crown ether (i.e. 18cr6) unit. It is shown that when moving from a sterically less demanding group such as -$SiMe_3$ to a more sterically hindered group such as -$SiMe_2{}^tBu$, the degree of pyramidalization increases. This is observed for both, the silicon and the germanium congener. Even (**17**) * 18cr6 shows higher pyramidalization than $(Me_3Si)_3GeK$ * 18cr6. However, this is not case for the tin compounds, where the purely trimethylsilyl substituted structure shows the highest degree of pyramidalization (∑ of ∢ Si-E-Si = 289.9°).

Furthermore, the E-M bond distances in (**17-19**) are elongated when compared to the $(Me_3Si)_3EK$ * 18cr6 compounds. Also, the average E-Si bond lengths do not change drastically when -$SiMe_3$ or -$SiMe_2{}^tBu$ are present as substituents.

**Table 3-8.** Comparison of relevant bond distances and angles of (**17**), (**18**), (**19**) and similar compounds from the literature

| Compound | ∑ of ∢ Si-E-Si [°] | E – M [Å] | mean E-Si [Å] | Ref. |
|---|---|---|---|---|
| **17** * 18cr6 | 300.9 | 3.70 | 2.35 | |
| **18** * 18cr6 | 297.4 | 3.67 | 2.39 | |
| **19** * 18cr6 | 290.2 | 3.71 | 2.60 | |
| $(Me_3Si)_3SiK$ * 18cr6 | 306.0 | 3.45 | 2.35 | (52) |
| $(Me_3Si)_3GeK$ * 18cr6 | 302.6 | 3.40 | 2.38 | (61) |
| $(Me_3Si)_3SnK$ * 18cr6 | 289.8 | 3.67 | 2.59 | (82) |

### 3.5.2 Formation of Me(SiMe$_2$$^t$Bu)(SiMe$_3$)EK * 18cr6 (E = Si, Ge, Sn)

To synthesize the chiral anions (**20-22**) the corresponding starting materials (**14-16**) were readily metalated with KOtBu in $Et_2O$. Again, 18cr6 was used as a host for the potassium cation to stabilize the structure. The anions were studied in means of $^1$H, $^{13}$C and $^{29}$Si NMR spectroscopy. The stannide was additionally characterized with $^{119}$Sn NMR spectroscopy. Suitable crystals for X-Ray analysis were obtained by recrystallization in $Et_2O$ at - 35°C.

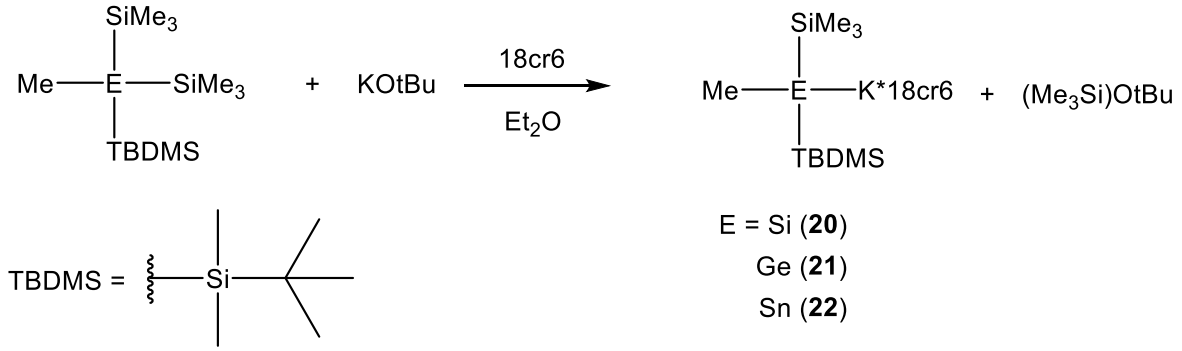


**Scheme 3-13.** Route of preparation for anions (**20**), (**21**) and (**22**)

In particular, the $^1$H and $^{13}$C NMR spectra provide exciting insights into the chiral anions. Here, the two diastereotropic methyl groups of the -SiMe$_2$$^t$Bu show two different signals in the $^1$H and $^{13}$C NMR at room temperature. The shifts for the diastereotropic methyl groups are given in Table 3-9.

**Table 3-9.** $^1$H and $^{13}$C NMR data for the diastereotropic methyl groups of -SiMe$_2$$^t$Bu in the chiral anions (**20-22**); Measured in $C_6D_6$.

| Compound | $^1$H NMR | | $^{13}$C NMR |
|---|---|---|---|
| | δ [ppm] | v [Hz] | δ [ppm] |
| (**20**) | 0.563/0.676 | 225/270 | - 0.85/- 1.71 |
| (**21**) | 0.041/0.097 | 16/39 | 2.04/2.05 |
| (**22**) | 0.578/0.723 | 231/289 | 0.06/1.03 |

Although a detailed temperature dependent NMR spectroscopic study of the chiral anions could not be performed due to problems with the NMR spectrometers, eq. (1) allows a crude estimation of the inversion barrier. Equation (1) is an approximation

based on the peak separation $\delta\upsilon\ [Hz]$ of the diastereotopic methyl groups in absence of exchange processes and the experimentally determined coalescence temperature. As only spectra at 25°C are experimentally available, the actual coalescence temperature $T_c$ is underestimated in all cases, but following eq. (1) amount to at least 62 kJ/mol for E = Si ($\delta\upsilon = 45\ Hz$), 63 kJ/mol for E = Ge ($\delta\upsilon = 23\ Hz$), and 61 kJ/mol for E = Sn ($\delta\upsilon = 58\ Hz$). Nevertheless, the absence of line broadening in $^{1}H$ and $^{13}C$ spectra of the tin homologous (**22**) suggests a much higher barrier.

$$\Delta G^{\ddagger} = 19.13 T_c \left(9.97 + log \frac{T_c}{\delta\upsilon}\right) \quad [Jmol^{-1}] \qquad (1)$$

The following figures (Figure 3-10 and -11) show the molecular structures obtained from X-Ray analysis of the compounds (**20**) and (**21**).

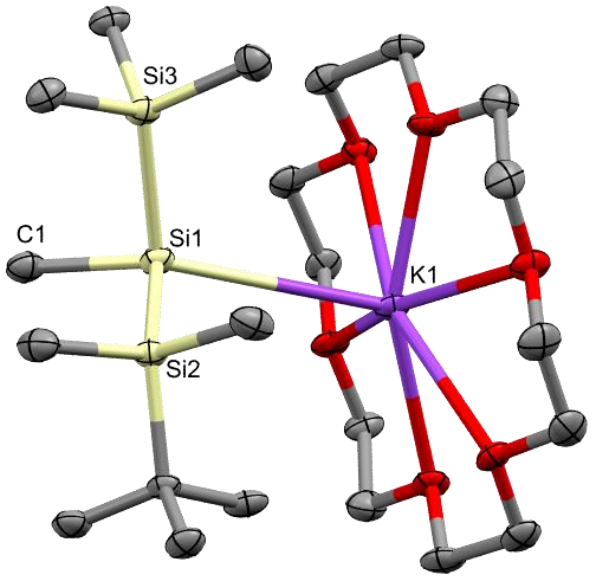


**Figure 3-10.** Crystal Structure of (**20**). H-atoms are omitted for clarity. Selected bond lengths [Å] and angles [°]: Si1-K1 3.667(2), Si1-Si2 2.347(2), Si1-Si3 2.342(2), Si1-C1 1.953(4); C1-Si1-Si2 101.3(2), C1-Si1-Si3 95.5(2), Si2-Si1-Si3 98.16(7).

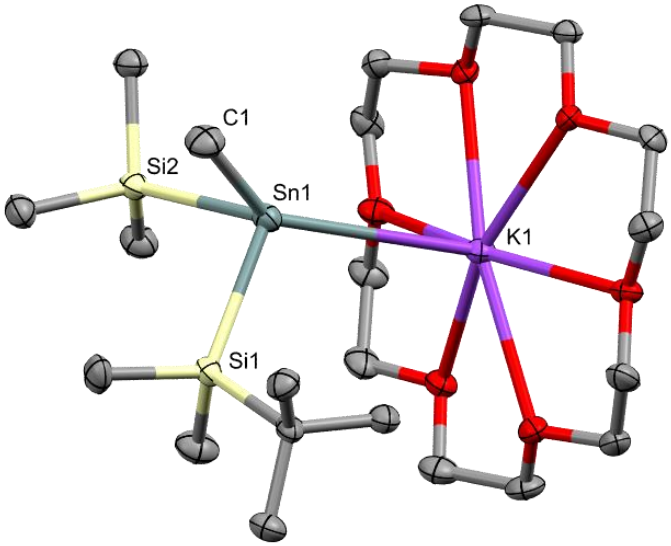


**Figure 3-11.** Crystal structure of (**22**). H-atoms are omitted for clarity. Selected bond lengths [Å] and angles [°]: Sn1-K1 3.741(2), Sn1-Si1 2.616(2), Sn1-Si2 2.608(2), Sn1-C1 2.229(6); Si1-Sn1-C1 96.2(2), Si1-Sn1-Si2 94.51(6), C1-Sn1-Si2 91.6(2).

The structures of the racemic mixtures of the chiral anionic compounds (**21-22**) were studied with X-Ray diffractometry. They all crystallize in the triclinic space group P-1. The bond distances between E-K are somewhat around 3.70 Å. The E-Si distances increase slightly when going from the silicon to the tin compound. Nevertheless, all structures show a high degree of pyramidalization (∑ of ∢ Si-E-R < 98.5°), since the Si-E-R (R = C, Si) angles are much smaller than it would be the case for an ideal tetrahedron (∑ of ∢ Si-E-R = 328.5°). The trend for the tin congener to have a higher degree of pyramidalization within the same compound class also holds here.

**Table 3-10.** Comparison of structural data between (**20**) and (**22**).

| Compound | ∑ of ∢ Si-E-R (R= C, Si) [°] | E – M [Å] | E – Si [Å] | E – $CH_3$ [Å] |
|---|---|---|---|---|
| **20** * 18cr6 | 98.5 | 3.67 | 2.34 | 1.95 |
| **22** * 18cr6 | 94.1 | 3.74 | 2.61 | 2.23 |

The following figures (Figure 3-12 to 3-15) show the $^{1}H$ and $^{13}C$ NMR spectra of the diastereotropic methyl groups measured on crystals (**20**) and (**21**).

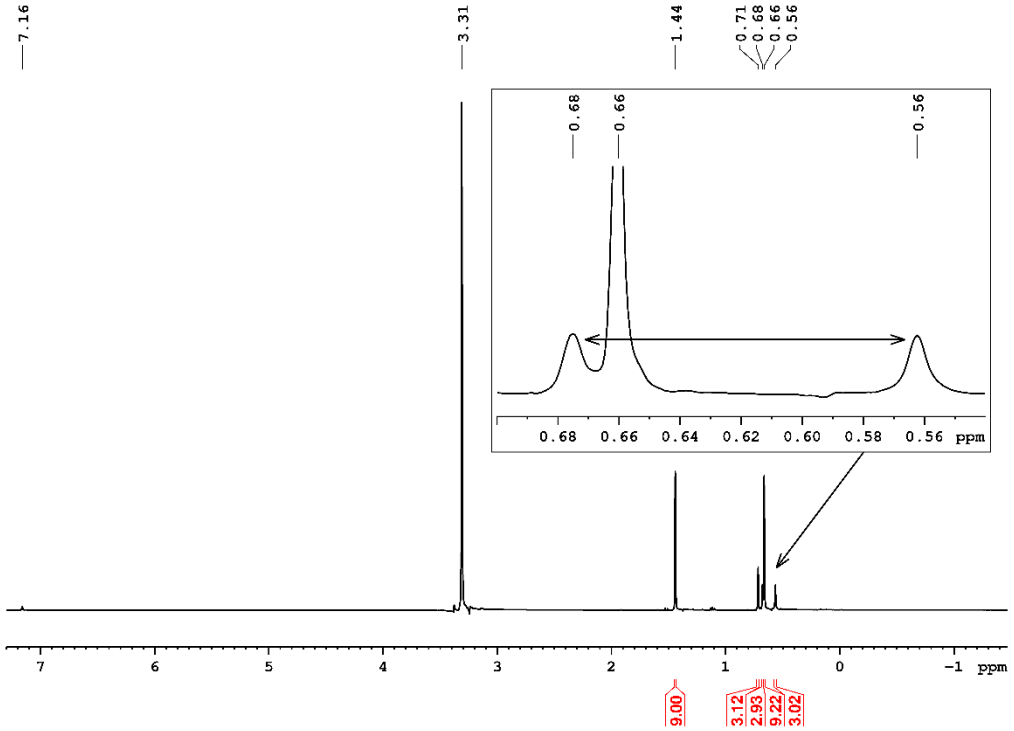


**Figure 3-12.** $^{1}$H NMR of (**20**) showing the diastereotropic methyl groups from -SiMe$_2$$^{t}$Bu

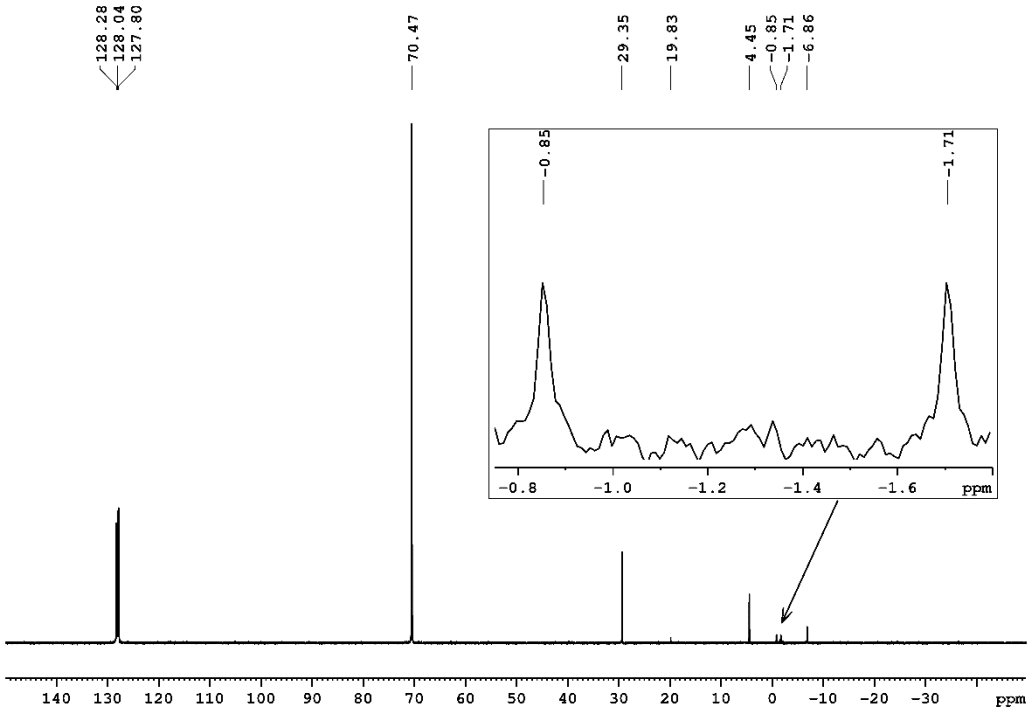


**Figure 3-13.** $^{13}$C NMR of (**20**) showing the diastereotropic methyl groups from -SiMe$_2$$^{t}$Bu

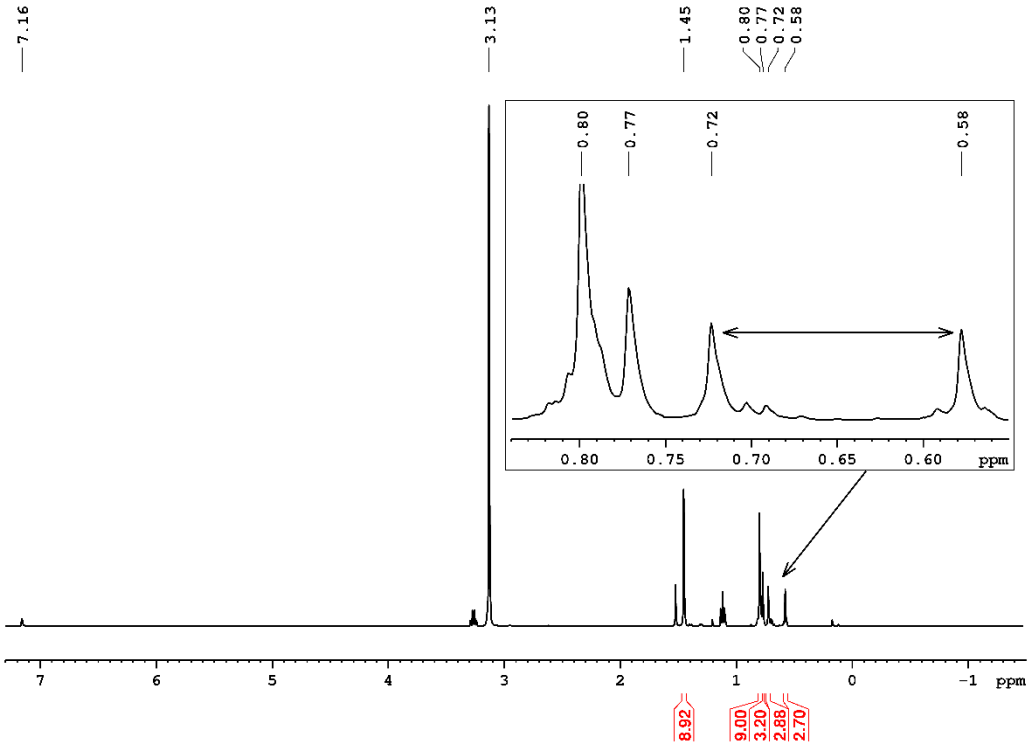


**Figure 3-14.** $^{1}$H NMR of (**22**) showing the diastereotropic methyl groups from -SiMe$_2$$^{t}$Bu; non assigned peaks are solvent peaks (i.e. Et$_2$O, acetone)

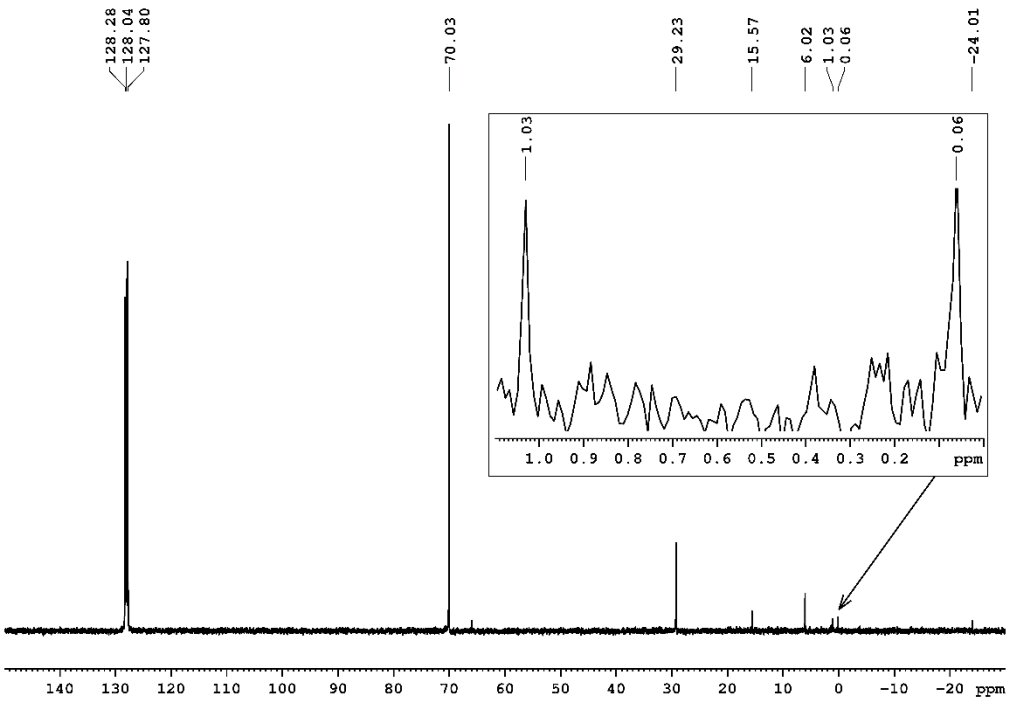


**Figure 3-15.** $^{13}$C NMR of (**22**) showing the diastereotropic methyl groups from -SiMe$_2$$^{t}$Bu

# 4 Conclusion & Outlook

The aim of this thesis was to investigate novel silyl substituted heavy Group 14 anions. To this end, we started from readily available starting materials such as the tetrakis(trimethylsilyl)-group 14 compounds (silicon, germanium and tin), where we introduced a *tert*-butyldimethylsilyl group by initial metalation with potassium *tert*-butoxide of the starting material. Further, a methyl group was introduced by replacing a trimethylsilyl group using, again potasisum *tert*-butoxide as initial metalating agent, followed by subsequent reaction with dimethyl sulfate. In addition, the tris(trimethylsilyl)phenylstannane could be prepared via Wurtz-type coupling. The compounds were characterized by multinuclear NMR ($^{1}$H, $^{13}$C, $^{29}$Si, $^{119}$Sn) spectroscopy.

The anions of the corresponding ($^{t}$BuMe$_2$Si)(Me$_3$Si)$_3$E and Me($^{t}$BuMe$_2$Si)(Me$_3$Si)$_2$E (E = Si, Ge, Sn) compounds were prepared in Et$_2$O with potassium *tert*-butoxide and 18crown6. The structures were studied by multinuclear NMR spectroscopy and X-Ray crystallography. It was interesting to study the NMR-shift change upon transition to the anionic form. In addition, the two diastereotropic methyl groups of Me($^{t}$Bu**Me$_2$**Si)(Me$_3$Si)EK*18cr6 showed two distinguishable peaks in the $^{1}$H and $^{13}$C NMR. Therefore, we were able to estimate a lower limit for the inversion barrier for these compounds. The crystal structures of the anions revealed details about the nature of the metal interaction, the degree of pyramidalization and the influence of introducing a sterically more hindered silyl group.

To determine the inversion barriers of the chiral anions, temperature dependent $^{1}$H NMR studies should be performed to obtain the rate constants. Further, the reaction of the anions towards electrophiles should be studied and compared with already known anions of group 14.

# 5 Experimental

## 5.1 General

Unless otherwise stated, all reactions were performed under $N_2$-atmosphere using standard Schlenk and glovebox techniques. Standard laboratory equipment at the Institute of Inorganic Chemistry, Technical University of Graz, was used. Chemicals and solvents were commercially available and used as supplied. Tetrakis(trimethylsilyl)silane was obtained as found in the laboratory. Dry solvents were purified using a Solvent Drying System, Innovative Technology Inc. (Molecular sieve pore size 4 Å).

### 5.1.1 NMR Spectroscopy

$^{1}H$, $^{13}C$, $^{29}Si$ and $^{119}Sn$ NMR spectra have been recorded with a Pulse 4$^{th}$ generation RS$^2$D 400 MHz spectrometer, with included Cameleon4, from RS$^2$D at 25 °C. The NMR frequencies and standards for the different nuclei are listed below (Table 5-1). To shorten the measurement time, {$^{1}H$} decoupled $^{13}C$ NMR and $^{29}Si$ (INEPT)[83] were used. Chemical shifts are given in ppm and are denotated as singlet (s), broad singlet (bs), doublet (d), triplet (t), multiplet (m) and are referred to the residual solvent peak.

**Table 5-1.** NMR-frequencies and standards for the different nuclei

| Nuclei | NMR- Frequency [MHz] | Standard |
|---|---|---|
| $^{1}H$ | 399.84 | $Me_4Si$ |
| $^{13}C$ | 100.54 | $Me_4Si$ |
| $^{29}Si$ | 79.43 | $Me_4Si$ |
| $^{119}Sn$ | 149.03 | $Me_4Sn$ |

### 5.1.2 X-Ray - crystallography

All suitable crystals were covered with a layer of silicone oil. A single crystal was selected, mounted on a glass rod with a copper pin, and placed in the cold $N_2$ stream of an Oxford Cryosystems cryometer (T=100 K). XRD data were obtained with a Bruker APEX II diffractometer using Mo Kα radiation (λ=0.71073 Å) from an IμS microsource and a CCD area detector. Empirical absorption corrections were performed using

SADABS or TWINABS.[84–86] The structures were analyzed using either direct methods or the Patterson option in SHELXS and solved by the full-matrix least-squares Methods in SHELXL to refine them.[84,87,88] The space group assignments and structure solutions were evaluated using PLATON.[84,89–91] All non-hydrogen atoms were refined anisotropically. All hydrogen atoms were placed in calculated positions corresponding to standard bond lengths, angles and angles using riding models. The Program Mercury was used for all crystal structure representations. The corresponding data of the measured crystals is listed in the Appendix.

## 5.2 Synthesis of literature known compounds

### 5.2.1 Dichlorodiphenylstannane (1)[67]

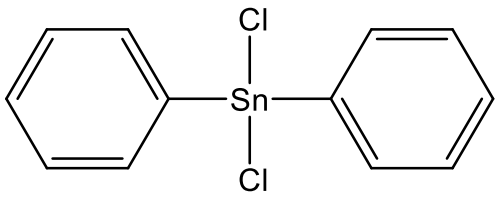


Chemical Formula: $C_{12}H_{10}Cl_2Sn$
Molecular Weight: 343,82

**Figure 5-1.** Structure of (**1**)

A 250 mL flask was charged with 40.48 g (105 mmol ,2 eq.) of $Ph_3SnCl$ and 6 mL (59.9 mmol, 1 eq.) of $SnCl_4$. The reaction mixture was heated up to 40°C to give a brownish palp and let stirring overnight. After 16h, the reaction mixture was gradually heated to 140°C over a period of 1h to give a brown oil. The temperature was maintained at 140°C for 2h and then slowly cooled to room temperature overnight. Recrystallization in n-hexane gave 45.7 g (85%) of a colorless, shiny solid.

$^{1}H$, $^{13}C$, $^{29}Si$ and $^{119}Sn$ NMR as reported in the literature.[92]

### 5.2.2 Trichlorophenylstannane (2)[68]

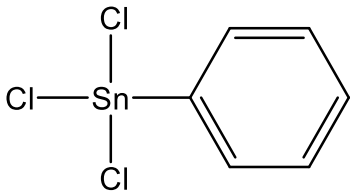


Chemical Formula: $C_6H_5Cl_3Sn$
Molecular Weight: 302,17

**Figure 5-2.** Structure of (**2**)

A 250 mL Schlenk flask was charged with 25.26 g (65.5 mmol, 1 eq.) of $Ph_3SnCl$ and 7.6 mL (65.9 mmol, 1.01 eq.) of $SnCl_4$. The resulting brownish palp was stirred for 20 minutes before an additional 7.6 mL (65.93 mmol, 1.01 eq.) of $SnCl_4$ was added. The brown reaction mixture was let stirring overnight. The reaction mixture was heated up to 80°C and stirred for 2 days to obtain 48.97g (82 %) of a dark brown liquid. The Product was kept at a constant 60°C to avoid disproportion and used without further purification steps.

$^{1}H$, $^{13}C$, $^{29}Si$ and $^{119}Sn$ NMR as reported in the literature.[92]

### 5.2.3 Diphenylbis(trimethylsilyl)stannane (3)[10]

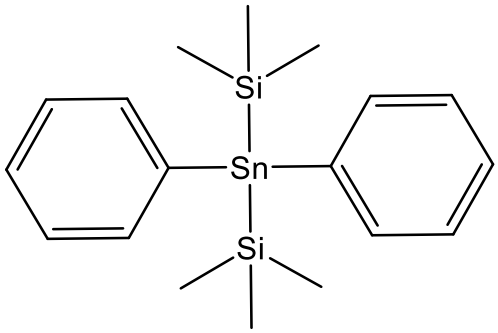


Chemical Formula: $C_{18}H_{28}Si_2Sn$
Molecular Weight: 419,30

**Figure 5-3.** Structure of (**3**)

4.3 mL of $Me_3SiCl$ (33.8 mmol, 2.3 eq) and 0.878 g (36.1 mmol, 2.5 eq) of Mg-turnings were added to a Schlenk flask with 100 mL dry THF. 5.04 g of $Ph_2SnCl_2$ (1) (14.7 mmol, 1 eq) were added at 0°C to obtain a yellow solution. The reaction mixture turned green after 5 minutes, was allowed to warm to r.t. and let stirring overnight. The dark gray suspension was concentrated *in vacuo* and 40 mL of dry heptane were added to the

residue. Stirred for some minutes and letting settle down overnight. Filtration and concentration of the filtrate *in vacuo* resulted into 4.25 g (69%) of a colorless oil.

$^{1}H$, $^{13}C$, $^{29}Si$ and $^{119}Sn$ NMR according to the literature.

### 5.2.4 Tetrakis(trimethylsilyl)germane (7)[7]

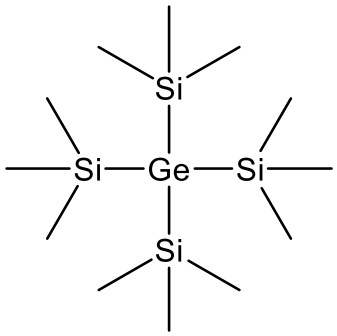


tetrakis(trimethylsilyl)germane
Chemical Formula: $C_{12}H_{36}GeSi_4$

**Figure 5-4.** Structure of (**7**)

A three necked flask with dropping funnel, reflux condenser and stop cock was charged with 300 mL dry THF, 7.65 g (1.10 mol, 8.06 eq.) lithium band and cooled to -50°C. During stirring 64.90 g (598 mmol, 4.37 eq.) of $SiMe_3Cl$ were added. The dropping funnel was charged with 29.33 g (137 mmol, 1 eq.) of $GeCl_4$ and 80 mL dry THF and added dropwise over a period of 1 1/2 h. After complete addition colling bath was taken away and reaction mixture was let warm to room temperature overnight. To the dark brown reaction mixture 8.54 g (78.6 mmol, 0.57 eq.) of $Me_3SiCl$ were added and refluxed for 3 h to consume all the reactive lithium metal. After the reaction mixture was cooled to room temperature it was filtrated through canula into a 300 mL cold degassed 5% $H_2SO_4$ and the phases were separated. The aqueous phase was washed with 3 times 50 mL $Et_2O$. The organic phase was dried over $Na_2SO_4$ and evaporated *in vacuo*. Sublimation (0.01 mbar, 100°C) of the yellow solid yielded 18.61 g (37 %) of a colorless solid.

$^{1}H$, $^{13}C$, $^{29}Si$ and $^{119}Sn$ NMR according to the literature.

### 5.2.5 Tetrakis(trimethylsilyl)stannane (8)[7]

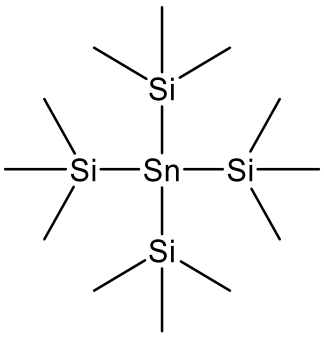


tetrakis(trimethylsilyl)stannane
Chemical Formula: $C_{12}H_{36}Si_4Sn$

**Figure 5-5.** Structure of (**8**)

A three necked flask with dropping funnel, reflux condenser and stop cock was charged with 250 mL dry THF, 7.24 g (1.04 mol, 8.1 eq.) lithium band and cooled to -78°C. During stirring 59,78 g (550 mmol, 4.3 eq.) of $SiMe_3Cl$ were added. The dropping funnel was charged with 33.55 g (129 mmol, 1 eq.) of $SnCl_4$ and 80 mL dry $Et_2O$ and added dropwise over a period of 1 h. After complete addition reaction was kept at – 50°C for 6 h. The colling bath was taken away and reaction mixture was let warm to room temperature overnight. To the ocker reaction mixture 8.54 g (78.6 mmol, 0.6 eq.) of $Me_3SiCl$ were added and refluxed for 3 h to consume all the reactive lithium metal. After the reaction mixture was cooled to room temperature it was dried *in vacuo* and the residue was washed with 3 x 50 mL dry pentane. The filtrate was concentrated *in vacuo*. Sublimation (0.01 mbar, 100°C) of the yellow solid yielded 9.76 g (18 %) of a colorless solid.

$^{1}H$, $^{13}C$, $^{29}Si$ and $^{119}Sn$ NMR according to the literature.

### 5.2.6 Tris(trimethylsilyl)germane (9)[13]

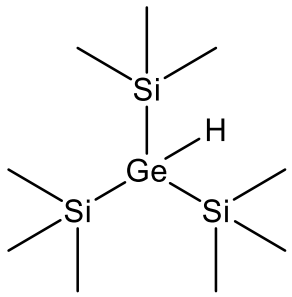


tris(trimethylsilyl)germane
Chemical Formula: $C_9H_{28}GeSi_3$

**Figure 5-6.** Structure of (**9**)

A Schlenk flask was charged with 7.95 g (21.8 mmol, 1 eq.) and 100 mL dry DME. The reaction mixture turned yellow upon addition of 2.68 g (23.9 mmol, 1.1 eq.) KOtBu. The reaction mixture was shortly evacuated and stirred overnight. The dark red reaction mixture was cannulated into 75 mL degassed 5 % $H_2SO_4$/$Et_2O$ mixture. The phases were separated, and the aqueous phase was washed with 2x 20 mL $Et_2O$. The combined organic phase was dried over $Na_2SO_4$ and dried *in vacuo* to obtain 1.1 g (17 %) of a colorless oil.

$^1$H NMR according to the literature.

### 5.2.7 Tris(trimethylsilyl)chlorogermane (10)[13]

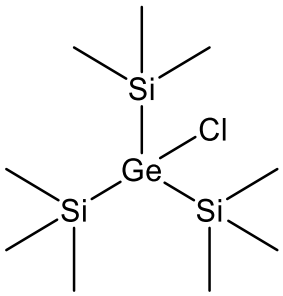


tris(trimethylsilyl)chlorogermane
Chemical Formula: $C_9H_{27}ClGeSi_3$

**Figure 5-7.** Structure of (**10**)

A Schlenk flask was charged with 6 mL $CCl_4$ and 1.1 g (3.75 mmol, 1 eq) of tris(trimethylsilyl)chlorogermane (9). The reaction was stirred overnight. The brownish reaction was concentrated *in vacuo* to yield 1.12 g (91%) of in places colorless needles

and a yellow oil. The colorless needles were found to be suitable for X-Ray analysis. $^{1}$H NMR showed formation of byproducts, purification of which was not successful.

$^{1}$H NMR according to the literature.

## 5.3 Synthesis of novel compounds

### 5.3.1 Tris(trimethylsilyl)phenylstannane (4)

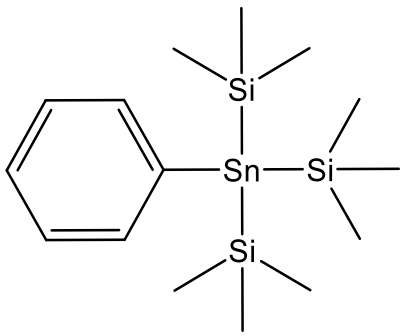


tris(trimethylsily)phenylstannane
Chemical Formula: $C_{15}H_{32}Si_3Sn$

**Figure 5-8.** Structure of (**4**)

A 3 necked flask, equipped with a dropping funnel, a reflux condenser and a stop cock, was charged with 350 mL dry $Et_2O$/THF mixture (7:2), 3.35 g (483 mmol, 6 eq.) lithium band and 25.62 g (234 mmol, 2.9 eq.) $Me_3SiCl$. The reaction mixture is cooled to -50 °C. The dropping funnel is charged with 24.28 g (80 mmol, 1 eq.) $PhSnCl_3$, 100 mL dry $Et_2O$/THF mixture (7:2) and 12.81 g (118 mmol, 1.5 eq) $Me_3SiCl$. Dropwise addition over 2 h at -50°C leaded to the formation of a yellow reaction mixture which was allowed to warm to room temperature overnight. Reaction control($^{119}$Sn-NMR) still showed starting material, therefore 2 mL of $SiMe_3Cl$ were added and the reaction mixture was stirred for another 24h. The orange reaction mixture was filtrated via cannula and dried *in vacuo*. The residue was washed with 2x 30 mL dry heptane, and the filtrate was concentrated *in vacuo* to obtain 14.96 g (45%) of a yellow oil as raw product. The residue was purified with flash column chromatography using dry heptane as eluent. Product separation was monitored with TLC under UV-light (350 nm). The fraction with the product was dried *in vacuo* to yield 952 mg (3 %) of a colorless oil.

**$^{1}$H NMR** ($C_6D_6$): δ = 0.358 ppm [s, 27H, Si-C**H$_3$**] $^{2}J(^{1}H\text{-}^{119}Sn)$ = 23.98 Hz $^{1}J(^{1}H\text{-}^{13}C)$ = 120. 15 Hz; 7.115 – 7.215 ppm [m, 3H, meta/para]; 7.571 – 7.679 ppm [m, 2H, ortho]

**$^{13}$C NMR** ($C_6D_6$): δ = 2.95 ppm [Si-**C**$H_3$] $^1J(^{13}C\text{-}^{29}Si)$ = 44.14 Hz; 127.34 ppm [para,meta] $^1J(^{13}C\text{-}^{1}H)$ = 9.04 Hz; 128.55 ppm [d, meta]; 139.27 ppm [Sn-**C**] $^1J(^{13}C\text{-}^{1}H)$ = 28.51 Hz

**$^{29}$Si NMR** ($C_6D_6$): δ = - 8.43 ppm $^1J(^{29}Si\text{-}^{117/119}Sn)$ = 398.7/417.4 Hz $^1J(^{29}Si\text{-}^{13}C)$ = 43.8 Hz

**$^{119}$Sn NMR** ($C_6D_6$) δ = - 409.8 ppm $^1J(^{119}Sn\text{-}^{29}Si)$ = 418.6 Hz $^1J(^{119}Sn\text{-}^{13}C)$ = 44.4 Hz $^2J(^{119}Sn\text{-}^{1}H)$ = 30.1 Hz.

**TLC:** Rf(heptane)= 0.62

### 5.3.2 Triphenyl(trimethylsilyl)stannane (5)

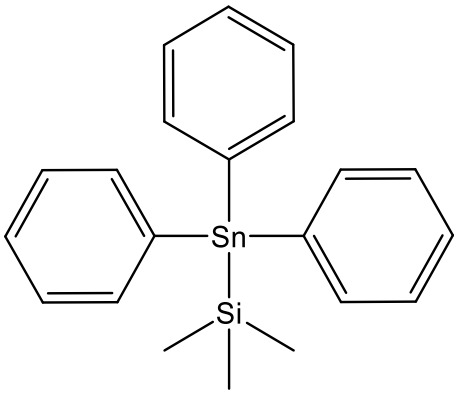


triphenyl(trimethylsilyl)stannane
Chemical Formula: $C_{21}H_{24}SiSn$

**Scheme 5-1.** Structure of (**5**)

Compound (**5**) was isolated via fractionated crystallization in heptane from the reaction mixture of compound (**4**) yielding 852 mg of colorless needles. The crystals were found suitable for X-Ray analysis.

$^1$H, $^{13}$C, $^{29}$Si and $^{119}$Sn NMR according to the literature.

### 5.3.3 Tris(trimethylsilyl)n-butylstannane (6)

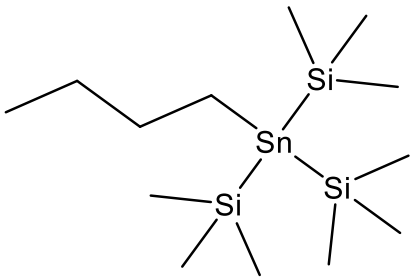


tris(trimethylsily)n-butylstannane
Chemical Formula: $C_{13}H_{36}Si_3Sn$

**Figure 5-9.** Structure of (**6**)

A 3 necked flask equipped with dropping funnel and reflux condenser was charged with 50 mL dry THF and cooled to – 50°C. Next, 6.94 g (352 mmol, 6.05 eq) of Li-band and 22.10 g (203 mmol, 3.5 eq.) of $Me_3SiCl$ were added to the flask. The dropping funnel was charged with 16.40 g (58 mmol, 1 eq.) of $nBuSnCl_3$ in 50 mL dry THF and added dropwise over 1 hour. The reaction mixture turned immediately yellow and changed to orange after some minutes. The reaction was kept at – 50°C for 5 h and warmed to room temperature overnight. The ocker reaction mixture was dried *in vacuo* and washed with 2x 25 mL dry pentane. Afterwards the solvent was removed *in vacuo* to obtain a black oily residue. After sublimation at 50°C and 0.1 mbar, 12.38 g (54 %) of a colorless oil was obtained. It was not able to isolate the pure product, as traces of $Sn(SiMe_3)_4$ remained.

**$^1$H NMR** ($C_6D_6$): δ = 0.340 ppm [s, 27H, Si-C**H$_3$**], 0.959 ppm [t, 3H, **H$_3$**C-$CH_2$-], 1.093 – 1.259 ppm [m, 2H, $H_3$C-C**H$_2$**-], 1.350 – 1.440 ppm [m, 2H, -C**H$_2$**-$CH_2$-Sn], 1.591 – 1.714 ppm [m, 2H, -C**H$_2$**-Sn]

**$^{13}$C NMR** ($C_6D_6$): δ = 2.19 ppm [**C**$H_3$-$CH_2$-], 3.02 ppm [Si-**Me$_3$**] $^1J(^{13}C\text{-}^{29}Si)$ = 42.04 Hz, 13.66 ppm [Sn-**C**$H_2$-], 27.99 ppm [Sn-$CH_2$-**C**$H_2$-] $^1J(^{13}C\text{-}^{29}Si)$ = 45.70 Hz, 33.60 ppm [$CH_3$-**C**$H_2$-] $^1J(^{13}C\text{-}^{1}H)$ = 17.46 Hz

**$^{29}$Si NMR** ($C_6D_6$): δ = - 9.91 ppm $^1J(^{29}Si\text{-}^{117/119}Sn)$ = 385.2/404.2 Hz

**$^{119}$Sn NMR** ($C_6D_6$) δ = - 438.1 ppm $^1J(^{119}Sn\text{-}^{29}Si)$ = 405.4 Hz $^1J(^{119}Sn\text{-}^{13}C)$ = 43.5 Hz

### 5.3.4 Tris(trimethylsilyl)(*tert*-butyldimethylsilyl)silane (11)

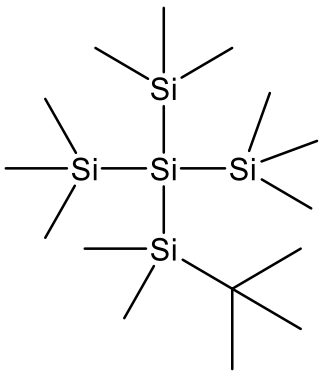


Tris(trimethylsilyl)(tert-butyldimethylsilyl)silane
Chemical Formula: $C_{15}H_{42}Si_5$

**Scheme 5-2.** Structure of (**11**)

A 150 mL Schlenk flask was charged with 40 mL dry THF and 4.05 g (12.6 mmol, 1.0 eq.) tetrakis(trimethylsilyl)silane. Next, 1.49 g (13.3 mmol, 1.05 eq.) of KOtBu were added at room temperature. The yellow reaction mixture was stirred overnight. A 2nd schlenk flask was charged with 40 mL dry toluene and 1.91 g (12.7 mmol, 1.0 eq.) of $(Me_3C)Me_2SiCl$ and cooled to 0°C. The anion was added dropwise over approx. 10 minutes to the 2nd Schlenk flask. The yellow reaction mixture was letting warm to room temperature overnight. The reaction mixture was concentrated *in vacuo* and washed with 2x 20 mL dry pentane. After aqueous workup the organic layer was dried *in vacuo* to obtain 3.66 g (80 %) of a colorless wax.

**$^{1}$H NMR** ($CDCl_3$): δ = 0.225 ppm [s, 6H, Si**Me$_2$**$^{t}$Bu]; 0.294 ppm [s, 27H, Si-C**H$_3$**]; 1.01 ppm [s, 9H, $SiMe_2$**$^{t}$Bu**]

**$^{13}$C NMR** ($CDCl_3$): δ = - 0.95 ppm [Si**Me$_2$**$^{t}$Bu], 3.45 ppm [Si**Me$_3$**] $^{1}J(^{13}C\text{-}^{29}Si)$ = 44.14 Hz, 18.78 ppm [$SiMe_2$(**C**$Me_3$)], 28.25 ppm [$SiMe_2$(C**Me$_3$**)]

**$^{29}$Si NMR** ($CDCl_3$): δ = - 138.68 ppm [Si-**Si**-Si], - 9.71 ppm [**Si**$Me_3$] $^{1}J(^{29}Si\text{-}^{13}C)$ = 44.39 Hz, 4.71 ppm [**Si**$Me_2$$^{t}$Bu]

NMR data according to the literature.[50]

### 5.3.5 Tris(trimethylsilyl)(*tert*-butyldimethylsilyl)germane (12)

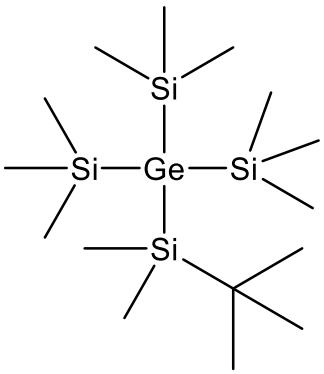


tris(trimethylsilyl)(tert-butyldimethylsilyl)germane
Chemical Formula: $C_{15}H_{42}GeSi_4$

**Figure 5-10.** Structure of (**12**)

A 150 mL Schlenk flask was charged with 50 mL dry THF and 5.02 g (13.7 mmol, 1 eq.) tetrakis(trimethylsilyl)germane (**7**). Next, 1.62 g (14.4 mmol, 1.05 eq.) of KOtBu were added at room temperature. The yellow reaction mixture was stirred for 3 hours. A 2nd schlenk flask was charged with 70 mL dry toluene and 2.17 g (14.4 mmol, 1.05 eq.) of $(Me_3C)Me_2SiCl$ and cooled to 0°C. The anion was added dropwise over approx. 10 minutes to the 2nd Schlenk flask. The yellow reaction mixture was letting warm to room temperature overnight. The reaction mixture was concentrated *in vacuo* and washed with 2x 20 mL dry pentane. After aqueous workup the organic layer was dried *in vacuo* to obtain 4.4 g (79 %) of a colorless wax.

**$^{1}$H NMR** ($CDCl_3$): δ = 0.257 ppm [s, 6H, Si**Me$_2$**$^{t}$Bu], 0.327 ppm [s, 27H, Si-C**H$_3$**], 1.01 ppm [s, 9H, $SiMe_2$***t*****Bu**]

**$^{13}$C NMR** ($CDCl_3$): δ = - 0.389 ppm [Si**Me$_2$**$^{t}$Bu]; 3.962 ppm [Si-**Me$_3$**] $^{1}J(^{13}C\text{-}^{29}Si)$ = 44.64 Hz; 18.66 ppm [Si-$Me_2$(**C**$Me_3$)]; 28.12 ppm [Si-$Me_2$(C**Me$_3$**)]

**$^{29}$Si NMR** ($CDCl_3$): δ = - 5.21 ppm [Ge-**Si**$Me_3$] $^{1}J(^{29}Si\text{-}^{13}C)$ = 44.22 Hz; 10.07 ppm [Ge-**Si**$Me_2(CMe_3)$]

### 5.3.6 Tris(trimethylsilyl)(*tert*-butyldimethylsilyl)stannane (13)

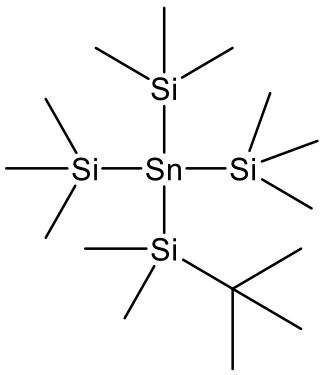


tris(trimethylsilyl)(tert-butyldimethylsilyl)stannane
Chemical Formula: $C_{15}H_{42}Si_4Sn$

**Figure 5-11.** Structure of (**13**)

A 150 mL Schlenk flask was charged with 40 mL dry THF and 3.24 g (7.9 mmol, 1 eq.) tetrakis(trimethylsilyl)stananne (**8**). Next, 0.93 g (8,3 mmol, 1.05 eq.) of KOtBu were added at room temperature. The yellow reaction mixture was stirred for one hour. A 2nd schlenk flask was charged with 40 mL dry toluene and 1.19 g (1 eq, 7.9 mmol) of $(Me_3C)Me_2SiCl$ and cooled to 0°C. The anion was added dropwise over approx. 10 minutes to the 2nd Schlenk flask. The bright orange reaction mixture was kept at 0°C for 6 h and put into the freezer overnight. The reaction mixture was concentrated *in vacuo* and washed with 2x 20 mL dry pentane. After aqueous workup the organic layer was dried *in vacuo* to obtain 3.08 g (86%) of a colorless wax.

**$^{1}$H NMR** ($C_6D_6$): δ = 0.310 ppm [s, 6H, Si**Me$_2$**$^t$Bu], 0.397 ppm [s, 27H, Si-C**H$_3$**]; 0.999 ppm [s, 9H, $SiMe_2$**$^t$Bu**]

**$^{13}$C NMR** ($C_6D_6$): δ = - 1.55 ppm [Si**Me$_2$**$^t$Bu]; 2.58 ppm [Si-**Me$_3$**] $^{1}J(^{13}C\text{-}^{29}Si)$ = 41.26 Hz; 16.70 ppm [Si-$Me_2$(**C**$Me_3$)]; 25.86 ppm [Si-$Me_2$(C**Me$_3$**)]

**$^{29}$Si NMR** ($C_6D_6$): δ = -10.51 ppm [**Si**$Me_3$] $^{1}J(^{29}Si\text{-}^{1177119}Sn)$ = 323.70/ 338.62 Hz, $^{1}J(^{29}Si\text{-}^{13}C)$ = 42.84 Hz; 10.35 ppm [**Si**$Me_2$$^t$Bu]

**$^{119}$Sn NMR** ($C_6D_6$) δ = - 672.8 ppm $^{1}J(^{119}Sn\text{-}^{29}Si)$ = 340.46 Hz, $^{1}J(^{119}Sn\text{-}^{13}C)$ = 38.88 Hz

### 5.3.7 Methyl(*tert*-butyldimethylsilyl)bis(trimethylsilyl)silane (14)

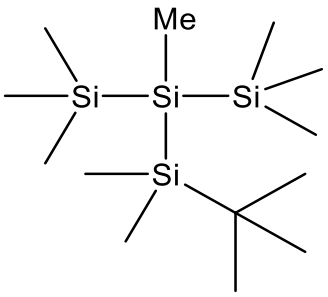


methyl(tert-butyldimethylsilyl)bis(trimethylsilyl)silane
Chemical Formula: $C_{15}H_{42}Si_5$

**Figure 5-12.** Structure of (**14**)

A Schlenk flask was charged with 2.74 g (7.55 mmol, 1 eq.) of (**11**) and 40 mL dry THF. Next, 892 mg (7.95 mmol, 1.05 eq.) of KOtBu were added and the following yellow reaction mixture was stirred overnight. In a 2nd Schlenk flask 957 mg (7.59 mmol, 1.0 eq) of dimethyl sulfate was dissolved in 40 mL dry toluene and cooled to -78°C. The anion was added over a period of 30 min at – 78°C. After, the reaction mixture was allowed to warm to room temperature. The reaction mixture was filtrated via canula. Aqueous workup, extraction with ether and drying *in vacuo* yielded 2.23 g (85%) of a colorless wax.

**$^{1}$H NMR** ($CDCl_3$): δ = 0.084 ppm [s, 6H, Si**Me$_2$**$^{t}$Bu], 0.112 ppm [s, 3H, Si-**Me**], 0.157 ppm [s, 18H, (Si**Me$_3$**)$_2$], 0.993 ppm [s, 9H, SiMe$_2$**$^{t}$Bu**]

**$^{13}$C NMR** ($CDCl_3$): δ = - 11.52 ppm [Si–**Me**], - 3.34 ppm [Si**Me$_2$**$^{t}$Bu], 0.76 ppm [Si**Me$_3$**] $^{1}J(^{13}C\text{-}^{29}Si)$ = 44.50 Hz, 18.51 ppm [SiMe$_2$(**C**Me$_3$)], 27.83 ppm [SiMe$_2$(C**Me$_3$**)], 31.72 ppm [SiMe$_2$(**C**Me$_3$)]

**$^{29}$Si NMR** ($CDCl_3$): δ = - 89.20 ppm [Si-**Si**-Si], – 12.13 ppm [**Si**Me$_3$], 0.68 ppm [**Si**Me$_2$$^{t}$Bu]

### 5.3.8 Methyl(*tert*-butyldimethylsilyl)bis(trimethylsilyl)germane (15)

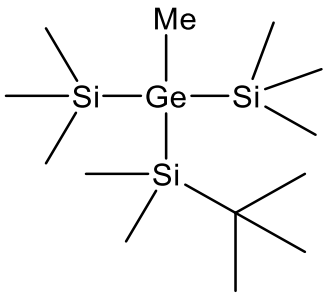


methyl(tert-butyldimethylsilyl)bis(trimethylsilyl)germane
Chemical Formula: $C_{13}H_{36}GeSi_3$

**Figure 5-13.** Structure of (**15**)

A Schlenk flask was charged with 3.82 g (9.37 mmol, 1 eq.) of (**12**) and 50 mL dry THF. Next, 1.12 g (9.98 mmol, 1.06 eq.) of KOtBu were added and the following yellow reaction mixture was stirred overnight. In a 2nd Schlenk flask 1.25 g (9.91 mmol, 1.05 eq) of dimethyl sulfate was dissolved in 40 mL dry toluene and cooled to -78°C. The anion was added over a period of 1 h at – 78°C. After, the reaction mixture was allowed to warm to room temperature. The reaction mixture was filtrated via canula. Aqueous workup, extraction with ether and drying *in vacuo* yielded 2.57 g (78%) of a colorless wax.

**$^{1}$H NMR** ($CDCl_3$): δ = 0.259 ppm [s, 6H, Si**Me$_2$**$^{t}$Bu], 0.313 ppm [s, 3H, Ge-**Me**], 0.330 ppm [s, 18H, (Si**Me$_3$**)$_2$], 1.012 ppm [s, 9H, SiMe$_2$-**$^{t}$Bu**]

**$^{13}$C NMR** ($CDCl_3$): δ = - 12.10 ppm [Ge–**Me**], - 2.76 ppm [Si**Me$_2$**$^{t}$Bu], 1.37 ppm [Si**Me$_3$**] $^{1}J(^{13}C\text{-}^{29}Si)$ = 44.64 Hz, 18.56 ppm [-SiMe$_2$(**C**Me$_3$)], 27.65 ppm [SiMe$_2$(C**Me$_3$**)].

**$^{29}$Si NMR** ($CDCl_3$): δ = - 5.22 ppm [**Si**Me$_3$] $^{1}J(^{29}Si\text{-}^{13}C)$ = 44.82 Hz, 10.07 ppm [**Si**Me$_2$$^{t}$Bu]

### 5.3.9 Methyl(*tert*-butyldimethylsilyl)bis(trimethylsilyl)stannane (16)

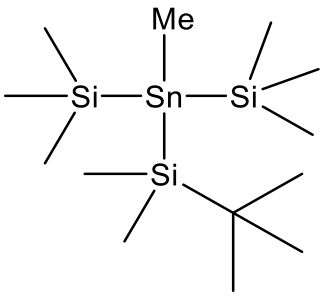


methyl(tert-butyldimethylsilyl)bis(trimethylsilyl)stannane
Chemical Formula: $C_{13}H_{36}Si_3Sn$

**Figure 5-14.** Structure of (**16**)

A Schlenk flask was charged with 2.52 g (5.5 mmol, 1 eq.) of (**13**) and 30 mL dry THF. Next, 0.660 g (5.9 mmol, 1.06 eq.) of KOtBu were added and the following yellow reaction mixture was stirred for 2h. In a 2nd Schlenk flask 0.931 g (7.4 mmol, 1.3 eq) of dimethyl sulfate was dissolved in 30 mL dry toluene and cooled to -78°C. The anion was added over a period of 1 h at – 78°C. After, the reaction mixture was allowed to warm to room temperature. The reaction mixture was filtrated via canula. Aqueous workup, extraction with ether and drying *in vacuo* yielded 1.64 g (75%) of a colorless wax.

**$^{1}$H NMR** ($C_6D_6$): δ = 0.251 ppm [s, 6H, Si**Me$_2$**$^{t}$Bu], 0.260 ppm [s, 3H, Sn-**Me**], 0.329 ppm [s, 18H, (Si**Me$_3$**)$_2$], 0.983 ppm [s, 9H, SiMe$_2$**$^{t}$Bu**]

**$^{13}$C NMR** ($C_6D_6$): δ = -23.70 ppm [Sn-**Me**], -3.32 ppm [Si**Me$_2$**($CMe_3$)] $^{1}J(^{13}C\text{-}^{29}Si)$ = 47.38 Hz, 0.72 ppm [Si**Me$_3$**] $^{1}J(^{13}C\text{-}^{29}Si)$ = 43.49 Hz, 16.72 ppm [SiMe$_2$(**C**Me$_3$)], 25.73 ppm [SiMe$_2$(C**Me$_3$**)]

**$^{29}$Si NMR** ($C_6D_6$): δ = - 10.43 ppm [**Si**Me$_3$] $^{1}J(^{29}Si\text{-}^{117/119}Sn)$ = 396.3/415.3 Hz $^{1}J(^{119}Sn\text{-}^{13}C)$ = 43.6 Hz, 8.15 ppm [**Si**Me$_2$$^{t}$Bu] $^{1}J(^{29}Si\text{-}^{117/119}Sn)$ = 390.3/409.5 Hz

**$^{119}$Sn NMR** ($C_6D_6$) δ = - 463.3 ppm $^{1}J(^{119}Sn\text{-}^{29}Si)$ = 414.8 Hz $^{1}J(^{119}Sn\text{-}^{13}C)$ = 45.6 Hz

## 5.4 Anion formation

### 5.4.1 General procedure for preparation of (17-19)

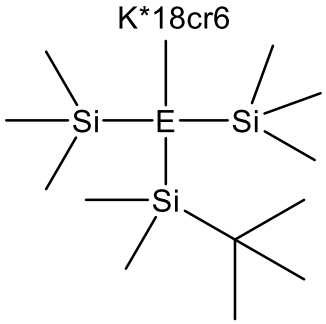


**Figure 5-15.** General structures of (**17**), (**18**) and (**19**), where E = Si, Ge, Sn.

The reactions were carried out in the Glovebox. Therefore, 100 mg of the starting material TBDMS($Me_3Si)_3$E (E = Si (**11**), Ge (**12**), Sn (**13**)) was dissolved in approx. 3 mL $Et_2O$. Next, one equivalent of KOtBu and one equivalent of 18cr6 were added to the yellow reaction mixture. Afterwards, the reaction mixture was filtrated, and the solvent evaporated. Recrystallization was done in $Et_2O$ at – 35°C.

### 5.4.2 Bis(trimethylsilyl)(*tert*-butyldimethylsilyl)silyl potassium * 18cr6 (17)

**$^1$H NMR** ($C_6D_6$): δ = 0.657 ppm [s, 6H, Si**$Me_2$**$^t$Bu], 0.690 ppm [s, 18H, Si-C**$H_3$**]; 1.372 ppm [s, 9H, $SiMe_2$**$^t$Bu**], 3.156 [s, $CH_2O$, 24H].

**$^{13}$C NMR** ($C_6D_6$): δ = 2.63 ppm [Si**$Me_2$**$^t$Bu]; 8.36 ppm [Si-**$Me_3$**]; 19.28 ppm [Si-$Me_2$(**C**$Me_3$)]; 29.44 ppm [Si-$Me_2$(C**$Me_3$**)], 69.95 ppm [18cr6].

**$^{29}$Si NMR** ($C_6D_6$): δ = -197.28 ppm [Si-**Si**-Si], -4.54 ppm [**Si**$Me_3$], 10.07 ppm [**Si**$Me_2$$^t$Bu].

### 5.4.3 Bis(trimethylsilyl)(*tert*-butyldimethylsilyl)germylpotassium * 18cr6 (18)

**$^1$H NMR** ($C_6D_6$): δ = 0.711 ppm [s, 6H, Si**$Me_2$**$^t$Bu], 0.740 ppm [s, 18H, Si-C**$H_3$**]; 1.380 ppm [s, 9H, $SiMe_2$**$^t$Bu**], 3.144 [s, $CH_2O$, 24H].

**$^{13}$C NMR** ($C_6D_6$): δ = 3.05 ppm [Si**$Me_2$**$^t$Bu]; 8.63 ppm [Si-**$Me_3$**]; 19.35 ppm [Si-$Me_2$(C**$Me_3$**)]; 29.39 ppm [Si-$Me_2$(**C**$Me_3$)], 69.96 ppm [18cr6]

**$^{29}$Si NMR** ($C_6D_6$): δ = - 3.72 ppm [**Si**$Me_3$], 12.01 ppm [**Si**$Me_2$$^t$Bu].

### 5.4.4 Bis(trimethylsilyl)(*tert*-butyldimethylsilyl)stannyl potassium * 18cr6 (19)

**$^{1}$H NMR** ($C_6D_6$): δ = 0.782 ppm [s, 6H, Si**Me$_2$**$^{t}$Bu], 0.807 ppm [s, 18H, Si-C**H$_3$**]; 1.379 ppm [s, 9H, SiMe$_2$**$^{t}$Bu**], 3.224 [s, $CH_2O$, 24H]

**$^{13}$C NMR** ($C_6D_6$): δ = 3.61 ppm [Si**Me$_2$**$^{t}$Bu], 8.88 ppm [Si-**Me$_3$**] $^{1}J(^{13}C\text{-}^{29}Si)$ = 23.26 Hz, 18.84 ppm [Si-Me$_2$(C**Me$_3$**)], 29.23 ppm [Si-Me$_2$(**C**Me$_3$)], 70.23 ppm [18cr6]

**$^{29}$Si NMR** ($C_6D_6$): δ = -13.44 ppm [**Si**Me$_3$] $^{1}J(^{29}Si\text{-}^{1177119}Sn)$ = 245.52/ 256.91 Hz, 7.28 ppm [**Si**Me$_2$$^{t}$Bu]

**$^{119}$Sn NMR** ($C_6D_6$) δ = - 904.4 ppm

### 5.4.5 General procedure for preparation of (17-19)

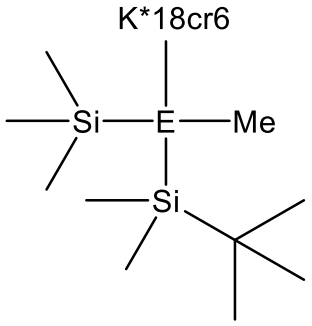


**Figure 5-16.** General structures of (**20**), (**21**) and (**22**), where E = Si, Ge, Sn.

The reactions were carried out in the Glovebox. Therefore, 100 mg of the starting material Me(TBDMS)(Me$_3$Si)$_2$E (E = Si (**14**), Ge (**15**), Sn (**16**)) was dissolved in approx. 3 mL $Et_2O$. Next, one equivalent of KOtBu and one equivalent of 18cr6 were added to the yellow reaction mixture and let stirring overnight. Next, the solvent was removed *in vacuo*. Recrystallization was done in $Et_2O$ at -35 °C.

### 5.4.6 Methyl(trimethylsilyl)(*tert*-butyldimethylsilyl)silyl potassium * 18cr6 (20)

**$^{1}$H NMR** ($C_6D_6$): δ = 0.563 ppm [ s, 3H, Si**Me$_2$**$^{t}$Bu], 0.661 ppm [s, 9H, Si**Me$_3$**], 0.676 ppm [s, 3H, Si**Me$_2$**$^{t}$Bu], 0.713 ppm [s, 3H, Si-**Me**], 1.440 ppm [s, 9H, SiMe$_2$**$^{t}$Bu**], 3.309 [s, 24H, $CH_2O$].

**$^{13}$C NMR** ($C_6D_6$): δ = - 6.86 ppm [Si-**Me**]; - 1.71 ppm [Si**Me$_2$**$^{t}$Bu], - 0.85 ppm [Si**Me$_2$**$^{t}$Bu] 4.45 ppm [Si-**Me$_3$**], 19.83 ppm [Si-Me$_2$(**C**Me$_3$)], 29.35 ppm [Si-Me$_2$(C**Me$_3$**)], 70.47 ppm [18cr6]

**$^{29}$Si NMR** ($C_6D_6$): δ = -133.2 ppm [Si-**Si**-Si], -5.8 ppm [**Si**Me$_3$], 7.1 ppm [**Si**Me$_2$$^{t}$Bu].

### 5.4.7 Methyl(trimethylsilyl)(*tert*-butyldimethylsilyl) germyl potassium * 18cr6 (21)

**$^{1}$H NMR** ($C_6D_6$): δ = 0.041 ppm [s, 3H, Si**Me**$_2$$^{t}$Bu], 0.097 ppm [s, 3H, Si**Me**$_2$$^{t}$Bu], 0.101 ppm [s, 3H, Ge-**Me**], 0.151 ppm [s, 9H, Si**Me$_3$**], 1.193 ppm [s, 9H, SiMe$_2$**$^{t}$Bu**], 3.362 ppm [s, 24H, $CH_2O$].

**$^{13}$C NMR** ($C_6D_6$): δ = - 6.42 ppm [Ge-**Me**]; 2.04 ppm [Si**Me**$_2$$^{t}$Bu], 2.05 ppm [Si**Me**$_2$$^{t}$Bu], 2.74 ppm [Si-**Me$_3$**],19.15 ppm [Si-Me$_2$(**C**Me$_3$)], 25.89 ppm [Si-Me$_2$(C**Me$_3$**)], 70.47 ppm [18cr6]

**$^{29}$Si NMR** ($C_6D_6$): δ = - 3.82 ppm [**Si**Me$_3$], 10.07 ppm [**Si**Me$_2$$^{t}$Bu].

### 5.4.8 Methyl(trimethylsilyl)(*tert*-butyldimethylsilyl) stannyl potassium * 18cr6 (22)

**$^{1}$H NMR** ($C_6D_6$): δ = 0.578 ppm [s, 3H, Si**Me**$_2$$^{t}$Bu], 0.723 ppm [s, 3H, Si**Me**$_2$$^{t}$Bu], 0.771 ppm [s, 3H, Sn-**Me**], 0.799 ppm [s, 9H, Si**Me$_3$**], 1.453 ppm [s, 9H, SiMe$_2$**$^{t}$Bu**], 3.132 [s, 24H, $CH_2O$].

**$^{13}$C NMR** ($C_6D_6$): δ = - 24.01 ppm [Sn-**Me**]; 0.06 ppm [Si**Me**$_2$$^{t}$Bu], 1.03 ppm [Si**Me**$_2$$^{t}$Bu], 6.02 ppm [Si-**Me$_3$**], 15.57 ppm [Si-Me$_2$(**C**Me$_3$)], 29.22 ppm [Si-Me$_2$(C**Me$_3$**)], 70.03 ppm [18cr6].

**$^{29}$Si NMR** ($C_6D_6$): δ = - 13.17 ppm [**Si**Me$_3$], 5.44 ppm [**Si**Me$_2$$^{t}$Bu].

**$^{119}$Sn NMR** ($C_6D_6$): δ = - 617.0 ppm.

# 6 References


(1) Sekiguchi, A.; Lee, V. Y.; Nanjo, M. Lithiosilanes and their application to the synthesis of polysilane dendrimers. *Coordination Chemistry Reviews* **2000**, *210*, 11–45.

(2) Fischer, R.; Frank, D.; Kayser, C.; Mechtler, C.; Baumgartner, J.; Marschner, C. Chemistry of Metalated Oligosilanes. In *Silicon Chemistry*; Jutzi, P., Schubert, U., Eds.; Wiley-VCH Verlag GmbH & Co. KGaA: Weinheim, Germany, **2003**; pp 118–128.

(3) Fischer, J.; Baumgartner, J.; Marschner, C. Silylgermylpotassium Compounds. *Organometallics* **2005**, *24*, 1263–1268.

(4) Rappoport, Z., Ed. *The Chemistry of Organic Germanium, Tin and Lead Compounds*; The chemistry of functional groups; John Wiley & Sons, Ltd: Chichester, UK, **2002**.

(5) Gilman, H.; Smith, C. L. Tetrakis(trimethylsilyl)silane. *J. Am. Chem. Soc.* **1964**, *86*, 1454.

(6) Merker, R. L.; Scott, M. J. Reactions of polyhalides with lithium and trimethylchlorosilane. *Journal of Organometallic Chemistry* **1965**, *4*, 98–100.

(7) Bürger, H.; Goetze, U. Trimethylsilyl Derivatives of Germanium and Tin.– Electron-balance Bonds of Silicon. *Angew. Chem. Int. Ed. Engl.* **1968**, *7*, 212–213.

(8) Rösch, L.; Starke, U. Tetrakis(trimethylsilyl)plumban, die erste Organosilicium-Blei-Verbindung. *Angewandte Chemie* **1983**, *95*, 572.

(9) Tortorelli, V. J.; Jones, M.; Wu, S.; Li, Z. Stereospecific additions of dimethylsilylene and diphenylsilylene to olefins. *Organometallics* **1983**, *2*, 759–764.

(10) Fischer, R.; Schollmeier, T.; Schürmann, M.; Uhlig, F. Syntheses of novel silylsubstituted distannanes. *Appl. Organometal. Chem.* **2005**, *19*, 523–529.

(11) Fritz, G.; Grunert, B. Bildung siliciumorganischer Verbindungen. 84 [1]. Synthese und thermische Umlagerung von verschieden substituierten linearen und cyclischen Silanen. *Z. Anorg. Allg. Chem.* **1981**, *473*, 59–79.

(12) Chenard, B. L.; van Zyl, C. M. Silylstannanes in organic synthesis. Scope and limitation of palladium-catalyzed reaction with acetylenes. *J. Org. Chem.* **1986**, *51*, 3561–3566.

(13) Brook, A. G.; Abdesaken, F.; Söllradl, H. Synthesis of some tris(trimethylsilyl)germyl compounds. *Journal of Organometallic Chemistry* **1986**, *299*, 9–13.

(14) Nanjo, M.; Oda, T.; Mochida, K. Preparation and Characterization of Tris(trimethylsilyl)germylzinc Chloride and Bis[tris(trimethylsilyl)germyl]zinc. *Chem. Lett.* **2002**, *31*, 108–109.

(15) GUIJARRO, A.; YUS, M. ChemInform Abstract: Polychlorinated Materials as a Source of Polyanionic Synthons. *ChemInform* **1996**, *27*, no-no.

(16) Dunogues, J.; Jousseaume, E.; Calas, R. Silylation de derives gem-polychlores. *Journal of Organometallic Chemistry* **1974**, *71*, 377–392.

(17) Wu, Q.; Qu, Z.-W.; Omann, L.; Irran, E.; Klare, H. F. T.; Oestreich, M. Cleavage of Unactivated Si-C(sp3 ) Bonds with Reed's Carborane Acids: Formation of Known and Unknown Silylium Ions. *Angew. Chem. Int. Ed. Engl.* **2018**, *57*, 9176–9179.

(18) Eisch, J. J.; Tsai, M.-R. 1, n-Triorganosilyl migrations in the rearrangements of silyl-substituted organolithium compounds. *Journal of Organometallic Chemistry* **1982**, *225*, 5–23.

(19) Herzog, U.; Roewer, G. Preparation of oligosilanes containing perhalogenated silyl groups and their hydrogenation by stannanes. *Journal of Organometallic Chemistry* **1997**, *544*, 217–223.

(20) Seitz, D. E.; Ferreira, L. An Efficient Preparation of Hexamethyldisilane. *Synthetic Communications* **1979**, *9*, 451–456.

(21) Bobbitt, K. L.; Maloney, V. M.; Gaspar, P. P. New photochemical routes to germylenes and germenes and kinetic evidence concerning the germylene-diene addition mechanism. *Organometallics* **1991**, *10*, 2772–2777.

(22) SHAW, C. FRANK, III. STUDIES OF TERT-BUTYL GERMANES AND METAL-METAL BONDS OF GROUP IV-M. Ph.D, Northwestern University, Ann Arbor, 1970.

(23) Eaborn, C.; Mahmoud, F. M. The mechanism of cleavage of Si□Ge bond by base. *Journal of Organometallic Chemistry* **1981**, *205*, 47–51.

(24) Chenard, B. L.; Laganis, E. D.; Davidson, F.; RajanBabu, T. V. Silyl stannanes: useful reagents for bis-functionalization of .alpha.,.beta.-unsaturated ketones and acetylenes. *J. Org. Chem.* **1985**, *50*, 3666–3667.

(25) Wells, A. F. *Structural inorganic chemistry*, 5. ed.; Oxford science publications; Clarendon Pr: Oxford, **1984**.

(26) Kutzelnigg, W. Chemical Bonding in Higher Main Group Elements. *Angew. Chem. Int. Ed. Engl.* **1984**, *23*, 272–295.

(27) Allred, A. L.; Rochow, E. G. Electronegativities of carbon, silicon, germanium, tin and lead. *Journal of Inorganic and Nuclear Chemistry* **1958**, *5*, 269–288.

(28) Baukov, Y. I.; Tandura, S. N. Hypervalent Compounds of Organic Germanium, Tin and Lead Derivatives. In *The Chemistry of Organic Germanium, Tin and Lead Compounds*; Rappoport, Z., Ed.; The chemistry of functional groups; John Wiley & Sons, Ltd: Chichester, UK, **2002**; pp 963–1239.

(29) Kano, N., Ed. *Penta- and Hexacoordinated Silicon (IV) Compounds: Organosilicon Compounds*; Academic Press An imprint of Elsevier: London, San Diego, Cambridge, Oxford, **2017**.

(30) Voronkov, M. G.; Egorochkin, A. N. Similarities and Differences of Organic Compounds of Germanium, Tin and Lead. In *PATAI'S Chemistry of Functional Groups*; Rappoport, Z., Ed.; John Wiley & Sons, Ltd: Chichester, UK, 2009; p 2269.

(31) Saito, K.; Hayakawa, S.; Takei, F.; Yamadera, H. Chemistry and Periodic Table. *Number* **1982**, *5*, 148–185.

(32) Bondi, A. van der Waals Volumes and Radii. *The Journal of Physical Chemistry* **1964**, *68*, 441–451.

(33) Auner, N.; Herrmann, W. A.; Klingebiel, U., Eds. *Synthetic Methods of Organometallic and Inorganic Chemistry, Volume 2, 1996: Volume 2: Groups 1,2, 13 and 14*, 1. Auflage; Thieme: Stuttgart, **2014**.

(34) Cottrell, T. L. *The Strength of CHemical Bonds*, 2nd Edition; Butterworth: London, **1958**.

(35) Ciccioli, A.; Gigli, G.; Meloni, G. The Si-Sn chemical bond: an integrated thermochemical and quantum mechanical study of the SiSn diatomic molecule and small Si-Sn clusters. *Chem. Eur. J.* **2009**, *15*, 9543–9560.

(36) Ciccioli, A.; Gigli, G.; Meloni, G.; Testani, E. The dissociation energy of the new diatomic molecules SiPb and GePb. *The Journal of chemical physics* **2007**, *127*, 54303.

(37) V. Grignard. Sur quelques nouvelles combinaisons organométalliques du magnèsium et leur application à des synthèses d'alcools et d'hydrocarbures. *CR Hebd. Séances Acad. Sci.* **1900**, 1322–1324.

(38) Schlenk, W.; Holtz, J. *Ber. Dtsch. Chem. Ges.* **1917**, 272.

(39) Marschner, C. Silicon-Centered Anions. In *Penta- and Hexacoordinated Silicon (IV) Compounds: Organosilicon Compounds*; Kano, N., Ed.; Academic Press An imprint of Elsevier: London, San Diego, Cambridge, Oxford, **2017**; pp 295–360.

(40) H. Gilman, J.M. Holmes, C. L. Smith. *Chem. Ind. (London)* **1965**, 848.

(41) Gutekunst, G.; G. Brook, A. Tris(trimethylsilyl)silyllithium · 3 THF: a stable crystalline silyllithium reagent. *Journal of Organometallic Chemistry* **1982**, *225*, 1–3.

(42) Preuss, F.; Wieland, T.; Perner, J.; Heckmann, G. Silyl-, Germyl-, Stannyl- und Plumbyl-Komplexe von Vanadium(V) / Silyl, Germyl, Stannyl, Plumbyl Complexes of Vanadium(V). *Zeitschrift für Naturforschung B* **1992**, *47*, 1355–1362.

(43) Kornev, A. N. The tris(trimethylsilyl)silyl group in organic, coordination and organometallic chemistry. *Russ. Chem. Rev.* **2004**, *73*, 1065–1089.

(44) Marschner, C. A New and Easy Route to Polysilanylpotassium Compounds. *Eur. J. Inorg. Chem.* **1998**, *1998*, 221–226.

(45) Wiberg, N.; Finger, C. M. M.; Polborn, K. Tetrakis(tri-tert-butylsilyl)-tetrahedro-tetrasilane (tBu3Si)4Si4: The First Molecular Silicon Compound with a Si4 Tetrahedron. *Angew. Chem. Int. Ed. Engl.* **1993**, *32*, 1054–1056.

(46) Marschner, C. Preparation and Reactions of Polysilanyl Anions and Dianions. *Organometallics* **2006**, *25*, 2110–2125.

(47) Klinkhammer, K. W.; Schwarz, W. ber die Synthese von Tris(trimethylsilyl)silyl-kalium, -rubidium und -caesium und die Molekl strukturen zweier Toluolsolvate. *Z. Anorg. Allg. Chem.* **1993**, *619*, 1777–1789.

(48) Klinkhammer, K. W. Tris(trimethylsilyl)silanides of the Heavier Alkali Metals—A Structural Study. *Chem. Eur. J.* **1997**, *3*, 1418–1431.

(49) Gilman, H.; Harrell, R. L. Hexakis(trimethylsilyl)disilane: A highly branched and symmetrical organopolysilane. *Journal of Organometallic Chemistry* **1967**, *9*, 67–76.

(50) Apeloig, Y.; Yuzefovich, M.; Bendikov, M.; Bravo-Zhivotovskii, D.; Klinkhammer, K. A New Method for the Synthesis of Branched Polysilane Anions. *Organometallics* **1997**, *16*, 1265–1269.

(51) Teng, W.; Ruhlandt-Senge, K. Syntheses and Structures of the First Heavy Alkaline Earth Metal Germanides M(THF) n (Ge(SiMe 3 ) 3 ) 2 (M = Ca, n = 3; M = Sr, n = 3; and M = Ba, n = 4). *Organometallics* **2004**, *23*, 952–956.

(52) Jenkins, D. M.; Teng, W.; Englich, U.; Stone, D.; Ruhlandt-Senge, K. Heavy Alkali Metal Tris(trimethylsilyl)silanides: A Synthetic and Structural Study. *Organometallics* **2001**, *20*, 4600–4606.

(53) Fischer, R.; Baumgartner, J.; Marschner, C.; Uhlig, F. Tris(trimethylsilyl)stannyl alkali derivatives: Syntheses and NMR spectroscopic properties. *Inorganica Chimica Acta* **2005**, *358*, 3174–3182.

(54) Ervin, K. M.; Gronert, S.; Barlow, S. E.; Gilles, M. K.; Harrison, A. G.; Bierbaum, V. M.; DePuy, C. H.; Lineberger, W. C.; Ellison, G. B. Bond strengths of ethylene and acetylene. *J. Am. Chem. Soc.* **1990**, *112*, 5750–5759.

(55) Norman, N. C. *Periodicity and the s- and p-block elements*, Second edition; Oxford University Press: Oxford, **2021**.

(56) Montgomery, C. D. Factors Affecting Energy Barriers for Pyramidal Inversion in Amines and Phosphines: A Computational Chemistry Lab Exercise. *J. Chem. Educ.* **2013**, *90*, 661–664.

(57) Fischer, R.; Marschner, C. Experimental Determination of the Inversion Barriers of Oligosilyl Anions. In *Organosilicon Chemistry V*; Auner, N., Weis, J., Eds.; Wiley-VCH Verlag GmbH: Weinheim, Germany, **2003**; pp 190–194.

(58) Kayser, C.; Fischer, R.; Baumgartner, J.; Marschner, C. Tailor-made Oligosilyl Potassium Compounds. *Organometallics* **2002**, *21*, 1023–1030.

(59) Heine, A.; Herbst-Irmer, R.; Sheldrick, G. M.; Stalke, D. Structural characterization of two modifications of tris(tetrahydrofuran)(tris(trimethylsilyl)silyl)lithium: a compound with a silicon-29-lithium-7 NMR coupling. *Inorg. Chem.* **1993**, *32*, 2694–2698.

(60) Freitag, S.; Herbst-Irmer, R.; Lameyer, L.; Stalke, D. Observation of a Ge−Li Bond: Donor-Base-Stabilized (Tris(trimethylsilyl)germyl)lithium. *Organometallics* **1996**, *15*, 2839–2841.

(61) Teng, W.; Ruhlandt-Senge, K. Syntheses and structures of the first heavy-alkali-metal tris(trimethylsilyl)germanides. *Chem. Eur. J.* **2005**, *11*, 2462–2470.

(62) Cardin, C. J.; Cardin, D. J.; Clegg, W.; Coles, S. J.; Constantine, S. P.; Rowe, J. R.; Teat, S. J. The molecular structure and one-pot synthesis of [Li(thf)3·Sn(SiMe3)3]. *Journal of Organometallic Chemistry* **1999**, *573*, 96–100.

(63) Nakamoto, M.; Fukawa, T.; Lee, V. Y.; Sekiguchi, A. Nearly planar nonsolvated monomeric silyl- and germyllithiums as a result of an intramolecular CH-Li agostic interaction. *J. Am. Chem. Soc.* **2002**, *124*, 15160–15161.

(64) Flock, M.; Marschner, C. Silylanions: Inversion Barriers and NMR Chemical Shifts. *Chem. Eur. J.* **2002**, *8*, 1024.

(65) Driess, M.; Merz, K.; Monsé, C. *Z. Anorg. Allg. Chem.* **2000**, *626*, 2264–2268.

(66) Fukawa, T.; Nakamoto, M.; Lee, V. Y.; Sekiguchi, A. Structural Diversity of the Tris(di- tert- butylmethylsilyl)stannyl Anion: Monomeric vs Dimeric, Lithium Coordinated vs Lithium Free. *Organometallics* **2004**, *23*, 2376–2381.

(67) Kozeschkow, K. A. Untersuchungen über metallorganische Verbindungen, I. Mitteilung: Eine neue Klasse von Arylzinnverbindungen: Phenyl-trihalogen-stannane. *Ber. dtsch. Chem. Ges. A/B* **1929**, *62*, 996–999.

(68) Kozeschkow, K. A. Untersuchungen über metallorganische Verbindungen, II. Mitteil.: Die Reaktion zwischen zinnorganischen Verbindungen der Fettreihe und Tetrahalogeniden des Zinns. *Ber. dtsch. Chem. Ges. A/B* **1933**, *66*, 1661–1665.

(69) Tagne Kuate, A. C.; Iovkova, L.; Hiller, W.; Schürmann, M.; Jurkschat, K. Organotin-Substituted [13]-Crown-4 Ethers: Ditopic Receptors for Lithium and Cesium Halides. *Organometallics* **2010**, *29*, 5456–5471.

(70) Blumenstein, M.; Lemmler, M.; Hayen, A.; Metzger, J. O. Enantioselective hydrogen transfer reactions from chiral binaphthyl variants of tin hydrides to prochiral radicals. *Tetrahedron: Asymmetry* **2003**, *14*, 3069–3077.

(71) Gielen, M.; Vanden Eynde, I. Organometallic compounds. *Journal of Organometallic Chemistry* **1981**, *217*, 205–213.

(72) Newcomb, M.; Horner, J. H.; Blanda, M. T. Macrocycles containing tin. Through space cooperative binding and high size selectivity in the complexation of chloride ion by Lewis acidic macrobicyclic hosts. *J. Am. Chem. Soc.* **1987**, *109*, 7878–7879.

(73) Uhlig, W. Synthese funktionell substituierter Disilane auf der Basis von Triflatderivaten. *Z. Anorg. Allg. Chem.* **1993**, *619*, 1479–1482.

(74) E.Zarl. Dissertation, TU Graz, **2008**.

(75) Sanganee, M. J.; Steel, P. G.; Whelligan, D. K. Novel one-pot synthesis of aryltris(trimethylsilyl)silanes. *J. Org. Chem.* **2003**, *68*, 3337–3339.

(76) Zarkadis, A. K.; Georgakilas, V.; Perdikomatis, G. P.; Trifonov, A.; Gurzadyan, G. G.; Skoulika, S.; Siskos, M. G. *CCDC 263099: Experimental Crystal Structure Determination*, **2006**.

(77) Parkányi, L.; Hengge, E. The crystal structure of trimethyltriephenyldisilane. *Journal of Organometallic Chemistry* **1982**, *235*, 273–276.

(78) Párkányi, L.; Hernandez, C.; Pannell, K. H. Organometalloidal derivatives of the transition metals. *Journal of Organometallic Chemistry* **1986**, *301*, 145–151.

(79) Kuzora, R.; Schulz, A.; Villinger, A.; Wustrack, R. Hypersilylated cyclodiphosphadiazanes and cyclodiphosphadiazenium salts. *Dalton transactions (Cambridge, England : 2003)* **2009**, 9304–9311.

(80) Xue, W.; Mao, W.; Zhang, L.; Oestreich, M. Mechanistic Dichotomy of Magnesium- and Zinc-Based Germanium Nucleophiles in the C(sp3 )-Ge Cross-Coupling with Alkyl Electrophiles. *Angew. Chem. Int. Ed. Engl.* **2019**, *58*, 6440–6443.

(81) Pedersen, C. J. Cyclic polyethers and their complexes with metal salts. *J. Am. Chem. Soc.* **1967**, *89*, 7017–7036.

(82) Roland Fischer. *unpublished results*; TU Graz.

(83) Morris, G. A.; Freeman, R. Enhancement of nuclear magnetic resonance signals by polarization transfer. *J. Am. Chem. Soc.* **1979**, *101*, 760–762.

(84) Sheldrick, G. M. A short history of SHELX. *Acta crystallographica. Section A, Foundations of crystallography* **2008**, *64*, 112–122.

(85) Blessing, R. H. An empirical correction for absorption anisotropy. *Acta crystallographica. Section A, Foundations of crystallography* **1995**, *51 (Pt 1)*, 33–38.

(86) Bruker. *APEX2 and SAINT. Bruker AXS Inc.*; Madison, Wisconsin, 2012.

(87) Sheldrick, G. M. SHELXT - integrated space-group and crystal-structure determination. *Acta crystallographica. Section A, Foundations and advances* **2015**, *71*, 3–8.

(88) Sheldrick, G. M. Phase annealing in SHELX-90: direct methods for larger structures. *Acta crystallographica. Section A, Foundations of crystallography* **1990**, *46*, 467–473.

(89) van der Sluis, P.; Spek, A. L. BYPASS: an effective method for the refinement of crystal structures containing disordered solvent regions. *Acta crystallographica. Section A, Foundations of crystallography* **1990**, *46*, 194–201.

(90) Spek, A. L. Structure validation in chemical crystallography. *Acta crystallographica. Section D, Biological crystallography* **2009**, *65*, 148–155.

(91) Spek, A. L. Single-crystal structure validation with the program PLATON. *J Appl Crystallogr* **2003**, *36*, 7–13.

(92) Zeppek, C.; Pichler, J.; Torvisco, A.; Flock, M.; Uhlig, F. Aryltin chlorides and hydrides: Preparation, detailed NMR studies and DFT calculations. *Journal of Organometallic Chemistry* **2013**, *740*, 41–49.

(93) Genser, D. Neue Methoden zur Knüpfung von Sn-Sn Bindungen. Diplomarbeit, TU Graz, **2010**.

# 7 Appendix

## 7.1 List of Figures, Tables and Schemes

### 7.1.1 List of Figures

### 7.1.2 List of Schemes

### 7.1.3 List of Tables

## 7.2 Crystallographic Data

**Table 7-1.** Crystallographic data for (**5**) and (**9**)

| **Compound** | (**5**) | (**9**) |
|---|---|---|
| Empirical formula | $C_{21}H_{24}SiSn$ | $C_{18}H_{54}Cl_2Ge_2Si_6$ |
| Formula weight | 423.18 | 655.23 |
| Temperature [K] | 293(2) | 100.27 |
| Crystal system | orthorhombic | cubic |
| Space group | $Pna2_1$ | Pa-3 |
| a [Å] | 20.4336(13) | 15.4017(7) |
| b [Å] | 12.2403(7) | 15.4017(7) |
| c [Å] | 7.8094(4) | 15.4017(7) |
| α [°] | 90 | 90 |
| β [°] | 90 | 90 |
| γ [°] | 90 | 90 |
| Volume [$Å^3$] | 1953.24(19) | 3653.5(5) |
| Z | 4 | 4 |
| $\rho_{calc}$ [$g*cm^{-3}$] | 1.439 | 1.191 |
| μ [$mm^{-1}$] | 1.367 | 1.994 |
| F(000) | 856.0 | 1376.0 |
| Crystal size [$mm^3$] | 0.19 × 0.14 × 0.09 | 0.22 × 0.19 × 0.16 |
| Radiation | MoKα (λ = 0.71073) | MoKα (λ = 0.71073) |
| 2Θ range for data collection [°] | 3.878 to 58.246 | 4.58 to 60.028 |
| Index ranges | -27 ≤ h ≤ 27, -16 ≤ k ≤ 16, -10 ≤ l ≤ 10 | -21 ≤ h ≤ 21, -21 ≤ k ≤ 21, -21 ≤ l ≤ 21 |
| Reflections collected | 35943 | 67574 |
| Independent reflections | 5186 [$R_{int}$ = 0.0420, $R_{sigma}$ = 0.0319] | 1796 [$R_{int}$ = 0.0858, $R_{sigma}$ = 0.0238] |
| Data/restraints/ parameters | 5186/1/211 | 1796/0/46 |
| Goodness of fit on $F^2$ | 1.035 | 1.166 |
| Final R indexes [I>=2σ (I)] | $R_1$ = 0.0212, $wR_2$ = 0.0387 | $R_1$ = 0.0226, $wR_2$ = 0.0480 |
| Final R indexes [all data] | $R_1$ = 0.0275, $wR_2$ = 0.0407 | $R_1$ = 0.0352, $wR_2$ = 0.0525 |
| Largest diff. peak/hole [e $Å^{-3}$] | 0.39/-0.37 | 0.34/-0.28 |

**Table 7-2.** Crystallographic data for (**17**), (**18**) and (**19**)

| **Compound** | (**17**) | (**18**) | (**19**) |
|---|---|---|---|
| Empirical formula | $C_{24}H_{57}KO_6Si_4$ | $C_{24}H_{57}GeKO_6Si_3$ | $C_{24}H_{57}KO_6Si_3Sn$ |
| Formula weight | 593.15 | 637.65 | 683.75 |
| Temperature [K] | 99.90 | 99.95 | 99.55 |
| Crystal system | monoclinic | monoclinic | monoclinic |
| Space group | $P2_1/n$ | $P2_1/n$ | $P2_1/c$ |
| a [Å] | 10.6318(11) | 10.6324(9) | 15.8383(13) |
| b [Å] | 17.0707(16) | 17.0576(14) | 14.0976(12) |
| c [Å] | 19.3336(17) | 19.3492(18) | 16.2047(16) |
| α [°] | 90 | 90 | 90 |
| β [°] | 99.462(5) | 99.249(5) | 97.190(3) |
| γ [°] | 90 | 90 | 90 |
| Volume [Å$^3$] | 3461.2(6) | 3463.6(5) | 3589.8(6) |
| Z | 4 | 4 | 4 |
| $\rho_{calc}$ [g*cm$^{-3}$] | 1.138 | 1.223 | 1.265 |
| μ [mm$^{-1}$] | 0.323 | 1.139 | 0.958 |
| F(000) | 1296.0 | 1368.0 | 1440.0 |
| Crystal size [mm$^3$] | 0.45 × 0.27 × 0.11 | 0.18 × 0.13 × 0.1 | 0.22 × 0.18 × 0.13 |
| Radiation | MoKα (λ = 0.71073) | MoKα (λ = 0.71073) | MoKα (λ = 0.71073) |
| 2Θ range for data collection [°] | 3.202 to 60.048 | 3.202 to 54.524 | 2.592 to 60.112 |
| Index ranges | -14 ≤ h ≤ 14, -23 ≤ k ≤ 23, -27 ≤ l ≤ 24 | -13 ≤ h ≤ 13, -21 ≤ k ≤ 21, -24 ≤ l ≤ 24 | -22 ≤ h ≤ 20, -19 ≤ k ≤ 19, -22 ≤ l ≤ 22 |
| Reflections collected | 157251 | 91631 | 222932 |
| Independent reflections | 10080 [$R_{int}$ = 0.1167, $R_{sigma}$ = 0.0581] | 7675 [$R_{int}$ = 0.1583, $R_{sigma}$ = 0.1102] | 10491 [$R_{int}$ = 0.0828, $R_{sigma}$ = 0.0358] |
| Data/restraints/ parameters | 10080/0/327 | 7675/0/327 | 10491/108/490 |
| Goodness of fit on $F^2$ | 1.017 | 1.009 | 1.170 |
| Final R indexes [I>=2σ (I)] | $R_1$ = 0.0570, $wR_2$ = 0.1394 | $R_1$ = 0.0500, $wR_2$ = 0.0816 | $R_1$ = 0.0428, $wR_2$ = 0.0640 |
| Final R indexes [all data] | $R_1$ = 0.0766, $wR_2$ = 0.1507 | $R_1$ = 0.1084, $wR_2$ = 0.0936 | $R_1$ = 0.0602, $wR_2$ = 0.0697 |
| Largest diff. peak/hole [e Å$^{-3}$] | 1.24/-0.70 | 0.98/-0.79 | 1.13/-0.84 |

**Table 7-3.** Crystallographic data for (**20**) and (**22**)

| **Compound** | (**20**) | (**22**) |
|---|---|---|
| Empirical formula | $C_{22}H_{51}KO_6Si_3$ | $C_{22}H_{51}KO_6Si_2Sn$ |
| Formula weight | 534.99 | 625.59 |
| Temperature [K] | 100.08 | 100.28 |
| Crystal system | triclinic | triclinic |
| Space group | P-1 | P-1 |
| a [Å] | 9.733(2) | 9.8988(7) |
| b [Å] | 10.087(2) | 10.2744(8) |
| c [Å] | 16.947(3) | 17.1578(14) |
| α [°] | 98.744(7) | 97.567(4) |
| β [°] | 104.320(6) | 104.854(3) |
| γ [°] | 106.387(6) | 107.781(3) |
| Volume [$Å^3$] | 1502.0(5) | 1563.8(2) |
| Z | 2 | 2 |
| $\rho_{calc}$ [$g*cm^{-3}$] | 1.183 | 1.329 |
| μ [$mm^{-1}$] | 0.328 | 1.056 |
| F(000) | 584.0 | 656.0 |
| Crystal size [$mm^3$] | 0.19 × 0.16 × 0.13 | ? × ? × ? |
| Radiation | MoKα (λ = 0.71073) | MoKα (λ = 0.71073) |
| 2Θ range for data collection [°] | 2.554 to 52 | 4.276 to 53.996 |
| Index Ranges | -11 ≤ h ≤ 11, -12 ≤ k ≤ 12, -20 ≤ l ≤ 19 | -12 ≤ h ≤ 12, -13 ≤ k ≤ 13, -21 ≤ l ≤ 21 |
| Reflections collected | 10502 | 29381 |
| Independent reflections | 5898 [$R_{int}$ = 0.1593, $R_{sigma}$ = 0.2156] | 6683 [$R_{int}$ = 0.0645, $R_{sigma}$ = 0.0571] |
| Data/restraints/ parameters | 5898/0/298 | 6683/0/298 |
| Goodness of fit on $F^2$ | 0.992 | 1.072 |
| Final R indexes [I>=2σ (I)] | $R_1$ = 0.0865, $wR_2$ = 0.1601 | $R_1$ = 0.0728, $wR_2$ = 0.1745 |
| Final R indexes [all data] | $R_1$ = 0.1734, $wR_2$ = 0.1823 | $R_1$ = 0.0912, $wR_2$ = 0.1895 |
| Largest diff. peak/hole [e $Å^{-3}$] | 0.65/-0.49 | 5.76/-3.30 |